


# Replacing the oxidation-sensitive triaminoaryl chemotype of problematic $K_{V7}$ channel openers: Exploration of a nicotinamide scaffold

Konrad W. Wurm | Frieda-Marie Bartz | Lukas Schulig | Anja Bodtke |  
Patrick J. Bednarski | Andreas Link 

Department of Pharmaceutical/Medicinal Chemistry, Institute of Pharmacy, University of Greifswald, Greifswald, Germany

## Correspondence

Andreas Link, Department of Pharmaceutical/Medicinal Chemistry, Institute of Pharmacy, University of Greifswald, Friedrich-Ludwig-Jahn-Str. 17, Greifswald 17489, Germany.  
Email: [link@uni-greifswald.de](mailto:link@uni-greifswald.de)

## Funding information

Deutsche Forschungsgemeinschaft, Grant/Award Numbers: BE 1287/6-2, LI 765/7-2

## Abstract

$K_{V7}$  channel openers have proven their therapeutic value in the treatment of pain as well as epilepsy and, moreover, they hold the potential to expand into additional indications with unmet medical needs. However, the clinically validated but meanwhile discontinued  $K_{V7}$  channel openers flupirtine and retigabine bear an oxidation-sensitive triaminoraryl scaffold, which is suspected of causing adverse drug reactions via the formation of quinoid oxidation products. Here, we report the design and synthesis of nicotinamide analogs and related compounds that remediate the liability in the chemical structure of flupirtine and retigabine. Optimization of a nicotinamide lead structure yielded analogs with excellent  $K_{V7.2/3}$  opening activity, as evidenced by  $EC_{50}$  values approaching the single-digit nanomolar range. On the other hand, weighted  $K_{V7.2/3}$  opening activity data including inactive compounds allowed for the establishment of structure–activity relationships and a plausible binding mode hypothesis verified by docking and molecular dynamics simulations.

## KEYWORDS

flupirtine, KCNQ,  $K_{V7}$ , nicotinamide, retigabine

## 1 | INTRODUCTION

$K_{V7}$  (KCNQ) channels are homo- or heterotetrameric, voltage-gated potassium channels expressed in various tissues,<sup>[1]</sup> whereby especially heterotetrameric neuronal  $K_{V7}$  channels predominantly composed of  $K_{V7.2}$  and  $K_{V7.3}$  subunits are validated pharmacological targets.<sup>[2]</sup> In general,  $K_{V7}$  activation induces hyperpolarization of cell membranes, through which the ion channels contribute to controlling neuronal excitability. By increasing the action potential threshold<sup>[3]</sup> and medium afterhyperpolarization while reducing spike frequency,<sup>[4]</sup>  $K_{V7}$  channels act as a “brake” for hyperexcitability.<sup>[5]</sup> Moreover, their

opening probability can be influenced by small-molecule ligands,<sup>[6]</sup> making them attractive therapeutic targets, particularly for a range of neurological diseases.<sup>[5]</sup>

For example, the administration of  $K_{V7}$  channel openers was recently discussed for the therapy of various forms of brain damage, including chronic stress-induced brain injury (CSBI) as well as traumatic brain injury (TBI), for which currently no pharmacotherapeutic treatment options exist. In both cases, animal models suggest that reducing the underlying neuronal hyperexcitability by enhancing  $K_{V7}$ -mediated potassium currents might offer a protective effect. Thus,  $K_{V7}$  channel activation may be a novel therapeutic intervention

This is an open access article under the terms of the Creative Commons Attribution License, which permits use, distribution and reproduction in any medium, provided the original work is properly cited.

© 2022 The Authors. *Archiv der Pharmazie* published by Wiley-VCH GmbH on behalf of Deutsche Pharmazeutische Gesellschaft.

strategy against post-TBI and CSBI brain damage.<sup>[7]</sup> Furthermore, a recent review by Costi et al. examined the promising potential of K<sub>v</sub>7 channel openers as novel antidepressants and concluded that existing preclinical and clinical studies provide initial evidence of a significant antidepressant effect.<sup>[8]</sup> Consequently, their conclusions support the conduct of larger randomized controlled clinical trials to validate the potential of K<sub>v</sub>7 channel openers as a treatment option for depressive disorders. These overall encouraging results are somewhat clouded by the fact that following the withdrawal of flupirtine (**1**, Figure 1) and retigabine (**2**, USAN: ezogabine) due to adverse drug reactions, no specific and safe K<sub>v</sub>7 channel opener is currently available for therapeutic use in humans, which may hamper further development of this class of drugs as potential TBI/CSBI therapeutics or antidepressants.

Moreover, the failure of the two established drugs with their unique mechanism of action also leaves the desire for a replacement in the clinically validated indications of pain<sup>[9]</sup> and epilepsy.<sup>[10]</sup> For example, in the case of K<sub>v</sub>7.2-related epilepsy due to loss-of-function variants, the use of K<sub>v</sub>7 channel openers proved indispensable. As a result, there are currently calls for the reintroduction of retigabine for personalized treatment, despite its side effects that led to a withdrawal decision.<sup>[11]</sup> A therapeutic gap with worrying consequences also remained in the field of pain therapy since metamizole, despite its known association with blood dyscrasias, is increasingly used in Germany as a substitute for flupirtine, which has led to a growing number of metamizole-induced neutropenia cases.<sup>[12]</sup> Against this background, there is an urgent need for a safe replacement for flupirtine and retigabine to close the existing therapeutic gaps and enable the expansion of the therapeutic potential of K<sub>v</sub>7 channel openers.

The reasons for the failure of flupirtine and retigabine have been analyzed in detail in our previous work.<sup>[13,14]</sup> In essence, the adverse drug reactions responsible for withdrawal, particularly hepatotoxicity with flupirtine<sup>[15]</sup> and discoloration of the skin and ocular tissues with retigabine,<sup>[16]</sup> seem not related to the activation of K<sub>v</sub>7 channels. Rather, they are most likely attributed to the oxidation-sensitive triaminoraryl scaffold both drugs have in common. As depicted in Figure 1, clear evidence points to the oxidative formation of reactive

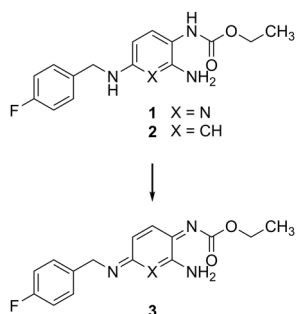


**FIGURE 1** Structures of flupirtine (**1**), retigabine (**2**), and their elusive *para* quinone diimine or azaquinone diimine oxidation products (**3**). *Ortho* quinone diimines or azaquinone diimines are also conceivable but not shown.

quinone diimine or azaquinone diimine metabolites such as **3** as the underlying cause of the adverse reactions in both cases.<sup>[17,18]</sup> Consequently, a possible approach to obtain safer replacements of flupirtine and retigabine is to screen for entirely new chemotypes, as done in the case of the very recently published compound ZK-21 (**8**, Figure 2), which has a 4-aminotetrahydroquinoline scaffold.<sup>[19]</sup> Moreover, the novel dual-mechanism K<sub>v</sub>7 channel opener GRT-X (**7**) that activates both K<sub>v</sub>7 potassium channels and the mitochondrial translocator protein (TSPO) likewise has no noteworthy structural similarities with the triaminoraryl type K<sub>v</sub>7 channel openers.<sup>[20]</sup> Hence, new chemotypes such as **7** or **8** could represent a conceivable way to prevent the adverse effects that are presumably closely linked to the metabolically and chemically labile structure of flupirtine and retigabine. However, radical structural changes also increase the risk of unexpected new toxicities, as in the case of PF-04895162, a structural distinct K<sub>v</sub>7 channel opener that was found to disrupt bile acid homeostasis and thus failed in phase I clinical trials.<sup>[21]</sup>

A more conservative but straightforward approach to obtain safer K<sub>v</sub>7 channel openers is to conduct minor structural changes in a ligand-based design. Such strategies have led to analogs with potent K<sub>v</sub>7 opening activity like HN37 (**4**) or the retigabine analog **5**. Although both compounds demonstrated improved chemical stability compared to retigabine, their design does not entirely exclude the formation of quinone diimine oxidation products as it still includes a *para* diaminobenzene and a triaminobenzene structural motif, respectively.<sup>[22]</sup>

Recently, our group also reported a ligand-based strategy, which in contrast to the approaches mentioned above, focused on completely avoiding structural motifs liable to quinoid metabolite formation. For this purpose, the substitution pattern of the central aromatic core of flupirtine and retigabine was redesigned.<sup>[23]</sup> In

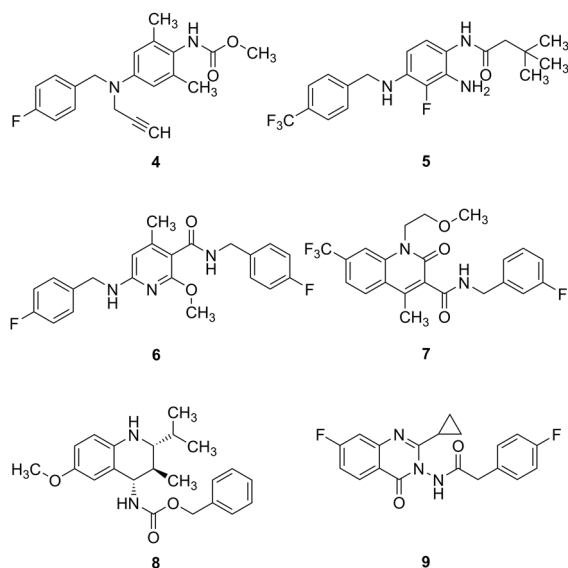


**FIGURE 2** Selection of recently published K<sub>v</sub>7 channel openers with scaffolds related to flupirtine and retigabine (**4–6**) and structurally distinct compounds with new chemotypes (**7–9**).

short, the oxidation-sensitive triaminoaryl structure was transformed into a nicotinamide scaffold without ortho/para-positioned nitrogen or oxygen atoms. However, further structural changes were necessary to maintain an acceptable  $K_{V7.2/3}$  opening activity, such as the introduction of an additional methyl group together with a benzylic amide side chain. The resulting compound **6** demonstrated good  $K_{V7.2/3}$  opening activity with an  $EC_{50}$  value of  $0.310 \mu\text{M}$ , hence ranging between flupirtine and retigabine in terms of potency. Unfortunately, due to its lipophilic character ( $\log D_{7.4} = 4.1$ ) and low fraction of  $sp^3$  hybridized carbon atoms, the compound proved to be poorly soluble in water, which limited the toxicity testing and, thus, requires additional structural optimization. To overcome this shortcoming of analog **6** and further improve the  $K_{V7.2/3}$  opening activity, a hybridization approach was intended, using the water-soluble and highly potent analog **10** ( $EC_{50} = 0.011 \mu\text{M}$ ) as a hybridization partner, which, however, is not devoid of the risk of azaquinone diimine formation (Figure 3).<sup>[24]</sup> To anticipate a selected result of the biological testing, the hybridization product **18a** showed promising  $K_{V7.2/3}$  channel opening activity and thus served as a starting point for further structural modifications. For this purpose, the structure of **18a** was divided into five zones (Figure 3a–e), each of which was subjected to substitution with selected structural elements to investigate structure–activity relationships, shed light on a possible binding mode, and further improve the  $K_{V7.2/3}$  opening activity. Particular 6-morpholinonicotinamides such as **18a** have been previously described in a patent by Grünenthal.<sup>[25]</sup> Still, a comprehensive description of the underlying SARs and a basic toxicological characterization were lacking and could be provided by this study. In addition, we expanded the existing work to include new substituents not previously considered, some of which may not be covered by the referenced patent.

## 2 | RESULTS AND DISCUSSION

### 2.1 | Chemistry

In the first step, the above-mentioned hybridization product **18a** and analogous compounds derived from it with modifications predominantly located in zones A and E were synthesized. The conducted structural changes in zone A were primarily aimed at elucidating the role of the morpholine ring in molecular recognition by the  $K_{V7.2/3}$  binding site. For this reason, the morpholine ring was replaced by carba analogs to help elucidate the possible role of the morpholine nitrogen atom. In particular, a tetrahydro-2H-pyran ring, a 3,6-dihydro-2H-pyran substituent, and a pyridin-4-yl residue were considered as morpholine replacements by synthesizing analogs **17**, **20**, and **21** (Scheme 1). In general, while the morpholine ring is deemed a privileged structure with advantageous physicochemical, biological, and metabolic properties,<sup>[26]</sup> in rare cases, it can be oxidized to reactive and potentially toxic iminium metabolites, as described for the multiple receptor tyrosine kinase inhibitor foretinib (not shown).<sup>[27]</sup> Consequently, the carba analogs **17**, **20**, and **21** also represent alternatives that do not possess this potential metabolic liability. In addition, the strategy of substituting a heteroatom for a methine or methylene group was also applied by synthesizing the piperidine derivative **18e**. Moreover, an attempt was made to further improve the water solubility of the analogs by reducing the compound lipophilicity. For this reason, a 2-oxa-6-azaspiro[3.3]heptane moiety was investigated in the case of analog **18f**. This bioisosteric replacement for a terminal morpholine ring had been shown to lower the lipophilicity of a corresponding molecule effectively.<sup>[28]</sup>

Regarding zone E, different strategies were followed. First, an additional effort was made to improve the aqueous solubility of the

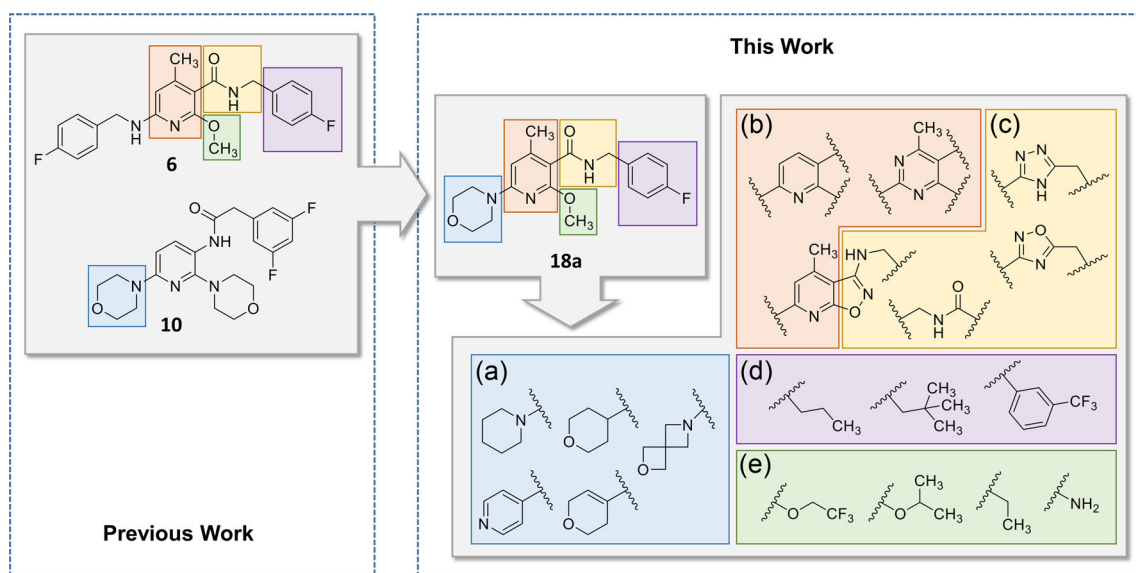
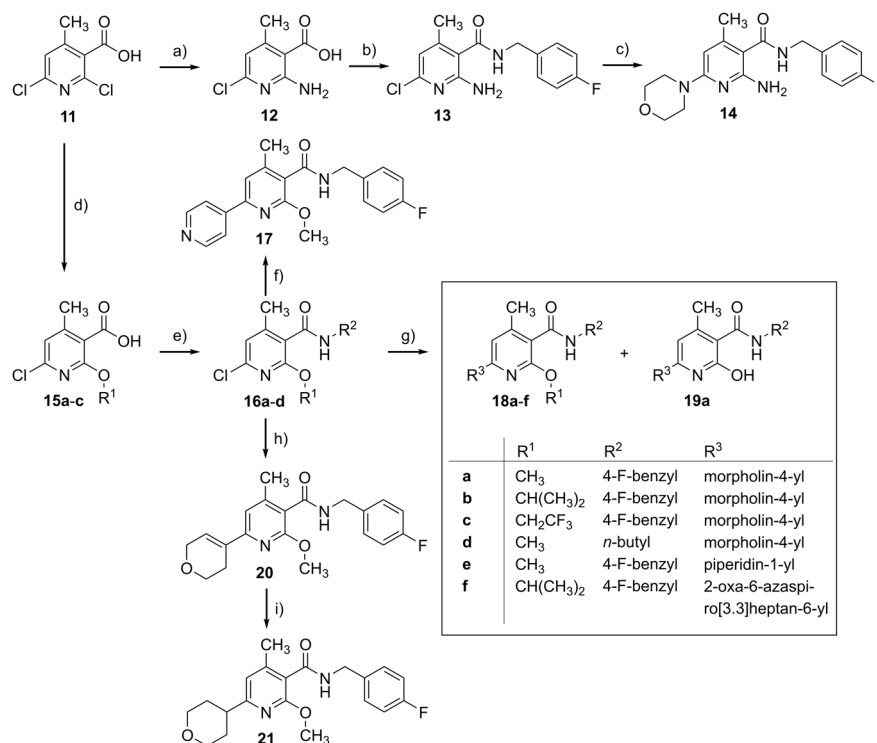


**FIGURE 3** Recently published  $K_{V7.2/3}$  openers **6** and **10**, the hybridization approach conducted in this work, yielding analog **18a**, and further structural modifications.



**SCHEME 1** Synthesis of nicotinamide analogs **14–21** with modifications in zones (a), (d), and (e). Reagents and conditions: (a) NaN<sub>3</sub>, K<sub>2</sub>CO<sub>3</sub>, CuI, ethane-1,2-diamine, EtOH, Ar, reflux, 28 h, 54%; (b) 1. CDI, THF, 50°C, 1 h, 2. 4-fluorobenzylamine, THF, rt, 12 h, 35%; (c) morpholine, NMP, 165°C,  $\mu$ W irradiation, 1 h, 73%; (d) appropriate alcohol, NaH, THF, 0°C–70°C, 7–23 h, 96%–99%; (e) 1. (COCl)<sub>2</sub>, DMF, DCM, 0°C–rt, 3 h, 2. amine, TEA, DCM, 0°C–rt, 16 h, 49%–61%; (f) pyridin-4-ylboronic acid, Pd(PPh<sub>3</sub>)<sub>4</sub>, Na<sub>2</sub>CO<sub>3</sub>, 1,4-dioxane, H<sub>2</sub>O, Ar, 140°C,  $\mu$ W irradiation, 0.5 h, 59%; (g) amine, NMP, 165°C, 0.5–1 h, 28%–53%; (h) 1-cyclohexeneboronic acid pinacol ester, Pd(PPh<sub>3</sub>)<sub>4</sub>, Na<sub>2</sub>CO<sub>3</sub>, 1,4-dioxane, H<sub>2</sub>O, Ar, 140°C,  $\mu$ W irradiation, 15 min, 86%; (i) H<sub>2</sub>, Pd/C, MeOH, rt, 5 h, 74%.

analogues by reintroducing the primary amino group from flupirtine and retigabine in analog **14**. Although the amino group, as a single ortho substituent of the amide function, led to inactive nicotinamide or benzamide analogues in our previous work, it has not yet been evaluated in combination with the advantageous ortho methyl group, which was also able to reconstitute the lost activity in the case of methoxy-substituted compounds such as **6**.<sup>[23]</sup> Second, a different approach was aimed at improving the K<sub>V7.2/3</sub> opening activity by varying the alkoxy residues. As described in our recent publication, the docking of **6** in combination with conformational analysis indicated that the methoxy group, together with the ortho methyl substituent, causes a favorable dihedral angle of the amide function.<sup>[23]</sup> By synthesizing analogues **18b** and **18c**, it was investigated whether bulkier alkoxy substituents may further enhance the beneficial effect on K<sub>V7.2/3</sub> opening by increasing steric interactions and rotational energy barriers.

The initial series of nicotinamide derivatives was synthesized starting from 2,6-dichloro-4-methylnicotinic acid (**11**), whereby various substituents were introduced in position 2 of the pyridine ring in the first reaction step (Scheme 1). In particular, an amino group was attached via a copper-catalyzed Ullmann-type reaction by using sodium azide as a nitrogen source to obtain aminopyridine **12**. According to Zhao et al., the reaction is supposed to proceed via an intermediate azidopyridine (not shown), which is reduced directly in

situ to the corresponding primary amine **12**.<sup>[29]</sup> In contrast, the introduction of alkoxy substituents, yielding **15a–c**, was performed via simple nucleophilic substitution reactions. The alcoholate, which served as the nucleophile, was generated in situ by reacting the corresponding alcohol with sodium hydride. Both reactions to introduce substituents at position 2 of the pyridine ring proceeded regioselectively at this specific position. The reason for the regioselectivity is probably a directing effect of the carboxyl function of **11**, which in both cases forms cyclic, five- or six-membered transition states, respectively, involving either a sodium alcoholate or a copper azide complex.<sup>[29,30]</sup>

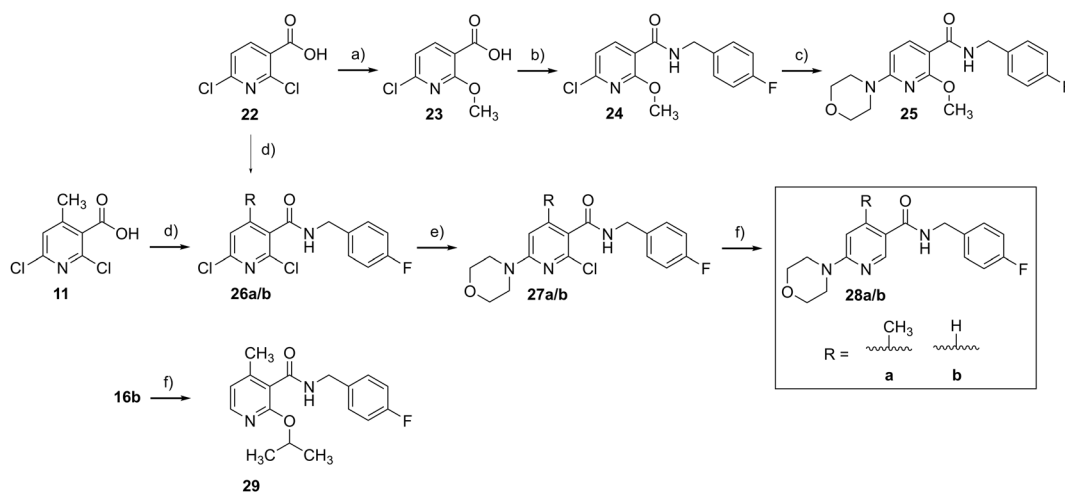
After introducing substituents at position 2 of the pyridine ring, the amide coupling allowed for the synthesis of all analogues. The activation of the nicotinic acid derivatives was performed either, as in the case of amino nicotinic acid derivative **12**, via the formation of an acyl imidazole after reaction with CDI or via generation of acyl chlorides in a DMF-catalyzed reaction with oxalyl chloride carried out in the case of **15a–c**. Both activated carboxylic acid species (not shown) were reacted directly, without prior isolation, with the corresponding amines to give the desired amides **13** and **16a–d**.

To introduce a substituent at position 6 of the pyridine ring, two different methods were principally applied. C–C bonds were formed via Suzuki coupling reactions by using the corresponding boronic acid or boronic acid pinacol ester to yield compounds **17** and **20**. The

tetrahydropyran substituent in the case of analog **21** was obtained by catalytic hydrogenation of the dihydropyran precursor **20**. In contrast, the introduction of amino substituents at position 6 in the case of compounds **18a–f** was not carried out with a palladium catalyst but by nucleophilic substitution reactions, which were performed by microwave-assisted heating. In the case of all methoxy-substituted compounds (**18a, d, e**), a by-product was formed, causing low yields of the desired products. In the synthesis of compound **18a**, it was isolated and identified as the demethylated analog **19a**. Contrary to a methoxy residue, a 1-methyl-ethoxy and a 2,2,2-trifluoroethoxy substituent incorporated in compounds **18b/c** were stable under identical reaction conditions. 2-Oxa-6-azaspiro [3.3]heptane oxalate required for synthesizing the spiro analog **18f** was prepared in a two-step synthesis according to a protocol described in the literature (not shown).<sup>[31]</sup> Briefly, 4-methylbenzenesulfonamide was reacted with pentaerythritol tri-bromide to generate the spiro partial structure in a double-ring closure reaction. In the second step, the tosyl protective group was cleaved reductively with magnesium, and the resulting amine was precipitated as an oxalate salt. In the synthesis of compound **18f**, the free amine was released from its salt in situ by adding the stronger base DBU to the reaction mixture.

Since the pronounced structural change from a 4-fluorobenzylamino residue in **6** to a morpholino substituent in **18a** was possible without significantly affecting the activity, the question of the pharmacophore arises. Analog **29** (Scheme 2) was synthesized to clarify whether the morpholine ring is part of the core pharmacophore or, on the contrary, molecular recognition might even be possible without a morpholine ring. Analogously, derivatives **25** and **28a/b** were synthesized in which the methyl group or the alkoxy group were missing to clarify the role of the specific substituents, thus testing our hypothesis that ortho disubstitution of the amide group might be essential for  $K_{v7.2/3}$  opening activity of nicotinamide analogs.

In general, nicotinamide derivatives with missing substituents in positions 2, 4, or 6 of the pyridine ring were prepared by synthetic routes similar to those of the nicotinamide analogs **18a–f** mentioned above. The synthesis of the nor-analog **25** was performed analogously to the synthesis of **18a** with the difference that 2,6-dichloronicotinic acid (**22**) was used as starting material instead of 2,6-dichloro-4-methylnicotinic acid (**11**). The amide coupling in the second reaction step to obtain **24** was done by using the coupling reagents DIC and HOBt (Scheme 2). In the case of the analogs **28a/b**, in which the substituents in position 2 or positions 2 and 4 are absent, the introduction of the methoxy group in the first step was skipped. After the amide coupling, yielding **26a/b**, the substitution reaction to introduce the morpholino substituent was carried out, which in this case required less drastic reaction conditions compared to the synthesis of analogs **18a–f**. Conventional heating to 80°C instead of microwave-assisted heating to 165°C proved sufficient. Since two chloro substituents were accessible for the reaction, a mixture of two regioisomers was formed and subsequently separated by silica gel column chromatography to obtain the desired morpholino nicotinamides **27a/b** and their corresponding regioisomers (not shown). Analytical discrimination of the regioisomers by NMR was not possible at this stage. However, after reductive cleavage of the chloro substituent in the following reaction step, confirmation of the identity of the desired analogs **28a/b** based on <sup>1</sup>H-NMR spectroscopy was possible by analyzing the pyridine proton signals. In the case of **28a**, two singlets were observed, unequivocally confirming the morpholino substituent in position 6 of the pyridine ring. The same applies to **28b**, where a doublet with <sup>3</sup>J coupling (9.0 Hz), a doublet with <sup>4</sup>J coupling (2.5 Hz), and a doublet of doublets (*J* = 9.0, 2.5 Hz) verify the desired 6-morpholino nicotinamide structure while excluding morpholino substitution at position 2. Analogously, the chloro substituent of compound **17b** was cleaved following the same catalytic hydrogenation procedure to obtain analog **29**, which lacks a substituent in zone A.



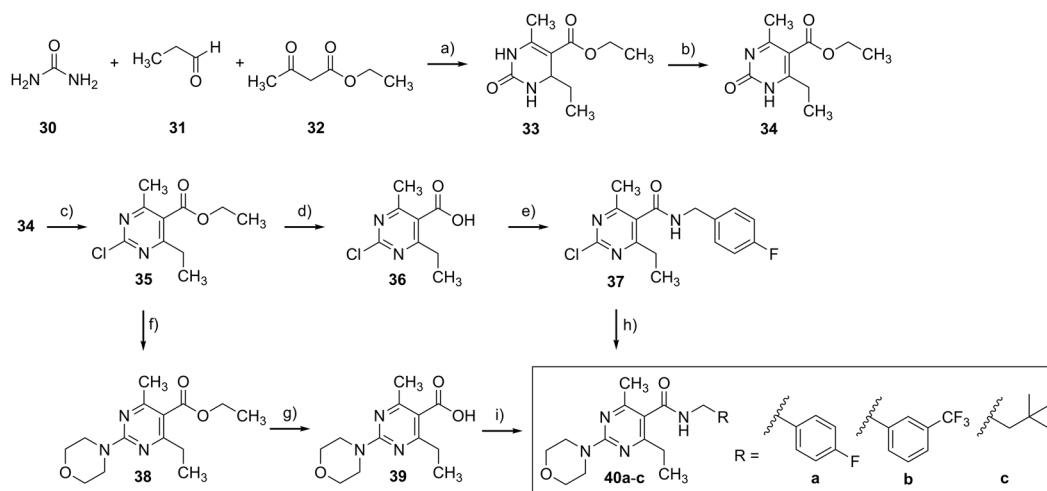
**SCHEME 2** Synthesis of nicotinamide analogs **25**, **28a/b**, and **29** lacking selected substituents of the central pyridine ring. Reagents and conditions: (a) MeOH, NaH, THF, 0°C–70°C, 7 h, 79%; (b) 4-fluorobenzylamine, DIC, HOBt, DMF, rt, 16 h, 65%; (c) morpholine, NMP, 165°C,  $\mu$ W irradiation, 30 min, 36%; (d) 4-fluorobenzylamine, DIC, HOBt, DMF, rt, 16 h, 46%–86%; (e) morpholine, MeOH or 2-propanol, reflux, 1–3 d, 23%–26%; (f) H<sub>2</sub>, Pd/C, TEA, MeOH, rt, 2–5 h, 64%–66%.

Regarding zone B, a replacement of the central pyridine ring of the nicotinamide scaffold with a pyrimidine ring could be an interesting structural change since various examples exist where this bioisosteric exchange led to improved biological activity on different targets.<sup>[32]</sup> In analogy to these literature cases, a pyrimidine ring with its altered electronic properties and reduced basicity may also influence the ligand binding to  $K_{V7.2/3}$  channels. The envisioned pyrimidine analogs were accessible via the Biginelli multicomponent reaction, which in its original form, however, does not provide access to alkoxy-substituted compounds. For this reason, the resulting analogs **40a-c** contain an ethyl group instead of a methoxy substituent in zone E.

The initial Biginelli reaction, which involved an acid-catalyzed cyclocondensation of ethyl acetoacetate (**32**), propionaldehyde (**31**), and urea (**30**), yielded the 3,4-dihydropyrimidin-2(1H)-one **33**, which was converted into the corresponding pyrimidin-2(1H)-one **34** in a subsequent oxidation step with nitric acid (Scheme 3). The following chlorination was carried out according to a modified procedure of Zhao et al. by heating **34** in excess phosphoryl chloride.<sup>[33]</sup> In the course of the reaction, the 3,4-dihydropyrimidin-2(1H)-one **34** probably forms an intermediate dichlorophosphate (not shown), as it was suggested for the chlorination of related quinazolin-4(3H)-ones.<sup>[34]</sup> Subsequently, the dichlorophosphate was attacked by a chloride ion in an  $S_NAr$  reaction, yielding the chloropyrimidine **35**. The additional use of a base such as triethylamine, sometimes described in the literature for similar reactions,<sup>[35]</sup> has been evaluated but did not result in an improved yield. After the chlorination, two different synthetic routes were investigated. For the synthesis of analog **40a**, the ethyl ester function of **35** was hydrolyzed under alkaline conditions, which gave the corresponding carboxylic acid **36**. This was followed by a coupling reaction with HATU yielding amide **37**. In the final step, the morpholino substituent was introduced by applying the same microwave-assisted method used for the nicotinamides to obtain the final

analog **40a**. For the entire six-step synthesis of **40a**, a poor cumulative yield of only 2.8% was calculated. In retrospect, the ester hydrolysis in the first reaction step has proven particularly unfavorable because the yield was reduced by an undesired by-product. The side product was not isolated, but the chloropyrimidine structure of **35** was suspected to be affected by the alkaline hydrolysis leading to a pyrimidinone by-product. For this reason, the reaction sequence was rearranged, resulting in an alternative synthetic route for analogs **40b/c**. In particular, compared to the synthesis of **40a**, the morpholino substituent was introduced first to give compound **38**, while the hydrolysis of the ethyl ester to obtain carboxylic acid **39** took place in the following step since hydrolysis of the chloropyrimidine structure is thus not a concern. Overall, the modified reaction sequence and the use of DIC and HOBt instead of HATU as amide coupling reagents in the last step to obtain the final amides **40b/c** enabled an improved cumulative yield of 7.7%.

The carbamate partial structure of retigabine is supposedly involved in the formation of hydrogen bonds to the  $K_{V7.2}$  binding site, which is also conserved in the case of nicotinamide derivative **6** as predicted by molecular docking.<sup>[23,36]</sup> Apart from that, mainly hydrophobic interactions contribute to the binding of compound **6**. Accordingly, the particular importance of the amide group can be anticipated, which was further explored by variation of the amide partial structure following three different approaches. The first structural change attempted in this direction was to replace the amide function with bioisosteric cyclic amide mimetics such as a 1,2,4-oxadiazole or a 1,2,4-triazole ring, resulting in analogs **47** and **54**. A similar approach was recently used successfully in the optimization of a GPR88 agonist (not shown), where an amide bioisosteric replacement with a variety of azoles, followed by lead optimization, provided a potent and efficacious triazole-based GPR88 agonist.<sup>[37]</sup> The second strategy was the incorporation of an amide-like structure into a fused ring system. Here, the isoxazolo[5,4-*b*]pyridin-3-amine **44** was synthesized, representing a conformationally restricted



**SCHEME 3** Synthesis of pyrimidine analogs **40a-c**. Reagents and conditions: (a) AcOH, EtOH, 90°C, 20 h, 32%; (b) HNO<sub>3</sub>, H<sub>2</sub>O, -10°C, 15 min, 87%; (c) POCl<sub>3</sub>, 110°C, 1 h, 45%; (d) KOH, H<sub>2</sub>O, THF, rt, 12 h, 72%; (e) 4-fluorobenzylamine, HATU, DIPEA, DMF, rt, 16 h, 42%; (f) morpholine, EtOH, 80°C, 2 h, 90%; (g) KOH, EtOH, H<sub>2</sub>O, 80°C, 4 h, 84%; (h) morpholine, NMP, 165°C,  $\mu$ W irradiation, 20 min, 73%; (i) amine, DIC, HOBt, DMF, rt, 16 h, 79%–81%.

analog. A comparable approach yielded, for example, highly potent benzo[d]isoxazol-3-amine-based sEH inhibitors with single-digit nanomolar IC<sub>50</sub> values from a benzamide lead structure.<sup>[38]</sup> The third structural change carried out in this context was a shift of the amide group realized by transforming the *N*-benzylnicotinamide **18a** to the *N*-(pyridin-3-ylmethyl) benzamide analog **49**; thus altering the hydrogen-bonding ability as well as the flexibility and conformation in this part of the scaffold.

The synthesis of the isoxazolo[5,4-*b*]pyridin-3-amine analog **44** as a cyclic and conformationally restricted nicotinamide replacement could be realized in three steps (Scheme 4). The starting point was 2,6-dichloro-4-methylnicotinonitrile (**41**), whose chloro substituent in position 6 was replaced by a morpholino residue through nucleophilic substitution. The reaction proceeded regioselectively with a preference for position 6, as reported by Antczak et al.<sup>[39]</sup> Nevertheless, a small amount of the regioisomer substituted at position 2 was formed. The mixture of the two resulting regioisomers was separated by chromatography, and the desired regioisomer **42** was cyclized to afford the corresponding isoxazolo[5,4-*b*]pyridin-3-amine **43** by reaction with acetohydroxamic acid. This method involved a convenient one-pot procedure where the *ortho* chloro nicotinonitrile forms an *N*-[(3-cyanopyridin-2-yl)oxy]acetamide intermediate after nucleophilic substitution of the chloro substituent with a hydroxamate anion, followed by in situ base-catalyzed intramolecular cyclization and subsequent elimination of the acetyl residue.<sup>[40]</sup> By reacting the amino group of compound **43** with 4-fluorobenzaldehyde, an imine (not shown) was formed in the last reaction step, which was reduced to the corresponding secondary amine without prior isolation by hydrosilylation with triethylsilane and trifluoroacetic acid to obtain the final analog **44**.

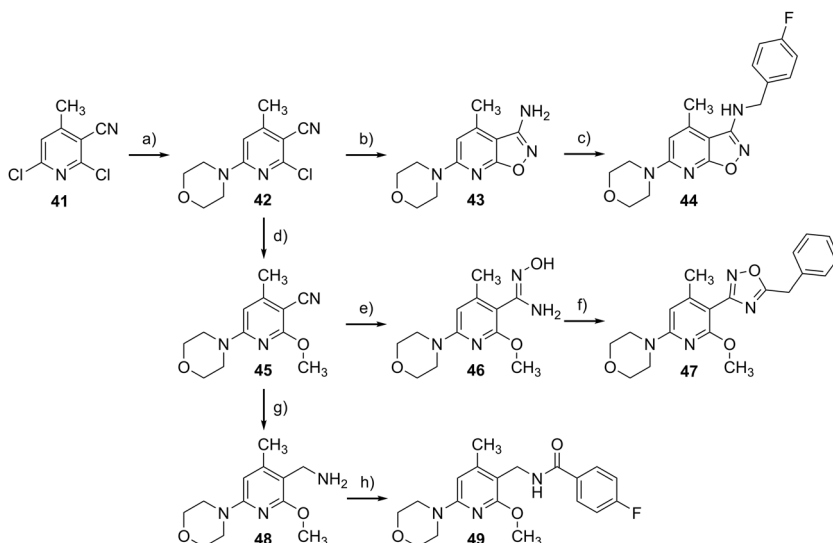
The synthesis of the oxadiazole derivative **47** began with the above-mentioned compound **42** (Scheme 4). In the first step, a methoxy group was introduced by substituting the remaining chloro substituent with sodium methoxide. The nitrile function of the resulting compound **45** was then converted to the corresponding amidoxime **46** by treatment with an aqueous solution of hydroxylamine. This reaction required an unusually long time (4 days) for

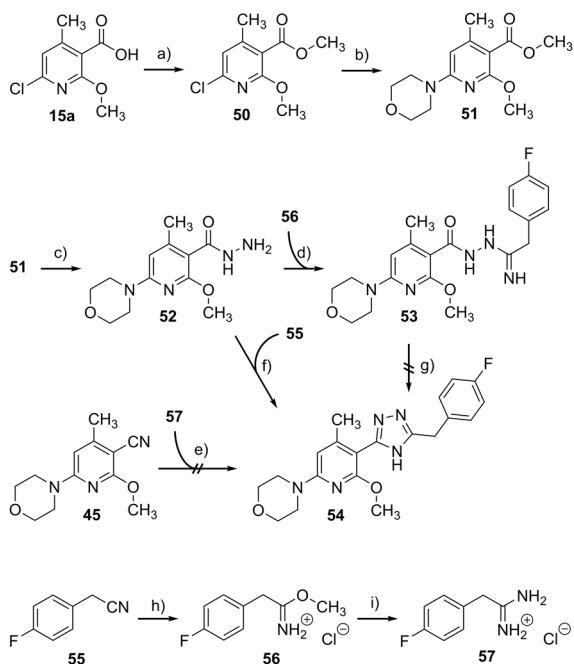
complete conversion, which is presumably attributed to the ortho-disubstitution of the nitrile function and the resulting restricted steric accessibility. The electron-donating properties of the morpholino and methoxy substituents may also have reduced the reactivity of the nitrile function for nucleophilic attack by hydroxylamine. While most syntheses of oxadiazoles reported in the literature proceed via amidoxime precursors such as **46**, the methods differ in the use of diverse activated carboxylic acid derivatives as acylating agents and in the reaction conditions applied for ring closure.<sup>[41]</sup> In this particular case, the amidoxime **46** was acylated with phenylacetyl chloride. The corresponding acylation product (not shown) was not isolated, but a ring closure was induced directly by the addition of tetrabutylammonium fluoride (TBAF) as a catalyst. Mechanistically, the ring closure reaction of the *O*-acyl amidoxime intermediate to the final oxadiazole analog **47** is supposed to proceed via an intramolecular attack of the amidoxime nitrogen atom on the carbonyl carbon atom of the acyl group, followed by dehydration of the resulting dihydro-oxadiazolol. Both steps are facilitated by TBAF, whose fluoride ion acts as a strong base in polar aprotic solvents such as THF.<sup>[42]</sup>

The *N*-(pyridin-3-ylmethyl)benzamide analog **49** with a shifted carbonyl group compared to the initial nicotinamide scaffold was synthesized from the nicotinonitrile **45** in two steps. First, the nitrile group of **45** was reduced by catalytic hydrogenation with Raney nickel as a catalyst to obtain the primary amine **48**. Then, in the second step, **48** was acylated by reaction with 4-fluorobenzoyl chloride, yielding the final analog **49**.

The above-mentioned nicotinic acid derivative **15a** was also used as a starting point for synthesizing the triazole derivative **54** (Scheme 5). In the first step, the corresponding methyl ester **50** was obtained by alkylation of **15a** with iodomethane. This was followed by substituting the chlorine atom of **50** to afford the morpholino derivative **51**, whose methyl ester function was subjected to hydrazinolysis yielding the hydrazide **52**. The following triazole formation proved problematic since two attempts to achieve a ring closure reaction were initially unsuccessful. The first approach

**SCHEME 4** Synthesis of analogs **44**, **47**, and **49** with modifications in zone C. Reagents and conditions: (a) morpholine, MeOH, 0°C–rt, 16 h, 70%; (b) acetohydroxamic acid, *t*-BuOK, Ar, DMF, RT–50°C, 5.5 h, 43%; (c) 4-fluorobenzaldehyde, (C<sub>2</sub>H<sub>5</sub>)<sub>3</sub>SiH, TFA, DCM, RT–60°C, 25 h, 80%; (d) NaOMe, MeOH, reflux, 24 h, 90%; (e) hydroxylamine (aq.), EtOH, reflux, 4 d, 99%; (f) 1. 2-phenylacetyl chloride, TEA, DCM, 0°C, 1 h, 2. TBAF, THF, rt, 2 h, 36%; (g) Ni, H<sub>2</sub>, NH<sub>3</sub>, MeOH, 50°C, 5 h, 71%; (h) 4-fluorobenzoyl chloride, TEA, DCM, rt, 16 h, 64%.





**SCHEME 5** Synthesis of the 1,2,4-triazole analog **54**. Reagents and conditions: (a)  $\text{CH}_3\text{I}$ ,  $\text{K}_2\text{CO}_3$ , DMF, rt, 8 h, 98%; (b) morpholine, TEA, NMP,  $90^\circ\text{C}$ , 2 d, 39%; (c)  $\text{N}_2\text{H}_4 \times \text{H}_2\text{O}$ , MeOH, reflux, 24 h, 67%; (d) NaOMe, MeOH,  $0^\circ\text{C}$ –rt, 24 h, 47%; (e)  $\text{CuBr}$ ,  $\text{Cs}_2\text{CO}_3$ , DMSO,  $120^\circ\text{C}$ , 24 h; (f)  $\text{K}_2\text{CO}_3$ , *n*-BuOH,  $150^\circ\text{C}$ ,  $\mu\text{W}$  irradiation, 4 h, 47%; (g)  $220^\circ\text{C}$ , 0.1 mbar, 10 min; (h) HCl, MeOH,  $0^\circ\text{C}$ , 3 h, 58%; (i)  $\text{NH}_3$ , MeOH, rt, 24 h, 61%.

was based on the reaction of hydrazide **52** with the Pinner salt **56** to give the *N'*-(1-iminoalkyl)-hydrazide **53**. According to the literature, ring closure to obtain the triazole structure should occur by heating compounds like **53** to the melting point under reduced pressure without solvent.<sup>[43]</sup> However, in this particular case, the procedure provided a complex mixture of products with little, if any, yield of the desired product according to TLC reaction control. A second unsuccessful attempt was based on a copper-catalyzed tandem addition–oxidative cyclization reaction described by Ueda and Nagasawa.<sup>[44]</sup> Unfortunately, in this specific case, the reaction between nitrile **45** and amidinium salt **57**, previously prepared by ammonolysis of the Pinner salt **56**, did not lead to any product formation. Finally, the triazole synthesis succeeded by applying the method of Yeung et al., which includes a one-step, base-catalyzed condensation of the hydrazide **52** with 4-fluorobenzonitrile (**55**).<sup>[45]</sup>

## 2.2 | Pharmacology/biology/modeling

### 2.2.1 | Evaluation of $\text{K}_{\text{V}7.2/3}$ opening activity

The  $\text{K}_{\text{V}7.2/3}$  opening activity was determined by applying a commercially available assay on HEK293 cells that overexpress the heterotetrameric  $\text{K}_{\text{V}7.2/3}$  channel. The assay exploits the permeability of potassium channels for thallium ions and is based on a thallium-

sensitive fluorescent dye, which is trapped inside the cell after esterase cleavage. Thallium influx through  $\text{K}_{\text{V}7.2/3}$  channels generates a fluorescence signal whose intensity correlates with the extent of channel opening. Based on the data generated this way,  $\text{EC}_{50}$  values were calculated, indicating the concentration at which the half-maximum fluorescence signal and, thus, the half-maximum  $\text{K}_{\text{V}7.2/3}$  opening activity was achieved. In addition to  $\text{EC}_{50}$  values, the efficacy, that is, the maximum response, of the analogs relative to flupirtine was calculated. Both values can be found in Table 1 for all analogs. Based on these results, structure–activity relationships were derived, which are systematically discussed below.

Regarding zone A, the replacement of the 4-fluorobenzylamino residue of **6** with a morpholine ring in **18a** improved the biological activity as intended by the hybridization approach. In particular, the  $\text{EC}_{50}$  value of **18a** decreased compared to **6** from 0.310 to 0.117  $\mu\text{M}$ , and at the same time, the efficacy increased from 105% to 144%. However, the difference in potency does not appear to be significant, and the reported outstanding  $\text{K}_{\text{V}7.2/3}$  opening activity of the second hybridization partner **10** was not quite reached. In contrast, the complete deletion of a substituent in zone A resulted in a total loss of activity in the case of analog **29**, which clearly confirmed the morpholine ring as part of the core pharmacophore.

Both heteroatoms of the morpholino substituent, on the other hand, do not appear to be of essential importance for  $\text{K}_{\text{V}7.2/3}$  opening. This was evident in the case of the morpholine oxygen atom, where a replacement with a methylene group even led to improved  $\text{K}_{\text{V}7.2/3}$  opening. The corresponding piperidine derivative **18e** exhibited a 2.9-fold reduced  $\text{EC}_{50}$  value compared to the direct morpholino counterpart **18a**. This observation correlates with molecular docking results (Figure 4b,c), which predicted the morpholine ring to occupy a hydrophobic cavity with no involvement of the oxygen atom in any hydrogen bond interactions.

In contrast, when considering only the activity data, it was initially presumed that the morpholine nitrogen atom might contribute substantially to binding since the corresponding hydroxy analog **21**, bearing a tetrahydropyran ring, showed a considerably 20-fold decrease in potency compared to the direct morpholino congener **18a**. However, the dihydropyran derivative **20**, which also has a carbon atom in place of the morpholine nitrogen atom, was approximately as potent as **18a**. This observation, combined with molecular docking results displayed in Figure 4, in turn, rather implies that the tertiary amino group of the morpholine ring does not participate in direct interactions with the  $\text{K}_{\text{V}7.2/3}$  binding site but instead might favor an advantageous molecular geometry. Specifically, the morpholine nitrogen nonbonding pair of electrons interacts with the electron-deficient pyridine  $\pi$ -system and thus probably favors a coplanar conformation, which is also assumed to be probable for the dihydropyran moiety of **20** since the double bond is in conjugation with the adjacent pyridine ring. These conformational considerations were confirmed by quantum mechanical calculations using density functional theory (DFT), which revealed energetic minima at a dihedral angle of approximately  $0/180^\circ$  and high rotational energy barriers for a morpholino as well as a dihydropyran



**TABLE 1**  $K_V7.2/3$  channel opening activity, in vitro toxicity, and  $\log D_{7.4}$  values of the synthesized compounds **14–54** in comparison to flupirtine and retigabine<sup>[a]</sup>

Entry	$\log D_{7.4}$	HEK-293 EC <sub>50</sub> <sup>[b]</sup> ( $\mu\text{M}$ )	Efficacy (%)	TAMH LD <sub>50</sub> <sup>[c]</sup> ( $\mu\text{M}$ )	LD <sub>25</sub> <sup>[d]</sup> ( $\mu\text{M}$ )	HEP-G2 LD <sub>50</sub> <sup>[c]</sup> ( $\mu\text{M}$ )	LD <sub>25</sub> <sup>[d]</sup> ( $\mu\text{M}$ )	LD <sub>25</sub> /EC <sub>50</sub> <sup>[f]</sup>
Flu <sup>[g]</sup>	2.0	1.837 ± 0.844	100	487 ± 51	103 ± 47	547 ± 111	74 ± 40	40
Ret <sup>[g]</sup>	2.1	0.249 ± 0.052	134 ± 16	>400	>400	>400	269 ± 166	1080
<b>6</b> <sup>[g]</sup>	4.1	0.310 ± 0.119	105 ± 12	>63	>63	>16	>16	52
<b>10</b> <sup>[g]</sup>	3.6	0.011 ± 0.004	111 ± 7	>500	212 ± 140	>500	231 ± 141	19273
<b>14</b>	2.2	6.858 ± 1.319	113 ± 28	>500	349 ± 36	>500	123 ± 73	18
<b>17</b>	2.7	0.500 ± 0.105	112 ± 11	>63	>63	>63	26 ± 20	52
<b>18a</b>	3.0	0.117 ± 0.029	144 ± 11	>63	>63	>63	>63	539
<b>18b</b>	3.8	0.017 ± 0.009	132 ± 16	>31	>31	>31	15 ± 1	882
<b>18c</b>	3.3	0.012 ± 0.004	117 ± 19	>15	>15	>15	>15	1250
<b>18d</b>	2.6	3.799 ± 1.730	170 ± 4	>250	>250	>250	>250	66
<b>18e</b>	4.7	0.040 ± 0.007	127 ± 1	>31	>31	>31	32 ± 11	775
<b>18f</b>	3.8	- <sup>[e]</sup>	- <sup>[e]</sup>	>63	>63	>63	>63	-
<b>19a</b>	2.4	- <sup>[e]</sup>	- <sup>[e]</sup>	>63	30 ± 17	>63	28 ± 16	-
<b>20</b>	3.1	0.143 ± 0.003	111 ± 11	>125	>125	>63	>63	440
<b>21</b>	3.1	2.402 ± 0.759	129 ± 16	>125	>125	>125	>125	52
<b>25</b>	3.8	- <sup>[e]</sup>	- <sup>[e]</sup>	>125	77 ± 35	>125	75 ± 24	-
<b>28a</b>	2.4	8.632 ± 1.876	76 ± 19	>250	169 ± 29	>250	126 ± 36	15
<b>28b</b>	2.3	- <sup>[e]</sup>	- <sup>[e]</sup>	>125	>125	>125	>125	-
<b>29</b>	2.6	- <sup>[e]</sup>	- <sup>[e]</sup>	>125	13 ± 3	>125	>125	-
<b>40a</b>	3.0	0.126 ± 0.035	114 ± 10	>31	>31	>31	20 ± 12	159
<b>40b</b>	3.5	0.035 ± 0.028	104 ± 12	>31	>31	>31	>31	886
<b>40c</b>	3.4	2.134 ± 0.591	52 ± 11	>63	>63	>63	>63	30
<b>44</b>	3.2	- <sup>[e]</sup>	- <sup>[e]</sup>	>125	>125	>125	>125	-
<b>47</b>	4.7	1.179 ± 0.193	45 ± 4	>30	>30	>30	>30	25
<b>49</b>	3.6	- <sup>[e]</sup>	- <sup>[e]</sup>	>31	>31	>63	29 ± 5	-
<b>54</b>	3.3	2.245 ± 0.338	149 ± 25	>30	>30	>30	>30	13

Note: [a]  $\log D_{7.4}$  values were estimated by employing an HPLC-based method. HEK293 cells overexpressing the  $K_V7.2/3$  channel were used to obtain the EC<sub>50</sub> values by applying a fluorimetric assay. LD values were determined by an MTT assay in TAMH and HEP-G2 cell lines after 24 h of exposure. EC<sub>50</sub> and LD values are means of  $\geq 3$  independent determinations  $\pm$  standard deviations. [b] Necessary concentration to reach half-maximal  $K_V7.2/3$  channel opening activity. [c] Concentration required to reduce cell viability to 50% compared to untreated controls. [d] Concentration required to reduce cell viability to 75% compared to untreated controls. [e] No  $K_V7.2/3$  channel opening activity up to a concentration of 20  $\mu\text{M}$ . [f] The lower of both LD<sub>25</sub> values was used to calculate the LD<sub>25</sub>/EC<sub>50</sub> ratio. If no LD<sub>25</sub> value could be determined, the maximum tested concentration was used for calculation. [g] Previously published values.<sup>[14,23,24]</sup>

substituent (Figure 5a,d). In contrast, a twisted conformation is probably energetically preferred by the 2-(tetrahydro-2H-pyran-4-yl) pyridine moiety of **21** owing to the  $sp^3$  hybridized hydroxy carbon atom, as verified by the dihedral scanning plot, which shows a global minimum at 60° and low rotational energy barriers (Figure 5c). Viewed in correlation with the corresponding docking poses, which also indicate a coplanar orientation of the pyridine ring with the adjacent heterocyclic substituent, the different molecular geometries

suggest that the inferior  $K_V7.2/3$  opening activity of **21** compared to **18a** and **20** is mainly due to a conformational preorganization of **18a** and **20**, which may reduce the entropic costs of ligand binding.

Regarding the other zone A substituents, an aromatic residue, such as a pyridine ring in analog **17**, was also found to be tolerated since the incorporated biaryl structure is expected to favor a coplanar conformation, too (Figure 5e). However, despite the beneficial coplanarity, compound **17** was still 4.3-fold less potent than the

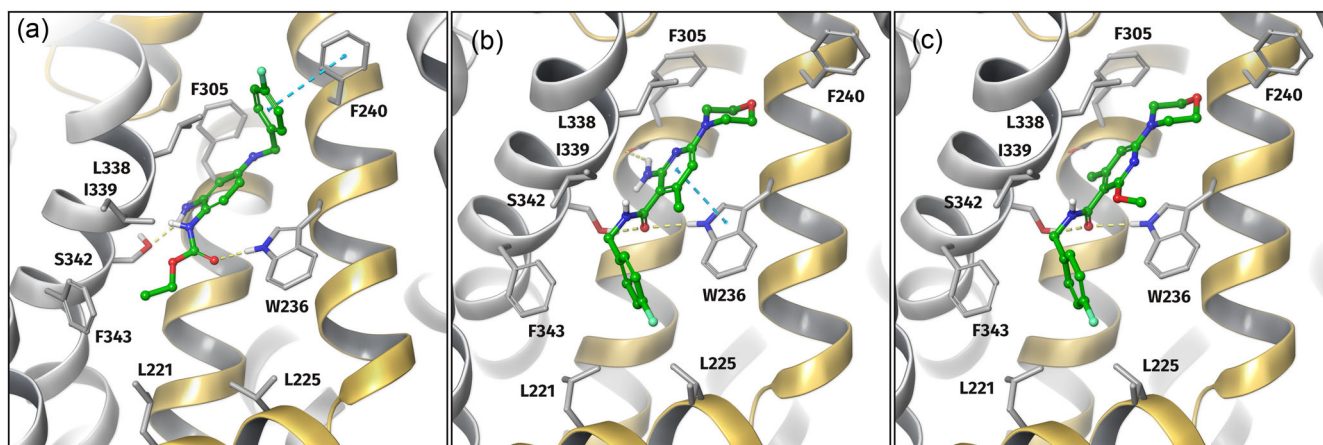


**FIGURE 4** Predicted binding poses of retigabine (a), **14** (b), and **18a** (c). The hydrogen bonds to W236 and S342 are maintained for all compounds, although the central pyridine ring is slightly displaced compared to retigabine. Therefore, the primary amino group of **14** does not participate in hydrogen bond formation with S342 as predicted for retigabine. Instead, it is shifted into a more hydrophobic cavity, which is also occupied by the methyl substituent of **18a**. The 4-fluorobenzyl group binds to a larger hydrophobic pocket formed by L221, L225, and F343 as previously reported for other derivatives.<sup>[23]</sup> The  $\pi$ - $\pi$  interactions to W236 (represented as blue dashed lines) can be observed for all three ligands during molecular dynamics simulations, depending on the distinct orientation of the aromatic rings. The color of the secondary structure elements represents the respective chains of Kv7.2 (gold) and Kv7.3 (silver) in the Kv7.2/3-heterotetramer.

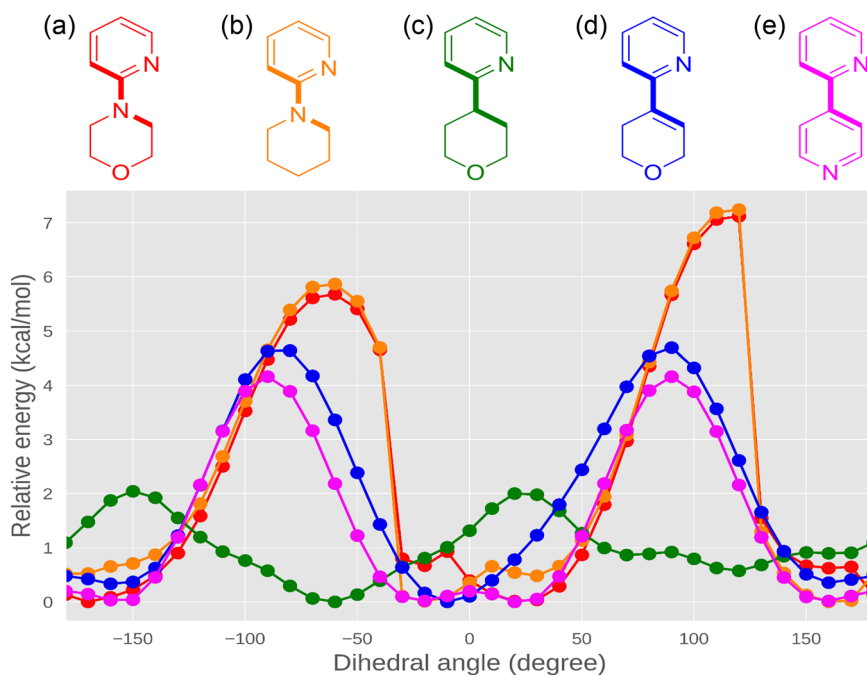


**FIGURE 5** Dihedral angle scanning for various pyridine scaffolds using B3LYP-D3/6-31G(d,p). The calculations were performed with Jaguar version 11.5 (Schrodinger, LLC, 2022).<sup>[46]</sup>

direct morpholino analog **18a**, but this may be attributed to other reasons, such as the flat and rigid geometry of the 4-pyridyl moiety, which deviates considerably from the chair conformation expected for a morpholine ring.<sup>[47]</sup> Consequently, this specific conformation of the morpholino substituent, which a pyridine substituent cannot adopt, might be required for good Kv7.2/3 channel opening since it is also observed in molecular dynamics simulations of corresponding analogs (Figure 4b,c).

Despite the presence of a tertiary amino partial structure as with a morpholino substituent, the spiro analog **18f** showed no Kv7.2/3

opening activity up to 20  $\mu$ M. Presumably, the 2-oxa-6-azaspiro[3.3]heptane substituent is slightly too long for an adequate fit into the Kv7.2/3 binding pocket since the distance between the nitrogen and the oxygen atom is 4.3  $\text{\AA}$  compared to 2.8  $\text{\AA}$  for morpholine.<sup>[28]</sup> Moreover, the substituent has a rather linear geometry and differs significantly from the chair conformation of morpholine, which is presumed to be favorable for Kv7.2/3 opening. Regarding physico-chemical properties, contrary to cases reported in the literature, the introduction of the 2-oxa-6-azaspiro[3.3]heptane substituent did not result in a decreased lipophilicity, as originally intended by this

structural change. Indeed, as with the corresponding morpholino substituted compound **18b**, the  $\log D_{7,4}$  value of the spiro analog **18f** was determined to be 3.8.

Concerning zone B, very potent pyrimidine analogs with nanomolar  $K_{V7.2/3}$  opening activity were obtained (**40a/b**), indicating that a central pyrimidine ring is well tolerated. However, since the corresponding analogs also bear an alkyl residue in zone E instead of an alkoxy substituent due to the chosen synthesis route via the Biginelli reaction, no final, conclusive statement can be made with certainty about the influence of the pyrimidine ring. Nevertheless, the almost identical  $EC_{50}$  values of the closely related analogs **18a** and **40a** suggest that the pyrimidine ring did not significantly affect the  $K_{V7.2/3}$  opening activity compared to a pyridine core, which is also supported by very similar docking poses of the corresponding analogs with no specific interaction of the additional pyrimidine nitrogen atom.

Contrary to the possible role of the pyrimidine ring, however, a valid judgment can be made on the importance of the methyl substituent in zone B, which must be considered in conjunction with the second ortho substituent of the amide group in zone E. In particular, compound **25**, which differs from the submicromolar active analog **18a** only in the absence of the methyl group, as well as compound **28b**, which lacks both ortho substituents of the amide group, were inactive up to a concentration of 20  $\mu$ M. In contrast, compound **28a**, which has a methyl substituent attached to the pyridine core but lacks the second ortho substituent in zone E, was still active, albeit weakly potent, with a 70-fold reduced  $EC_{50}$  value compared to **18a**. Based on these observations, two conclusions can be drawn concerning the possible role of the methyl group in zone B. First, viewed in isolation, the methyl group seems to be slightly more important for  $K_{V7.2/3}$  opening than the second ortho substituent of the amide group since the methylated analog **28a** was still weakly active while **25** and **28b**, both lacking the methyl group, were completely inactive. Second, however, only the presence of both amide ortho substituents, as in the case of **18a**, allows sufficient  $K_{V7.2/3}$  opening activity with submicromolar potency. Essentially, these results complete the evidence supporting our earlier hypothesis that the ortho disubstitution of the amide function is necessary to favor a molecular geometry that matches the bound-state conformation of the nicotinamide analogs in which the amide group is rotated out of the aromatic plane.<sup>[23]</sup> In contrast, a methoxy residue as the only amide ortho substituent, as in **25**, probably stabilizes an unfavorable coplanar orientation of the amide group through intramolecular hydrogen bonding. This negative effect is impossible with a methyl group as the sole ortho substituent, which is why the methylated analog **28a**, in contrast to compound **25** bearing a methoxy residue, was at least weakly active.

By modifying zone C, the possible role of the N-substituted amide group was investigated, which is presumed to be a crucial structural element of the initial nicotinamide scaffold. A first structural change based on the incorporation of an amide-analogous partial structure into an isoxazolo[5,4-*b*]hydroxyl-3-amine scaffold proved clearly detrimental to  $K_{V7.2/3}$  opening since the

corresponding analog **44** was inactive up to a concentration of 20  $\mu$ M. This observation essentially confirms the hypothesis formulated above that the amide group in the bound state conformation is probably rotated out of the pyridine plane, which of course, is not possible in the case of the conformationally restricted isoxazolo[5,4-*b*]pyridine analog **44**.

A different attempt to replace the amide function of **18a** with heterocyclic amide bioisosteres was slightly more successful, yielding the weakly to moderately active compounds **47** and **54**, which provided valuable SAR insights despite their overall inferior  $K_{V7.2/3}$  opening activity. As suggested by docking and molecular dynamics simulations, the amide group of nicotinamide analogs could be involved in direct interactions with the  $K_{V7.2/3}$  binding site as both a hydrogen bond donor and acceptor. In particular, the role of the amide function as a hydrogen bond donor was partially elucidated by the cyclic amide bioisosteres since the triazole ring of analog **54** provides a hydrogen atom similar to an amide group. In contrast, the oxadiazole structure of **47** is not able to act as a hydrogen bond donor. Consistent with this assumption, docking predicted the triazole ring of **54** to mimic the original amide group by forming both hydrogen bond interactions, and moreover, it may even be involved in a third hydrogen bond to S342 (Figure 6b). Contrary, the docking pose of the oxadiazole analog **47** shows a different orientation due to the lack of hydrogen bonding with I339 and S342 (Figure 6a). Albeit the hydrogen bond donor ability seems not essential for  $K_{V7.2/3}$  opening, it may still play an important role, as the triazole analog **54** had a superior efficacy of 149%, whereas the oxadiazole analog **47** was on the verge of inactivity with an efficacy of only 45%. Presumably, the putative hydrogen bond interactions of the triazole derivative **54** result in a slight shift of the S6'  $\alpha$  helix, which is part of the pore-forming domain, thereby enhancing the  $K_{V7.2/3}$  opening of **54** compared to the oxadiazole analog **47**.

In addition to these findings regarding the possible role of a hydrogen bond donor ability, analog **54** also provided a novel substance class of  $K_{V7.2/3}$  openers since, to our knowledge, **54** is the first 1,2,4-triazole derivative described to address this target. Indeed, there is still room for improvement in terms of potency, but considering the superior efficacy of **54**, it was even slightly more active than flupirtine, indicated by an overall left-shifted concentration-activity curve.

The third structural modification affecting the amide region again resulted in an inactive compound. The *N*-(hydroxyl-3-ylmethyl) benzamide analog **49** with a displaced amide carbonyl group compared to the original nicotinamide scaffold demonstrated no  $K_{V7.2/3}$  opening activity up to 20  $\mu$ M, thus underlining the crucial importance of the amide group for  $K_{V7.2/3}$  opening and confirming the postulated binding mode. By shifting the carbonyl group of the original amide partial structure while maintaining the position of the amide NH moiety, two important mechanisms contributing to ligand binding are disrupted at once. In detail, steric interactions of the amide group with ortho substituents on the pyridine core are vastly reduced, and one of the two presumed hydrogen bonds of the amide function is also prevented.

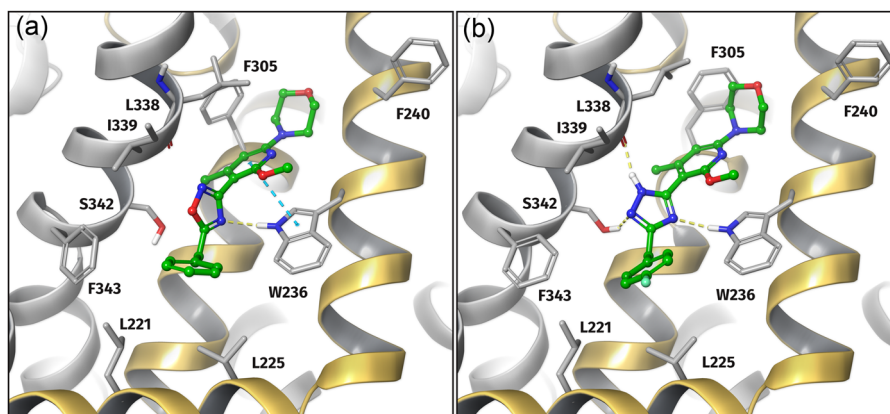


**FIGURE 6** Predicted binding poses of **47** (a) and **54** (b). The triazole ring forms hydrogen bonds to the S342 side chain and the I339 backbone carbonyl oxygen atom, probably affecting the S6' alpha helix, which is part of the pore-forming domains. The color of the secondary structure elements represents the respective chains of K<sub>v</sub>7.2 (gold) and K<sub>v</sub>7.3 (silver) in the K<sub>v</sub>7.2/3-heterotetramer.

According to molecular docking, the amide side chain in zone D is likely to occupy a hydrophobic cavity formed essentially by L221, L225, and F343, which has so far been mainly addressed with benzyl moieties. However, from a physicochemical point of view, this type of amide side chain, inherited from lead **6**, remains a certain hindrance to the desired increased aqueous solubility. Therefore, while incorporating polar structural elements in this region of the scaffold did not seem expedient, attempts were made to replace the benzyl moiety with aliphatic side chains to increase the overall sp<sup>3</sup> fraction and thus possibly improve the water solubility. The corresponding compounds **18d** and **40c** were both found to be moderately active with EC<sub>50</sub> values slightly inferior to flupirtine but showed a remarkable difference in efficacy. Whereas analog **40c** bearing a bulky 3,3-dimethylbutyl side chain achieved only 52% efficacy, an *n*-butyl side chain in **18d** resulted in an impressive 170% efficacy, which was the best of all compounds tested in this study (Figure 7). Consequently, despite the clear negative impact on the EC<sub>50</sub> value, an *n*-butyl side chain may still represent an attractive structural element for future designs since analog **18d** not only showed the best efficacy but was also one of the most soluble substances in the toxicity tests carried out where it could be tested up to 250 μM. The detrimental effect of the *n*-butyl amide side chain on the EC<sub>50</sub> value might be partially compensated when combined with successful substituents in zones A and E of the scaffold. However, considering only the K<sub>v</sub>7.2/3 opening activity while leaving aside physicochemical properties, a benzylic amide side chain was still clearly superior. The beneficial effect could even be enhanced by replacing the initially used 4-fluorobenzyl moiety with a 3-(trifluoromethyl)benzyl residue, as revealed by a **40a** and **40b** comparison, where this structural change led to a 3.6-fold increase in potency. The observed boost in K<sub>v</sub>7.2/3 opening activity might be attributed to a π–π interaction between the benzyl side chain and F343 being strengthened upon trifluoromethylation. This is consistent with computational studies by Mottishaw and Sun, which demonstrated that trifluoromethylation of an aromatic core results in improved π–π

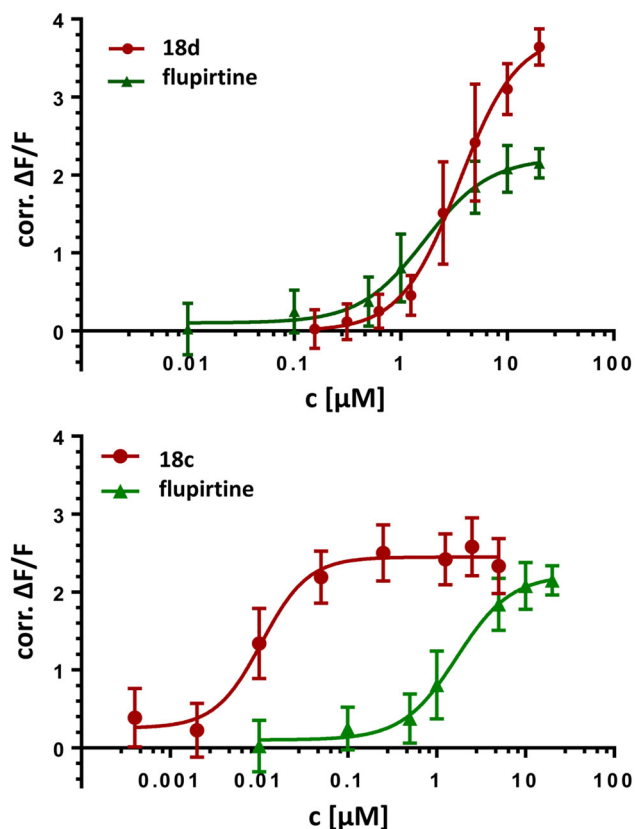


**FIGURE 7** The concentration-activity curves for K<sub>v</sub>7.2/3 opening of analogs **18c** and **18d** in comparison to flupirtine demonstrate the excellent potency of **18c** (EC<sub>50</sub> = 0.012 μM) as well as the superior efficacy of **18d** (E<sub>max</sub> = 170%).

interactions compared to direct monofluorination, as indicated by increased intermolecular interaction energies and reduced π–π distances.<sup>[48]</sup>

Regarding the investigated substituents in zone E, the impression emerged that sterically more demanding substituents with increased

lipophilicity favor  $K_{V7.2/3}$  opening. A replacement of the methoxy group of **18a** with a 2,2,2-trifluoroethoxy or a 1-methyl-ethoxy substituent increased the potency of the corresponding analogs **18b** and **18c** significantly by a factor of 6.9 and 9.8, respectively, leading to an excellent  $EC_{50}$  value of 0.012  $\mu$ M in the case of **18c** (Figure 7). This is noteworthy since the predicted binding poses of the nicotinamide analogs indicate that the alkoxy substituents do not interact directly with the binding pocket but rather point in the opposite direction toward the vicinity of the  $K_{V7.2/3}$  channel (Figure 4c). Consistent with the assumption about the orientation of the alkoxy substituents, an exchange of the methoxy group for an isosteric ethyl residue in analog **40a** was also tolerated well, as there are no specific interactions of the alkoxy oxygen atom with the  $K_{V7.2/3}$  binding site predicted.

However, without direct contact with the binding site, the question arises of how the bulky and lipophilic alkoxy substituents were able to improve  $K_{V7.2/3}$  opening. Remarkably, the position of the  $K_{V7.2/3}$  binding site may be relevant in this case since it is situated in the transmembrane region of the channel on the protein-phospholipid interface (Figure 8). Hence, the bulky and lipophilic alkoxy substituents in zone E, which are presumed to face in the direction of the cell membrane, may improve possible interactions with adjacent lipid tails. Such ligand-lipid interactions have so far been underestimated as influencing factors of drug activity. However, they are becoming increasingly important in drug design as a growing number of intramembrane binding sites are revealed by X-ray crystallography and cryogenic electron microscopy.<sup>[49]</sup> Consequently, for various small molecules and targets, it is assumed that ligand-lipid interactions are significantly involved in ligand binding. A prominent and impressive example of ligand-lipid interactions is ivacaftor (not shown), a potentiator of the cystic fibrosis transmembrane conductance regulator (CFTR) that binds to a site within

the transmembrane region of the CFTR chloride channel. The molecule bears two *tert*-butyl groups that interact with lipids of the adjacent membrane and shield the polar part of the ligand, which is responsible for molecular recognition via hydrogen bonds, against the phospholipid interface.<sup>[49]</sup> Conceivably, the lipophilic alkoxy substituents of **18b** and **18c** function in a similar way as the *tert*-butyl groups of ivacaftor. To confirm the postulated ligand-lipid interactions, a molecular dynamics simulation was performed with **18c** and a  $K_{V7.2/3}$  channel, which was inserted in a phosphatidylcholine bilayer simulating the cell membrane. The result presented in Figure 8 clearly shows that the trifluoroethoxy group, together with the 4-fluorophenyl ring, is able to shield the polar part of the molecule, that is, the amide group and the pyridine nitrogen atom, from the adjacent lipid layer, thus improving hydrophobic interactions with lipid tails.

In contrast to the alkoxy substituents, the considerably more hydrophilic primary amino function of **14** resulted in a reduced  $\log D_{7.4}$  value and, as intended, in an improved solubility in toxicity testing, but at the same time caused an unexpected drastic loss of  $K_{V7.2/3}$  opening activity. Consequently, the question arises why the primary amino function is well tolerated in flupirtine and retigabine, whereas it appears to be clearly disadvantageous in nicotinamide analogs. In this case, there are probably several reasons to consider. First, molecular dynamics simulations indicate that the amino function of **14** is slightly shifted in the binding pocket compared to the amino group of retigabine. As a result, the hydrogen bond to S342, which is assumed to be advantageous, is not predicted as with retigabine (Figure 4b). Second, in the case of **14**, the methyl group is located on the lipid-facing side of the molecule. Therefore, the shielding against the cell membrane is likely reduced compared to bulky lipophilic alkoxy residues of analogs **18b/c**. Finally, with a  $\log D_{7.4}$  value of 2.2, compound **14** is also the most hydrophilic of the

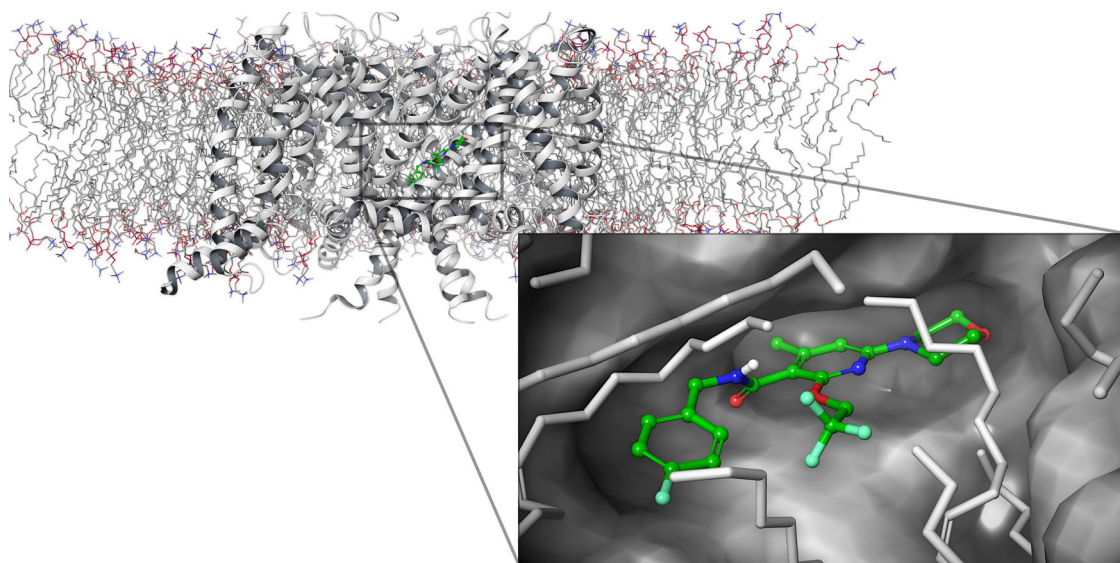


**FIGURE 8** Predicted binding mode of **18c** from combined ligand docking and all-atom molecular dynamics simulations. The trifluoroethoxy group points toward the membrane and shields it from the hydrophilic parts of the ligand.

nicotinamide analogs, which may inhibit diffusion through the lipid layer and thus impede the compound from reaching the intramembrane binding site.

The same may also apply to analog **19a**, which has a hydroxyl group in place of the primary amino substituent of **14**. Remarkably, in contrast to the still weakly active compound **14**, analog **19a** turned out to be completely inactive up to a concentration of 20  $\mu\text{M}$ . The even worse performance of a hydroxyl group compared to the amino substituent of **14** might be attributed to a tautomeric relationship of **19a**, whose 2-hydroxypyridine form is likely in equilibrium with the 2-pyridone form. This is particularly relevant as docking suggests that the central pyridine ring of nicotinamide analogs is involved in  $\pi$ - $\pi$  interactions with the W236 indole side chain, similar to the phenyl ring of retigabine (Figure 4). This specific interaction is presumed to be highly relevant for ligand binding since it could be shown that a mutation of W236 completely abolishes the effect of retigabine.<sup>[50]</sup> Consequently, this crucial interaction might be weakened in the case of the nonaromatic 2-pyridone tautomer of **19a**, hence leading to the observed inactivity.

## 2.2.2 | Evaluation of in vitro toxicity

Flupirtine-induced severe hepatotoxicity is a very rare phenomenon with a reporting rate of 1.68 cases per 100,000 patient years.<sup>[51]</sup> For this reason, it was not reported in any in vitro or in vivo toxicity studies during preclinical and clinical development, and thus flupirtine has long been considered a well-tolerated analgesic.<sup>[9,52]</sup> In accordance, in vitro LD<sub>50</sub> values of flupirtine were determined in the range of 500  $\mu\text{M}$ , hence significantly exceeding therapeutically relevant concentrations, which are in the low single-digit micromolar range.<sup>[53]</sup> In general, idiosyncratic toxicity, as suspected for flupirtine, is very difficult to reproduce in an in vitro toxicity model due to the multifactorial causes,<sup>[54]</sup> which in the case of flupirtine probably include both the formation of potentially toxic metabolites and involvement of the adaptive immune system.<sup>[18,55]</sup> Despite all efforts, currently, no in vitro or in vivo model exists that reliably predicts idiosyncratic drug-induced liver injury (DILI),<sup>[56]</sup> which is reflected in the fact that idiosyncratic hepatotoxicity is still one of the two most common reasons for drug withdrawals, restrictions and project terminations.<sup>[57]</sup> For these reasons, since flupirtine usually behaves uncritically in standard toxicity tests and no adequate assay for idiosyncratic hepatotoxicity exists, the toxicological evaluation carried out in this work should not be understood as a proof of concept to verify the design hypothesis but rather as a general examination of the new scaffolds for potential intrinsic toxicity. This standard toxicological characterization was carried out on two hepatic cell lines with an MTT assay, which essentially measures metabolic activity as an indicator of cell viability. The method is based on the mitochondrial reduction of 3-(4,5-dimethylthiazol-2-yl)-2,5-diphenyltetrazolium bromide (MTT) to the corresponding formazan, which can be quantified colorimetrically.<sup>[58]</sup> The human HEP-G2 and mouse TAMH cell lines used for this assay are well established for in vitro hepatotoxicity testing.<sup>[59]</sup>

A limitation in toxicity testing that inherently demands that much higher concentrations are applied than in activity testing continued to be the relatively poor water solubility of most analogs, which was already problematic for compound **6**.<sup>[23]</sup> Remarkably, the introduction of a morpholino substituent in **18a** did not result in significantly improved solubility. Like analog **6**, the morpholino derivative **18a** could only be tested up to a concentration of 63  $\mu\text{M}$ , which was surprising since the log $D_{7.4}$  value was reduced from 4.1 to 3.0, and at the same time, the fraction of sp<sup>3</sup> hybridized carbon atoms was increased from 0.18 to 0.37. However, the three-dimensional structure of **18a** and the other morpholino-substituted analogs is probably still rather flat due to the coplanar conformation of the morpholino substituent and the central aromatic ring, which might favor aggregation and thus prevent noticeably improved water solubility. This hypothesis is supported by the increased aqueous solubility of analog **21**, which could be tested up to a concentration of 125  $\mu\text{M}$  and was thus about twice as soluble as **18a**. The reason for this difference is probably the tetrahydropyran ring of **21**, which does not prefer a coplanar conformation like the morpholine ring of **18a**, as discussed above. Since no LD<sub>50</sub> value could be determined for any analog due to the limited water solubility, LD<sub>25</sub> values were calculated, which indicate the concentration that was necessary to reduce the cell viability to 75% to enable a comparison of the analogs regarding their hepatotoxic potential. Nevertheless, for 12 of the 22 analogs, no LD<sub>25</sub> value could be determined for either cell line because the required concentrations could not be reached. However, apart from the poor water solubility, the lack of LD values principally indicates that most of the analogs do not possess a pronounced level of in vitro hepatotoxicity at concentrations required for K<sub>v</sub>7.2/3 opening.

While it was possible to derive structure-activity relationships for K<sub>v</sub>7.2/3 opening, an analysis of the toxicity data displayed in Table 1 does not allow a clear correlation with certain structural elements to set up any valid structure-toxicity relationships. However, the nicotinamide scaffold per se does not appear to be of toxicological concern. This becomes apparent when the analogs with low water solubility are initially left aside, and instead, the focus is placed on the more soluble substances such as **14**, **18d**, **21**, or **28a/b**. These analogs displayed rather uncritical levels of in vitro hepatotoxicity with higher LD<sub>25</sub> values compared to flupirtine. Nevertheless, focusing on the remaining analogs, there are some compounds that appear to perform worse than flupirtine and retigabine. This applies, for example, to the nanomolar active analogs **18b** and **18e**, for which LD<sub>25</sub> values of 15 and 32  $\mu\text{M}$ , respectively, were determined for the HEP-G2 cell line. However, the structural similarity of the compounds to the significantly less toxic analogs **14** and **18d** suggests that the specific chemical structure may not be responsible for the reduced LD<sub>25</sub> values. Instead, the reason could be the overall increased lipophilicity of **18b** and **18e**, which was among the highest of the current analogs as indicated by log $D_{7.4}$  values of 3.8 and 4.7, respectively. This would be consistent with an analysis of 1036 FDA-approved drugs suggesting that compound lipophilicity is statistically significantly associated with DILI risk.<sup>[60]</sup>

However, it must be emphasized that it is not possible to define a general LD limit at which a substance is to be classified as hepatotoxic. Tham et al. reported LD<sub>50</sub> values of 10 proven hepatotoxic drugs determined by the MTT assay on HEP-G2 cells, which extend over a wide concentration range from 25  $\mu$ M to 20 mM.<sup>[61]</sup> Therefore, LD values on their own are not very meaningful and must always be considered in relation to the biological activity, which among other factors, ultimately determines the necessary therapeutic concentration. For this reason, LD<sub>25</sub>/EC<sub>50</sub> ratios were calculated for all active analogs, thus enabling a preliminary estimation of the therapeutic range. Considering these LD<sub>25</sub>/EC<sub>50</sub> ratios, the highly potent analogs **18b** and **18e** appear to have significantly improved therapeutic safety windows compared to flupirtine despite lower absolute LD<sub>25</sub> values. The same applies to compound **18c** with an LD<sub>25</sub>/EC<sub>50</sub> ratio of 1,250 that even surpasses retigabine, for which no hepatotoxic effect is known. Overall, only the weakly to moderately active analogs **14**, **28a**, **40c**, **47**, and **54** have a poorer preliminary therapeutic range than flupirtine, whereby the exact LD<sub>25</sub>/EC<sub>50</sub> ratios of **40c**, **47**, and **54** are actually unknown since the maximum soluble concentrations were used for the calculation due to the lack of LD<sub>25</sub> values; therefore the calculated LD<sub>25</sub>/EC<sub>50</sub> ratios represent worst-case scenarios. In summary, the potential to cause intrinsic hepatotoxicity appears to be low for most analogs based on preliminary in vitro toxicity data. However, as mentioned above, the results of the MTT assay may not be predictive of idiosyncratic hepatotoxicity.

### 3 | CONCLUSION

The K<sub>v</sub>7.2/3 opening activity of nicotinamide lead compound **6** could be successfully improved by introducing a morpholino substituent and a 2,2,2-trifluoroethoxy group. The resulting compound **18c** was 150 times more potent than flupirtine and 20 times more potent than retigabine while also demonstrating a superior toxicity/activity ratio. The water solubility of **18c** and related compounds was still low, but considering the nanomolar activity, it might be sufficient for further development, which in perspective also includes in vivo assays. Moreover, the K<sub>v</sub>7.2/3 activity data of the structurally distinct analogs provided profound structure–activity relationships, which could be correlated with docking and molecular dynamics simulations to hypothesize a plausible binding mechanism for the nicotinamide derivatives. As a result, the ortho disubstitution of the amide function was confirmed as an essential structural feature. In addition, the role of a cyclic substituent in position 6 of the pyridine ring was clarified, which must be aligned coplanar to the central pyridine ring but still has to allow for a flexible conformation to fit into the binding pocket adequately. Finally, a bulky alkoxy group is presumed to better shield the analogs in their intramembrane binding site from the adjacent lipid layer by improving ligand–lipid interactions. Taken together, the SAR findings obtained in this work provide a strong basis for future drug design.

## 4 | EXPERIMENTAL

### 4.1 | Chemistry

#### 4.1.1 | General remarks

The starting materials, reagents, and solvents were commercially available and purchased from Sigma Aldrich, VWR, TCI, or ABCR. All chemicals were used as received unless specified otherwise. Anhydrous solvents were obtained from Acros Organics, except THF, which was dried by refluxing over sodium. Microwave-supported syntheses were conducted using an Anton Paar Mono-wave 300 reactor in closed vessel mode with an integrated IR sensor for temperature control. NMR spectra were recorded on a Bruker Avance III device at 400 MHz (<sup>1</sup>H) and 100 MHz (<sup>13</sup>C), respectively, using CDCl<sub>3</sub>, DMSO-*d*<sub>6</sub>, or MeOH-*d*<sub>4</sub> as solvents. The chemical shifts were referenced to the internal standard tetramethylsilane (TMS) and reported in parts per million (ppm). The coupling constants (*J*) are in Hz, and the following abbreviations were used to designate the multiplicities: br = broad, s = singlet, d = doublet, t = triplet, q = quartet, m = multiplet, and combinations thereof. MIR spectroscopy was performed with an ALPHA FT-IR instrument from Bruker Optics equipped with a diamond ATR accessory unit. A Bruker Elute UHPLC with Bruker compact QTOF-MS, a Bruker maXis LC-QTOF-MS, or a Shimadzu LCMS-IT-TOF system, each operated with ESI ionization, were used to measure the HRAM-MS data. HPLC analysis with UV detection at 220 nm using the 100% method determined the purity of all final compounds to be >95%. The melting points were measured with an automated Büchi Melting Point M-565 device. Analytical thin-layer chromatography was carried out on silica gel 60 F<sub>254</sub> aluminum plates obtained from Merck, and visualization was accomplished with UV light. Column chromatography on silica gel was performed using silica gel 60 from Carl Roth with a particle size of 20–45  $\mu$ m. Flash chromatographic separations were conducted using the Sepacore system from Büchi with 25 or 50 g Biotage SNAP KP-SIL columns, or alternatively, an Interchim puriFlash XS 520Plus system in combination with 80 g puriFlash 30SI-HP or 25 g puriFlash 15SI-HP columns. The InChI codes of the investigated analogs are provided as Supporting Information. The Supporting Information also contains <sup>1</sup>H-NMR and <sup>13</sup>C-NMR spectra of all synthesized compounds as well as HPLC traces of the final compounds. All new compounds were fully characterized, including purity by HPLC and HRAM-MS data within 4 ppm accuracy.

#### 4.1.2 | Synthesis and characterization

##### *General procedure A: introduction of alkoxy substituents*

A 60% suspension of NaH in mineral oil (2.5 equiv., 1.21 mmol/ml) was suspended in dry THF under an argon atmosphere, and the resulting suspension was cooled to 0°C. A solution of the chosen alcohol (1.2 equiv., 0.58 mmol/ml) in dry THF and a solution of the required chloropyridine (5.2–24.3 mmol, 0.49 mmol/ml) in dry THF

were added successively. Afterward, the reaction mixture was heated to 70°C and stirred at 70°C until the TLC control indicated complete conversion (7–23 h). The reaction was quenched by the addition of water (100 ml). The resulting aq. mixture was adjusted to pH 12 by the addition of a 2 M aq. NaOH solution and extracted with ethyl acetate (100 ml). The organic phase was discarded, and the aq. phase was adjusted to pH 2–3 with conc. HCl. Subsequently, it was extracted with ethyl acetate again (2 × 50–235 ml). Finally, the combined organic phases were washed with brine, dried over Na<sub>2</sub>SO<sub>4</sub>, filtrated, and concentrated under reduced pressure.

*General procedure B: Amide coupling with oxalyl chloride*

Under an argon atmosphere, the required nicotinic acid derivative (2.5–12.1 mmol, 0.2 mmol/ml) was dissolved in dry DCM, and a catalytic amount of dry DMF was added. The mixture was cooled to 0°C, and a solution of oxalyl chloride (3.0 equiv., 2.0 mmol/ml) in dry DCM was added dropwise. After complete addition, the cooling was discontinued, and the reaction mixture was stirred at room temperature for 3 h. Subsequently, all volatiles were removed under reduced pressure, and the residue was redissolved in dry DCM (10–48 ml). The resulting solution was added dropwise to a solution of amine reactant (1.2 equiv., 0.3 mmol/ml) and triethylamine (2.0 equiv., 0.5 mmol/ml) in dry DCM at 0°C under stirring. Afterward, the cooling was discontinued, and the reaction mixture was stirred at room temperature. After 16 h, additional DCM (50–240 ml) was added. The resulting solution was extracted successively with an equal volume of a saturated aq. NaHCO<sub>3</sub> solution and a 2 M aq. HCl solution. Finally, the organic phase was washed with brine, dried over Na<sub>2</sub>SO<sub>4</sub>, filtrated, and concentrated under reduced pressure to obtain the crude product.

*General procedure C: Microwave-assisted nucleophilic substitution*

The required chloropyridine (0.9–3.0 mmol, 0.33 mmol/ml) was dissolved in NMP. Subsequently, the corresponding amine (5.0 equiv.) was added, and the mixture was heated in a microwave reactor at 165°C in a closed vessel under stirring. After complete conversion (30–60 min), the reaction mixture was cooled to room temperature, dissolved in ethyl acetate (100 ml), and extracted with water (2 × 100 ml). Finally, the organic phase was washed with brine, dried over Na<sub>2</sub>SO<sub>4</sub>, filtrated, and concentrated under reduced pressure to obtain the crude product.

*General procedure D: Amide coupling with DIC and HOBt*

The required carboxylic acid (1.0–5.8 mmol, 0.15 mmol/ml) was dissolved in DMF. HOBt (2.0 equiv.), DIC (2.0 equiv.) and the corresponding amine (1.5 equiv.) were added successively, and the reaction mixture was stirred at room temperature. After 16 h, the solution was partitioned between ethyl acetate (50–290 ml) and an equal volume of water. The organic phase was extracted with the same volume of water again (2×), washed with brine, dried over Na<sub>2</sub>SO<sub>4</sub>, filtrated, and concentrated under reduced pressure to obtain the crude product.

*General procedure E: Dechlorination by catalytic hydrogenation*

The required chloropyridine (0.3–3.0 mmol, 0.02 mmol/ml) was dissolved in methanol. Pd/C (10% Pd, 50% water wet, 0.1 equiv.) and triethylamine (1.5 equiv.) were added. Subsequently, the suspension was carefully set under a hydrogen atmosphere (balloon pressure) and stirred at room temperature. After complete conversion (2–5 h), the reaction mixture was filtered through a pad of celite, and the filtrate was concentrated under reduced pressure to obtain the crude product.

*2-Amino-6-chloro-4-methylnicotinic acid (12)*

2,6-Dichloro-4-methylnicotinic acid (950 mg, 4.61 mmol), K<sub>2</sub>CO<sub>3</sub> (1275 mg, 9.22 mmol, 2.0 equiv.), CuI (176 mg, 0.92 mmol, 0.2 equiv.), NaN<sub>3</sub> (1199 mg, 18.44 mmol, 4.0 equiv.), and ethane-1,2-diamine (62 µl, 0.92 mmol, 0.2 equiv.) were successively dissolved/suspended in ethanol (90 ml). The reaction mixture was set under an atmosphere of argon and stirred under reflux. After 23 h, additional amounts of K<sub>2</sub>CO<sub>3</sub> (382 mg, 2.77 mmol, 0.6 equiv.), CuI (53 mg, 0.28 mmol, 0.06 equiv.), NaN<sub>3</sub> (360 mg, 5.5 mmol, 1.2 equiv.) and ethane-1,2-diamine (19 µl, 0.28 mmol, 0.06 equiv.) were added, and the reaction was continued for 5 h under the same conditions. Afterward, the reaction mixture was filtered through a pad of silica gel. Subsequently, the silica gel pad was rinsed with ethanol, and the combined eluates were concentrated under reduced pressure. The residue was dissolved in a 1 M aq. KOH solution and the product was precipitated by the addition of conc. HCl. Finally, the precipitate was filtered off to obtain **12** as a brown solid (467 mg, 2.50 mmol, 54%). *R*<sub>f</sub> = 0.63 (toluene/ethanol/AcOH 5:4:1); mp = 178°C; <sup>1</sup>H-NMR (400 MHz, DMSO-*d*<sub>6</sub>): δ(ppm) = 13.36 (s, 1H), 7.20 (s, 2H), 6.54 (s, 1H), 2.38 (s, 3H); <sup>13</sup>C-NMR (100 MHz, DMSO-*d*<sub>6</sub>): δ(ppm) = 168.8, 159.7, 154.0, 151.1, 113.86, 106.23, 22.21; IR (ATR):  $\tilde{\nu}$  = 3406, 3282 (m,  $\nu_{\text{N-H}}$ ), 3300–2500 (b,  $\nu_{\text{O-H}}$ ), 1681 (s,  $\nu_{\text{C=O}}$ ), 1619 (s,  $\delta_{\text{N-H}}$ ).

*2-Amino-6-chloro-N-(4-fluorobenzyl)-4-methylnicotinamide (13)*

Compound **12** (424 mg, 2.27 mmol) was dissolved in THF (22 ml). CDI (737 mg, 4.56 mmol, 2.0 equiv.) was added in one portion, and the mixture was stirred at 50°C. After 1 h, the solution was cooled to room temperature, 4-fluorobenzylamine (1040 µl, 9.09 mmol) was added, and the mixture was continued to stir at room temperature. After 12 h, ethyl acetate (100 ml) was added. The resulting solution was extracted with a saturated aq. NaHCO<sub>3</sub> solution (100 ml), washed with brine, dried over Na<sub>2</sub>SO<sub>4</sub>, filtrated, and concentrated under reduced pressure. Finally, the crude residue was purified by silica gel column chromatography (ethyl acetate/*n*-hexane 2:3) to obtain **13** as a slightly yellow solid (236 mg, 0.80 mmol, 35%). *R*<sub>f</sub> = 0.70 (ethyl acetate/*n*-hexane 7:3); mp = 169°C; <sup>1</sup>H-NMR (400 MHz, DMSO-*d*<sub>6</sub>): δ(ppm) = 8.87 (t, *J* = 6.0 Hz, 1H), 7.43–7.33 (m, 2H), 7.22–7.11 (m, 2H), 6.49 (s, 1H), 6.14 (s, 2H), 4.41 (d, *J* = 5.9 Hz, 2H), 2.10 (s, 3H); <sup>13</sup>C-NMR (100 MHz, DMSO-*d*<sub>6</sub>): δ (ppm) = 166.3, 161.2 (d, *J* = 242.4 Hz), 156.6, 148.0, 147.9, 135.4 (d, *J* = 3.1 Hz), 129.6 (d, *J* = 8.2 Hz), 115.2, 115.0 (d, *J* = 21.3 Hz), 112.4, 41.9, 18.8; IR (ATR):  $\tilde{\nu}$  = 3441, 3278 (m,  $\nu_{\text{N-H}}$ ), 1613 (s,  $\nu_{\text{C=O}}$ ).



*2-Amino-N-(4-fluorobenzyl)-4-methyl-6-morpholinicotinamide (14)*

The synthesis was conducted from **13** (350 mg, 1.19 mmol) and morpholine in accordance with general procedure C. The crude residue was purified by silica gel column chromatography (ethyl acetate/*n*-hexane 7:3) and successive recrystallization (methanol/water) to obtain **14** as a slightly yellow solid (300 mg, 0.87 mmol, 73%).  $R_f = 0.34$  (ethyl acetate/*n*-hexane 7:3); mp = 177°C;  $^1\text{H-NMR}$  (400 MHz, DMSO- $d_6$ ):  $\delta$ (ppm) = 8.41 (t,  $J = 6.0$  Hz, 1H), 7.41–7.31 (m, 2H), 7.20–7.10 (m, 2H), 5.86 (s, 1H), 5.63 (s, 2H), 4.39 (d,  $J = 6.0$  Hz, 2H), 3.67–3.60 (m, 4H), 3.41–3.34 (m, 4H), 2.14 (s, 3H);  $^{13}\text{C-NMR}$  (100 MHz, DMSO- $d_6$ ):  $\delta$ (ppm) = 168.1, 161.1 (d,  $J = 242.0$  Hz), 157.9, 156.2, 146.5, 135.9 (d,  $J = 2.9$  Hz), 129.4 (d,  $J = 8.1$  Hz), 115.0 (d,  $J = 21.3$  Hz), 105.6, 96.7, 66.0, 44.9, 41.8, 20.5; IR (ATR):  $\tilde{\nu} = 3458, 3346, 3254$  (m,  $\nu_{\text{N-H}}$ ), 3049, 2974 (w,  $\nu_{\text{C-H}}$ ), 1583 (s,  $\nu_{\text{C=O}}$ ), 1531 (m,  $\delta_{\text{N-H}}$ ); ESI-HRAM-MS ( $m/z$ ): calcd. for  $[\text{C}_{18}\text{H}_{21}\text{N}_4\text{O}_2\text{F}+\text{H}]^+$  345.1721, found 345.1708; cpd purity (220 nm): 99.6%.

*6-Chloro-2-methoxy-4-methylnicotinic acid (15a)*

The synthesis was conducted from 2,6-dichloro-4-methylnicotinic acid (5.00 g, 24.3 mmol) and methanol in accordance with general procedure A to obtain **15a** as a beige-colored solid (4.72 g, 23.4 mmol, 96%).  $R_f = 0.78$  (*n*-butanol/AcOH/water 8:1:1); mp: 166°C;  $^1\text{H-NMR}$  (400 MHz, DMSO- $d_6$ ):  $\delta$ (ppm) = 13.39 (s, 1H), 7.09 (s, 1H), 3.87 (s, 3H), 2.17 (s, 3H);  $^{13}\text{C-NMR}$  (100 MHz, DMSO- $d_6$ ):  $\delta$  (ppm) = 166.6, 159.4, 149.8, 147.0, 118.0, 117.4, 54.3, 18.4; IR (ATR):  $\tilde{\nu} = 3002, 2954$  (w,  $\nu_{\text{C-H}}$ ), 3300–2500 (b,  $\nu_{\text{O-H}}$ ), 1686 (s,  $\nu_{\text{C=O}}$ ).

*6-Chloro-2-isopropoxy-4-methylnicotinic acid (15b)*

The synthesis was carried out from 2,6-dichloro-4-methylnicotinic acid (2.50 g, 12.1 mmol) and 2-propanol following general procedure A to obtain **15b** as a beige-colored solid (2.75 g, 12.0 mmol, 99%), which was used for the following reaction without any further characterization and purification.

*6-Chloro-4-methyl-2-(2,2,2-trifluoroethoxy)nicotinic acid (15c)*

The synthesis was conducted from 2,6-dichloro-4-methylnicotinic acid (1.25 g, 6.1 mmol) and 2,2,2-trifluoroethanol in accordance with general procedure A to obtain **15c** as a beige-colored solid (1.62 g, 6.0 mmol, 99%), which was used for the following reaction without any further characterization and purification.

*6-Chloro-N-(4-fluorobenzyl)-2-methoxy-4-methylnicotinamide (16a)*

The synthesis was carried out from **15a** (500 mg, 2.48 mmol) and 4-fluorobenzylamine according to general procedure B. The crude residue was purified by silica gel column chromatography (ethyl acetate/*n*-hexane 3:2), which yielded **16a** as a colorless solid (402 mg, 1.30 mmol, 53%).  $R_f = 0.29$  (ethyl acetate/*n*-hexane 1:1); mp: 127°C;  $^1\text{H-NMR}$  (400 MHz, DMSO- $d_6$ ):  $\delta$ (ppm) = 8.89 (t,  $J = 6.0$  Hz, 1H), 7.43–7.33 (m, 2H), 7.24–7.08 (m, 2H), 7.05 (d,  $J = 0.6$  Hz, 1H), 4.42 (d,  $J = 6.0$  Hz, 2H), 3.86 (s, 3H), 2.18 (d,  $J = 0.6$  Hz, 3H);  $^{13}\text{C-NMR}$  (100 MHz, DMSO- $d_6$ ):  $\delta$ (ppm) = 164.5, 161.2 (d,  $J = 242.1$  Hz), 159.6, 149.9, 146.4, 135.3 (d,  $J = 3.0$  Hz), 129.1 (d,  $J = 8.1$  Hz), 119.9, 117.9,

115.0 (d,  $J = 21.3$  Hz), 54.1, 41.5, 18.0; IR (ATR):  $\tilde{\nu} = 3310$  (m,  $\nu_{\text{N-H}}$ ), 3067, 2954 (w,  $\nu_{\text{C-H}}$ ), 1635 (s,  $\nu_{\text{C=O}}$ ), 1604 (m,  $\delta_{\text{N-H}}$ ).

*6-Chloro-N-(4-fluorobenzyl)-2-(propan-2-yloxy)-4-methylnicotinamide (16b)*

The synthesis was carried out from **15b** (2.78 g, 12.1 mmol) and 4-fluorobenzylamine according to general procedure B. The crude residue was purified by flash chromatography (mobile phase: ethyl acetate/*n*-hexane with 0%–30% ethyl acetate), which yielded **16b** as a colorless solid (2.10 g, 6.2 mmol, 51%).  $R_f = 0.83$  (ethyl acetate/*n*-hexane 2:1); mp: 122°C;  $^1\text{H-NMR}$  (400 MHz, DMSO- $d_6$ ):  $\delta$ (ppm) = 8.82 (t,  $J = 6.1$  Hz, 1H), 7.45–7.35 (m, 2H), 7.21–7.11 (m, 2H), 7.00 (s, 1H), 5.16 (sept,  $J = 6.2$  Hz, 1H), 4.42 (d,  $J = 6.1$  Hz, 2H), 2.19 (s, 3H), 1.26 (d,  $J = 6.1$  Hz, 6H);  $^{13}\text{C-NMR}$  (100 MHz, DMSO- $d_6$ ):  $\delta$ (ppm) = 164.6, 161.2 (d,  $J = 242.0$  Hz), 158.9, 149.9, 146.3, 135.4 (d,  $J = 3.0$  Hz), 129.0 (d,  $J = 8.1$  Hz), 120.4, 117.4, 114.8 (d,  $J = 21.0$  Hz), 69.4, 41.3, 21.7, 18.0; (ATR):  $\tilde{\nu} = 3267$  (m,  $\nu_{\text{N-H}}$ ), 3078, 2982 (w,  $\nu_{\text{C-H}}$ ), 1632 (s,  $\nu_{\text{C=O}}$ ).

*6-Chloro-N-(4-fluorobenzyl)-4-methyl-2-(2,2,2-trifluoroethoxy)nicotinamide (16c)*

The synthesis was conducted from **15c** (1.25 g, 4.64 mmol) and 4-fluorobenzylamine following general procedure B. The crude residue was purified by silica gel column chromatography (ethyl acetate/*n*-hexane 2:3), which yielded **16c** as a beige-colored solid (855 mg, 2.27 mmol, 49%).  $R_f = 0.67$  (ethyl acetate/*n*-hexane 1:1); mp: 127°C;  $^1\text{H-NMR}$  (400 MHz, DMSO- $d_6$ ):  $\delta$ (ppm) = 8.98 (t,  $J = 6.0$  Hz, 1H), 7.43–7.32 (m, 2H), 7.21 (d,  $J = 0.6$  Hz, 1H), 7.18–7.07 (m, 2H), 4.96 (q,  $J = 9.0$  Hz, 2H), 4.44 (d,  $J = 6.0$  Hz, 2H), 2.24 (d,  $J = 0.6$  Hz, 3H);  $^{13}\text{C-NMR}$  (100 MHz, DMSO- $d_6$ ):  $\delta$ (ppm) = 163.7, 161.2 (d,  $J = 242.1$  Hz), 157.1, 151.1, 146.1, 135.1 (d,  $J = 3.0$  Hz), 129.0 (d,  $J = 8.1$  Hz), 123.7 (q,  $J = 277.7$  Hz), 120.0, 119.6, 114.9 (d,  $J = 21.3$  Hz), 62.3 (q,  $J = 35$  Hz), 41.5, 18.1; (ATR):  $\tilde{\nu} = 3404$  (m,  $\nu_{\text{N-H}}$ ), 3013, 2924 (w,  $\nu_{\text{C-H}}$ ), 1613 (s,  $\nu_{\text{C=O}}$ ).

*N-Butyl-6-chloro-2-methoxy-4-methylnicotinamide (16d)*

The synthesis was carried out from **15a** (2.19 g, 10.87 mmol) and *n*-butylamine according to general procedure B. The crude residue was purified by silica gel column chromatography (ethyl acetate/*n*-hexane 3:7), which yielded **16d** as a colorless solid (1.71 g, 6.7 mmol, 61%).  $R_f = 0.81$  (ethyl acetate/*n*-hexane 2:1); mp: 57°C;  $^1\text{H-NMR}$  (400 MHz, DMSO- $d_6$ ):  $\delta$ (ppm) = 8.30 (t,  $J = 5.7$  Hz, 1H), 7.04 (s, 1H), 3.82 (s, 3H), 3.19 (td,  $J = 6.9, 5.7$  Hz, 2H), 2.19 (s, 3H), 1.51–1.40 (m, 2H), 1.43–1.27 (m, 2H), 0.89 (t,  $J = 7.3$  Hz, 3H);  $^{13}\text{C-NMR}$  (100 MHz, DMSO- $d_6$ ):  $\delta$ (ppm) = 164.1, 159.6, 149.7, 146.1, 120.4, 117.8, 54.0, 38.3, 31.0, 19.5, 18.0, 13.6; IR (ATR):  $\tilde{\nu} = 3220$  (m,  $\nu_{\text{N-H}}$ ), 3068, 2961 (w,  $\nu_{\text{C-H}}$ ), 1645 (s,  $\nu_{\text{C=O}}$ ), 1624 (m,  $\delta_{\text{N-H}}$ ).

*N-(4-Fluorobenzyl)-6-methoxy-4-methyl-(2,4'-bipyridine)-5-carboxamide (17)*

In a microwave vessel, compound **16a** (210 mg, 0.68 mmol) was dissolved in 1,4-dioxane (2 ml). Eight hundred and eighty microliters of a 2 M aq. solution of  $\text{Na}_2\text{CO}_3$  (1.76 mmol, 2.6 equiv.), tetrakis (triphenylphosphine)palladium(0) (79 mg, 0.07 mmol, 0.1 equiv.) and

pyridin-4-ylboronic acid (100 mg, 0.82 mmol, 1.2 equiv.) were added. Argon was passed through the reaction mixture for 30 min. Afterward, the mixture was heated in a microwave reactor at 140°C under stirring. After 30 min, the reaction mixture was cooled to room temperature, water (100 ml) was added, and the aq. suspension was extracted with ethyl acetate (100 ml). The organic phase was washed with brine, dried over Na<sub>2</sub>SO<sub>4</sub>, filtrated, and concentrated under reduced pressure. The crude residue was purified by flash chromatography (ethyl acetate/*n*-hexane, 70%–90% ethyl acetate) and subsequent recrystallization (methanol/water), which yielded **17** as a beige-colored solid (140 mg, 0.40 mmol, 59%). *R*<sub>f</sub> = 0.29 (ethyl acetate/*n*-hexane 3:1); mp: 139°C; <sup>1</sup>H-NMR (400 MHz, DMSO-*d*<sub>6</sub>): δ(ppm) = 8.93 (t, *J* = 6.1 Hz, 1H), 8.74–8.68 (m, 2H), 8.10–8.04 (m, 2H), 7.69 (d, *J* = 0.7 Hz, 1H), 7.47–7.38 (m, 2H), 7.26–7.15 (m, 2H), 4.46 (d, *J* = 6.0 Hz, 2H), 4.01 (s, 3H), 2.29 (s, 3H); <sup>13</sup>C-NMR (100 MHz, DMSO-*d*<sub>6</sub>): δ(ppm) = 165.2, 161.2 (d, *J* = 242.1 Hz), 159.8, 150.3, 150.0, 147.7, 144.8, 135.5 (d, *J* = 3.1 Hz), 129.1 (d, *J* = 8.2 Hz), 121.5, 120.6, 116.0, 115.0 (d, *J* = 21.3 Hz), 53.4, 41.5, 18.4; (ATR):  $\tilde{\nu}$  = 3330 (m,  $\nu_{\text{N-H}}$ ), 3023, 2951 (w,  $\nu_{\text{C-H}}$ ), 1633 (s,  $\nu_{\text{C=O}}$ ), 1594 (m,  $\delta_{\text{N-H}}$ ); ESI-HRAM-MS (*m/z*): calcd. for [C<sub>20</sub>H<sub>19</sub>N<sub>3</sub>O<sub>2</sub>F+H]<sup>+</sup> 352.1456, found 352.1463; cpd purity (220 nm): 99.5%.

#### N-(4-Fluorobenzyl)-2-methoxy-4-methyl-6-morpholinonicotinamide (**18a**)

The synthesis was conducted from **16a** (300 mg, 0.97 mmol) and morpholine in accordance with general procedure C. The crude residue was purified by flash chromatography (mobile phase: ethyl acetate/*n*-hexane with 50%–100% ethyl acetate) and successive recrystallization (methanol/water), which yielded **18a** as a colorless solid (126 mg, 0.35 mmol, 36%). *R*<sub>f</sub> = 0.60 (ethyl acetate/*n*-hexane 3:2); mp: 192°C; <sup>1</sup>H-NMR (400 MHz, DMSO-*d*<sub>6</sub>): δ(ppm) = 8.52 (t, *J* = 6.2 Hz, 1H), 7.43–7.33 (m, 2H), 7.21–7.10 (m, 2H), 6.22 (s, 1H), 4.38 (d, *J* = 6.1 Hz, 2H), 3.80 (s, 3H), 3.73–3.65 (m, 4H), 3.47–3.40 (m, 4H), 2.13 (s, 3H); <sup>13</sup>C-NMR (100 MHz, DMSO-*d*<sub>6</sub>): δ(ppm) = 166.1, 161.1 (d, *J* = 241.7 Hz), 158.8, 157.0, 148.6, 135.9 (d, *J* = 2.9 Hz), 128.9 (d, *J* = 8.1 Hz), 114.9 (d, *J* = 21.0 Hz), 109.6, 99.5, 65.9, 52.7, 45.0, 41.5, 19.2; IR (ATR):  $\tilde{\nu}$  = 3330 (m,  $\nu_{\text{N-H}}$ ), 3049, 2997 (w,  $\nu_{\text{C-H}}$ ), 1627 (s,  $\nu_{\text{C=O}}$ ); ESI-HRAM-MS (*m/z*): calcd. for [C<sub>19</sub>H<sub>23</sub>N<sub>3</sub>O<sub>3</sub>F+H]<sup>+</sup> 360.1718, found 360.1717; cpd purity (220 nm): 100.0%.

#### N-(4-Fluorobenzyl)-2-(propyl-2-oxy)-4-methyl-6-morpholinonicotinamide (**18b**)

The synthesis was conducted from **16b** (596 mg, 1.77 mmol) and morpholine in accordance with general procedure C. The crude residue was purified by silica gel column chromatography (ethyl acetate/*n*-hexane 1:1) and successive recrystallization (ethanol/water), which yielded **18b** as a colorless solid (356 mg, 0.92 mmol, 52%). *R*<sub>f</sub> = 0.54 (ethyl acetate/*n*-hexane 2:1); mp: 134°C; <sup>1</sup>H-NMR (400 MHz, DMSO-*d*<sub>6</sub>): δ(ppm) = 8.41 (t, *J* = 6.2 Hz, 1H), 7.45–7.36 (m, 2H), 7.19–7.09 (m, 2H), 6.20 (s, 1H), 5.16 (sept, *J* = 6.2 Hz, 1H), 4.39 (d, *J* = 6.1 Hz, 2H), 3.73–3.63 (m, 4H), 3.47–3.36 (m, 4H), 2.14 (s, 3H), 1.24 (d, *J* = 6.2 Hz, 6H); <sup>13</sup>C-NMR (100 MHz, DMSO-*d*<sub>6</sub>): δ(ppm) = 166.2, 161.0 (d, *J* = 241.7 Hz), 158.1,

157.0, 148.6, 135.9 (d, *J* = 3.0 Hz), 128.9 (d, *J* = 8.0 Hz), 114.7 (d, *J* = 21.2 Hz), 110.0, 99.4, 67.6, 65.8, 45.0, 41.4, 22.0, 19.2; (ATR):  $\tilde{\nu}$  = 3277 (m,  $\nu_{\text{N-H}}$ ), 2967 (w,  $\nu_{\text{C-H}}$ ), 1619 (s,  $\nu_{\text{C=O}}$ ), 1591 (m,  $\delta_{\text{N-H}}$ ); ESI-HRAM-MS (*m/z*): calcd. for [C<sub>21</sub>H<sub>27</sub>N<sub>3</sub>O<sub>3</sub>F+H]<sup>+</sup> 388.2031, found 388.2030; cpd purity (220 nm): 99.8%.

#### N-(4-Fluorobenzyl)-4-methyl-6-morpholino-2-(2,2,2-trifluoroethoxy)nicotinamide (**18c**)

The synthesis was conducted from **16c** (500 mg, 1.33 mmol) and morpholine in accordance with general procedure C. The crude residue was purified by silica gel column chromatography (ethyl acetate/*n*-hexane 1:1) and successive recrystallization (methanol/water), which yielded **18c** as a colorless solid (212 mg, 0.50 mmol, 37%). *R*<sub>f</sub> = 0.56 (ethyl acetate/*n*-hexane 3:2); mp: 164°C; <sup>1</sup>H-NMR (400 MHz, DMSO-*d*<sub>6</sub>): δ(ppm) = 8.61 (t, *J* = 6.1 Hz), 7.42–7.32 (m, 2H), 7.17–7.05 (m, 2H), 6.35 (s, 1H), 4.89 (q, *J* = 9.2 Hz, 2H), 4.39 (d, *J* = 6.0 Hz, 2H), 3.72–3.65 (m, 4H), 3.49–3.42 (m, 4H), 2.16 (s, 3H); <sup>13</sup>C-NMR (100 MHz, DMSO-*d*<sub>6</sub>): δ(ppm) = 165.38, 161.1 (d, *J* = 241.8 Hz), 156.7, 156.3, 149.4, 135.6 (d, *J* = 2.9 Hz), 128.8 (d, *J* = 8.0 Hz), 124.1 (q, *J* = 278.1 Hz), 114.7 (d, *J* = 21.2 Hz), 109.4, 101.0, 65.8, 61.2 (q, *J* = 34.5 Hz), 44.9, 41.5, 19.1; (ATR):  $\tilde{\nu}$  = 3291 (m,  $\nu_{\text{N-H}}$ ), 2978 (w,  $\nu_{\text{C-H}}$ ), 1617 (s,  $\nu_{\text{C=O}}$ ), 1602 (s,  $\delta_{\text{N-H}}$ ); ESI-HRAM-MS (*m/z*): calcd. for [C<sub>20</sub>H<sub>22</sub>N<sub>3</sub>O<sub>3</sub>F<sub>4</sub>+H]<sup>+</sup> 428.1592, found 428.1591; cpd purity (220 nm): 98.2%.

#### N-Butyl-2-methoxy-4-methyl-6-morpholinonicotinamide (**18d**)

The synthesis was conducted from **16d** (770 mg, 3.0 mmol) and morpholine in accordance with general procedure C. The crude residue was purified by flash chromatography (mobile phase: ethyl acetate/*n*-hexane with 0%–100% ethyl acetate) and successive recrystallization (ethanol/water), which yielded **18d** as a colorless solid (250 mg, 0.85 mmol, 28%). *R*<sub>f</sub> = 0.43 (ethyl acetate/*n*-hexane 2:1); mp: 135°C; <sup>1</sup>H-NMR (400 MHz, DMSO-*d*<sub>6</sub>): δ(ppm) = 7.93 (t, *J* = 5.7 Hz, 1H), 6.20 (s, 1H), 3.76 (s, 3H), 3.71–3.65 (m, 4H), 3.46–3.39 (m, 4H), 3.15 (td, *J* = 6.9, 5.7 Hz, 2H), 2.13 (s, 3H), 1.50–1.38 (m, 2H), 1.42–1.26 (m, 2H), 0.89 (t, *J* = 7.3 Hz, 3H); <sup>13</sup>C-NMR (100 MHz, DMSO-*d*<sub>6</sub>): δ(ppm) = 165.7, 158.7, 156.9, 148.3, 110.3, 99.4, 65.9, 52.6, 45.1, 38.4, 31.1, 19.5, 19.1, 13.7; (ATR):  $\tilde{\nu}$  = 3303 (m,  $\nu_{\text{N-H}}$ ), 3067, 2967 (w,  $\nu_{\text{C-H}}$ ), 1625 (s,  $\nu_{\text{C=O}}$ ), 1594 (m,  $\delta_{\text{N-H}}$ ); ESI-HRAM-MS (*m/z*): calcd. for [C<sub>16</sub>H<sub>26</sub>N<sub>3</sub>O<sub>3</sub>+H]<sup>+</sup> 308.1969, found 308.1968; cpd purity (220 nm): 99.7%.

#### N-(4-Fluorobenzyl)-2-methoxy-4-methyl-6-(piperidin-1-yl)nicotinamide (**18e**)

The synthesis was conducted from **16a** (400 mg, 1.30 mmol) and piperidine in accordance with general procedure C. The crude residue was purified by flash chromatography (mobile phase: ethyl acetate/*n*-hexane with 30%–70% ethyl acetate) and successive recrystallization (methanol/water), which yielded **18e** as a colorless solid (161 mg, 0.45 mmol, 35%). *R*<sub>f</sub> = 0.76 (ethyl acetate/*n*-hexane 1:1); mp: 147°C; <sup>1</sup>H-NMR (400 MHz, DMSO-*d*<sub>6</sub>): δ(ppm) = 8.49 (t, *J* = 6.2 Hz, 1H), 7.48–7.30 (m, 2H), 7.26–7.05 (m, 2H), 6.19 (s, 1H), 4.38 (d, *J* = 6.1 Hz, 2H), 3.79 (s, 3H), 3.65–3.40 (m, 4H), 2.13 (s, 3H), 1.67–1.57 (m, 2H), 1.57–1.48 (m, 4H); <sup>13</sup>C-NMR (100 MHz, DMSO-*d*<sub>6</sub>): δ(ppm) = 166.2, 161.0 (d, *J* = 241.8 Hz), 158.9, 156.7, 148.6, 136.0 (d, *J* = 2.9 Hz), 128.9 (d,

$J = 8.2$  Hz), 114.8 (d,  $J = 21.1$  Hz), 108.1, 99.4, 52.6, 45.5, 41.5, 24.9, 24.3, 19.3; (ATR):  $\tilde{\nu} = 3335$  (m,  $\nu_{N-H}$ ), 2948 (w,  $\nu_{C-H}$ ), 1626 (s,  $\nu_{C=O}$ ), 1593 (s,  $\delta_{N-H}$ ); ESI-HRAM-MS ( $m/z$ ): calcd. for  $[C_{20}H_{25}N_3O_2F+H]^+$  358.1925, found 358.1954; cpd purity (220 nm): 99.7%.

*N*-(4-Fluorobenzyl)-2-isopropoxy-4-methyl-6-(2-oxa-6-azaspiro[3.3]heptan-6-yl)nicotinamide (**18f**)

The synthesis was conducted from **16b** (500 mg, 1.49 mmol) and 2-oxa-6-azaspiro[3.3]heptane oxalate (856 mg, 2.97 mmol, 2.0 equiv.) following general procedure C. Deviating from general procedure C, DBU (665  $\mu$ l, 4.45 mmol, 3.0 equiv.) was added to the reaction mixture. The crude residue was purified by flash chromatography (mobile phase: ethyl acetate/*n*-hexane with 60%–100% ethyl acetate), which yielded **18f** as a slightly yellow solid (314 mg, 0.79 mmol, 53%).  $R_f = 0.32$  (ethyl acetate/*n*-hexane 1:1); mp: 146°C;  $^1H$ -NMR (400 MHz, DMSO- $d_6$ ):  $\delta$ (ppm) = 8.39 (t,  $J = 6.2$  Hz, 1H), 7.45–7.36 (m, 2H), 7.19–7.09 (m, 2H), 5.77 (s, 1H), 5.17 (sept,  $J = 6.2$  Hz, 1H), 4.71 (s, 4H), 4.38 (d,  $J = 6.1$  Hz, 2H), 4.06 (s, 4H), 2.11 (s, 3H), 1.25 (d,  $J = 6.2$  Hz, 6H);  $^{13}C$ -NMR (100 MHz, DMSO- $d_6$ ):  $\delta$  (ppm) = 166.3, 161.0 (d,  $J = 241.6$  Hz), 158.7, 158.5, 148.0, 135.9 (d,  $J = 2.9$  Hz), 128.9 (d,  $J = 8.0$  Hz), 114.7 (d,  $J = 21.1$  Hz), 109.7, 98.3, 79.9, 67.5, 59.6, 41.4, 38.3, 22.0, 18.9; (ATR):  $\tilde{\nu} = 3329$  (m,  $\nu_{N-H}$ ), 2932 (m,  $\nu_{C-H}$ ), 1628 (s,  $\nu_{C=O}$ ), 1591 (s,  $\delta_{N-H}$ ); ESI-HRAM-MS ( $m/z$ ): calcd. for  $[C_{22}H_{27}N_3O_3F+H]^+$  400.2031, found 400.2033; cpd purity (220 nm): 98.4%.

*N*-(4-Fluorobenzyl)-4-methyl-6-morpholino-2-oxo-1,2-dihydropyridine-3-carboxamide (**19a**)

Compound **19a** was a side product in the synthesis of **18a**. It was separated from the main product by flash chromatography and further purified by recrystallization (methanol/water). The title compound was obtained as a colorless solid (132 mg, 0.38 mmol, 39%).  $R_f = 0.42$  (ethyl acetate); mp: 225°C (decomp.);  $^1H$ -NMR (400 MHz, DMSO- $d_6$ ):  $\delta$  (ppm) = 11.12 (s, 1H), 9.73 (s, 1H), 7.39–7.29 (m, 2H), 7.18–7.08 (m, 2H), 5.76 (s, 1H), 4.40 (d,  $J = 5.9$  Hz, 2H), 3.70–3.63 (m, 4H), 3.42–3.35 (m, 4H), 2.41 (s, 3H);  $^{13}C$ -NMR (100 MHz, DMSO- $d_6$ ):  $\delta$ (ppm) = 166.3, 162.4, 161.0 (d,  $J = 241.8$  Hz), 155.8, 152.8, 136.3 (d,  $J = 3.0$  Hz), 129.0 (d,  $J = 8.0$  Hz), 114.9 (d,  $J = 21.2$  Hz), 106.3, 95.2, 65.5, 46.0, 41.2, 22.7; IR (ATR):  $\tilde{\nu} = 3303$  (m,  $\nu_{N-H}$ ), 3060, 2924 (w,  $\nu_{C-H}$ ), 1656 (s,  $\nu_{C=O}$ ); ESI-HRAM-MS ( $m/z$ ): calcd. for  $[C_{18}H_{20}N_3O_3F+H]^+$  346.1561, found 346.1564; cpd purity (220 nm): 100.0%.

6-(3,6-Dihydro-2H-pyran-4-yl)-*N*-(4-fluorobenzyl)-2-methoxy-4-methylnicotinamide (**20**)

In a microwave vessel, **16a** (600 mg, 1.94 mmol) was dissolved in 1,4-dioxane (4 ml). 1.76 ml of a 2 M aq. solution of  $Na_2CO_3$  (3.5 mmol, 1.8 equiv.), tetrakis(triphenylphosphine)palladium(0) (112 mg, 0.10 mmol, 0.05 equiv.) and 2-(cyclohex-1-en-1-yl)-4,4,5,5-tetramethyl-1,3,2-dioxaborolane (490 mg, 2.33 mmol, 1.2 equiv.) were added. Argon was passed through the reaction mixture for 30 min. Afterward, the mixture was heated in a microwave reactor at 140°C. After 15 min, the reaction mixture was cooled to room temperature, water (100 ml) was added, and the aq. suspension was extracted with ethyl acetate (100 ml). The organic phase was washed with brine, dried over

$Na_2SO_4$ , filtrated, and concentrated under reduced pressure. The crude residue was purified by flash chromatography (ethyl acetate/*n*-hexane, 10%–30% ethyl acetate) and successive recrystallization (methanol/water), which yielded **20** as a colorless solid (595 mg, 1.67 mmol, 86%).  $R_f = 0.50$  (ethyl acetate/*n*-hexane 1:1); mp: 167°C;  $^1H$ -NMR (400 MHz,  $CDCl_3$ ):  $\delta$ (ppm) = 7.48–7.30 (m, 2H), 7.14–6.96 (m, 2H), 6.89–6.78 (m, 2H), 6.58 (s, 1H), 4.64 (d,  $J = 5.8$  Hz, 2H), 4.49–4.32 (m, 2H), 3.98 (s, 3H), 3.94 (t,  $J = 5.5$  Hz, 2H), 2.65–2.54 (m, 2H), 2.45 (s, 3H);  $^{13}C$ -NMR (100 MHz,  $CDCl_3$ ):  $\delta$ (ppm) = 166.5, 162.4 (d,  $J = 245.4$  Hz), 159.8, 154.3, 150.1, 134.3 (d,  $J = 3.3$  Hz), 133.4, 129.5 (d,  $J = 8.1$  Hz), 127.1, 117.2, 115.7 (d,  $J = 21.4$  Hz), 114.7, 66.0, 64.5, 53.7, 43.2, 25.8, 20.4; (ATR):  $\tilde{\nu} = 3325$  (m,  $\nu_{N-H}$ ), 1631 (s,  $\nu_{C=O}$ ), 1590 (m,  $\delta_{N-H}$ ); ESI-HRAM-MS ( $m/z$ ): calcd. for  $[C_{20}H_{22}N_2O_3F+H]^+$  357.1609, found 357.1607; cpd purity (220 nm): 99.5%.

*N*-(4-Fluorobenzyl)-2-methoxy-4-methyl-6-(oxan-4-yl)nicotinamide (**21**)

Compound **20** (250 mg, 0.70 mmol) was dissolved in methanol (20 ml). Pd/C (10% Pd, 50% water wet, 150 mg) was added, the suspension was carefully set under a hydrogen atmosphere (balloon pressure), and the reaction mixture was stirred at room temperature. After 5 h, the resulting mixture was filtered through a pad of celite, and the filtrate was concentrated under reduced pressure. The crude residue was purified by silica gel column chromatography (ethyl acetate/*n*-hexane 2:3) and successive recrystallization (methanol/water) to obtain **21** as a colorless solid (186 mg, 0.52 mmol, 74%).  $R_f = 0.46$  (ethyl acetate/*n*-hexane 1:1); mp: 124°C;  $^1H$ -NMR (400 MHz, DMSO- $d_6$ ):  $\delta$ (ppm) = 8.81 (t,  $J = 6.1$  Hz, 1H), 7.50–7.31 (m, 2H), 7.28–7.06 (m, 2H), 6.77 (s, 1H), 4.41 (d,  $J = 6.1$  Hz, 2H), 4.02–3.90 (m, 2H), 3.86 (s, 3H), 3.50–3.36 (m, 2H), 2.91–2.73 (m, 1H), 2.16 (s, 3H), 1.83–1.70 (m, 4H);  $^{13}C$ -NMR (100 MHz, DMSO- $d_6$ ):  $\delta$ (ppm) = 165.6, 161.3, 160.8 (d,  $J = 241.0$  Hz), 159.2, 146.7, 135.6 (d,  $J = 3.0$  Hz), 129.0 (d,  $J = 8.1$  Hz), 118.8, 115.5, 114.9 (d,  $J = 21.2$  Hz), 67.0, 53.0, 41.8, 41.4, 31.7, 18.2; (ATR):  $\tilde{\nu} = 3351$  (m,  $\nu_{N-H}$ ), 3051, 2949 (w,  $\nu_{C-H}$ ), 1634 (s,  $\nu_{C=O}$ ), 1596 (m,  $\delta_{N-H}$ ); ESI-HRAM-MS ( $m/z$ ): calcd. for  $[C_{20}H_{24}N_2O_3F+H]^+$  359.1765, found 359.1759; cpd purity (220 nm): 100.0%.

6-Chloro-2-methoxynicotinic acid (**23**)

The synthesis was conducted from 2,6-dichloronicotinic acid (1.00 g, 5.2 mmol) and methanol in accordance with general procedure A. The crude residue was purified by recrystallization (toluene/*n*-hexane) to obtain **23** as a slightly pink-colored solid (768 mg, 4.09 mmol, 79%).  $R_f = 0.68$  (ethyl acetate/toluene/acetic acid 5:5:1); mp: 176°C;  $^1H$ -NMR (400 MHz, DMSO- $d_6$ ):  $\delta$ (ppm) = 13.14 (s, 1H), 8.16 (d,  $J = 7.8$  Hz, 1H), 7.18 (d,  $J = 7.9$  Hz, 1H), 3.92 (s, 3H);  $^{13}C$ -NMR (100 MHz, DMSO- $d_6$ ):  $\delta$  (ppm) = 165.1, 161.4, 150.2, 143.9, 116.5, 113.8, 54.4; (ATR):  $\tilde{\nu} = 2958$  (w,  $\nu_{C-H}$ ), 3200–2500 (b,  $\nu_{O-H}$ ), 1687 (s,  $\nu_{C=O}$ ).

6-Chloro-*N*-(4-fluorobenzyl)-2-methoxynicotinamide (**24**)

The synthesis was conducted from **23** (300 mg, 1.60 mmol) and 4-fluorobenzylamine in accordance with general procedure D. The crude residue was purified by flash chromatography (mobile phase: ethyl acetate/*n*-hexane with 10–70% ethyl acetate) and successive

recrystallization (methanol/water), which yielded **24** as a beige-colored solid (308 mg, 1.05 mmol, 65%).  $R_f = 0.52$  (ethyl acetate/*n*-hexane 1:3); mp: 101°C;  $^1\text{H-NMR}$  (400 MHz, DMSO- $d_6$ ):  $\delta(\text{ppm}) = 8.80$  (t,  $J = 6.0$  Hz, 1H), 8.15 (d,  $J = 7.9$  Hz, 1H), 7.42–7.32 (m, 2H), 7.22 (d,  $J = 7.9$  Hz, 1H), 7.21–7.11 (m, 2H), 4.48 (d,  $J = 6.1$  Hz, 2H), 3.98 (s, 3H);  $^{13}\text{C-NMR}$  (100 MHz, DMSO- $d_6$ ):  $\delta(\text{ppm}) = 162.9$ , 161.1 (d,  $J = 241.6$  Hz), 159.9, 148.8, 142.9, 135.5 (d,  $J = 3.0$  Hz), 129.1 (d,  $J = 8.1$  Hz), 117.0, 116.6, 115.0 (d,  $J = 21.4$  Hz), 54.6, 42.0; (ATR):  $\tilde{\nu} = 3416$  (m,  $\nu_{\text{N-H}}$ ), 3091, 2953 (w,  $\nu_{\text{C-H}}$ ), 1652 (s,  $\nu_{\text{C=O}}$ ), 1582 (m,  $\delta_{\text{N-H}}$ ).

#### *N*-(4-Fluorobenzyl)-2-methoxy-6-morpholinonicotinamide (**25**)

The synthesis was conducted from **24** (250 mg, 0.85 mmol) and morpholine in accordance with general procedure C. The crude residue was purified by flash chromatography (mobile phase: ethyl acetate/*n*-hexane with 70%–100% ethyl acetate) and successive recrystallization (methanol/water), which yielded **25** as a colorless solid (105 mg, 0.30 mmol, 36%).  $R_f = 0.46$  (ethyl acetate/*n*-hexane 1:1); mp: 129°C;  $^1\text{H-NMR}$  (400 MHz, DMSO- $d_6$ ):  $\delta(\text{ppm}) = 8.41$  (t,  $J = 6.1$  Hz, 1H), 8.05 (d,  $J = 8.5$  Hz, 1H), 7.42–7.26 (m, 2H), 7.20–7.08 (m, 2H), 6.46 (d,  $J = 8.7$  Hz, 1H), 4.46 (d,  $J = 6.1$  Hz, 2H), 3.94 (s, 3H), 3.76–3.63 (m, 4H), 3.62–3.49 (m, 4H);  $^{13}\text{C-NMR}$  (100 MHz, DMSO- $d_6$ ):  $\delta(\text{ppm}) = 163.7$ , 161.0 (d,  $J = 242.0$  Hz), 159.7, 158.5, 142.3, 136.3 (d,  $J = 3.0$  Hz), 129.0 (d,  $J = 8.1$  Hz), 114.9 (d,  $J = 21.2$  Hz), 103.4, 98.8, 65.8, 53.2, 44.6, 41.8; (ATR):  $\tilde{\nu} = 3403$  (m,  $\nu_{\text{N-H}}$ ), 2987 (w,  $\nu_{\text{C-H}}$ ), 1642 (s,  $\nu_{\text{C=O}}$ ), 1596 (s,  $\delta_{\text{N-H}}$ ); ESI-HRAM-MS ( $m/z$ ): calcd. for  $[\text{C}_{18}\text{H}_{21}\text{N}_3\text{O}_3\text{F}+\text{H}]^+$  346.1561, found 346.1558; cpd purity (220 nm): 98.7%.

#### 2,6-Dichloro-*N*-(4-fluorobenzyl)-4-methylnicotinamide (**26a**)

The synthesis was conducted from 2,6-dichloro-4-methylnicotinic acid (1.19 g, 5.8 mmol) and 4-fluorobenzylamine in accordance with general procedure D. The crude residue was purified by flash chromatography (mobile phase: ethyl acetate/*n*-hexane with 10%–50% ethyl acetate) and successive recrystallization (acetone/water), which yielded **26a** as a pale yellow solid (835 mg, 2.66 mmol, 46%).  $R_f = 0.77$  (ethyl acetate/*n*-hexane 1:1); mp: 161°C;  $^1\text{H-NMR}$  (400 MHz, DMSO- $d_6$ ):  $\delta(\text{ppm}) = 9.17$  (t,  $J = 5.9$  Hz, 1H), 7.57 (d,  $J = 0.8$  Hz, 1H), 7.46–7.36 (m, 2H), 7.25–7.14 (m, 2H), 4.46 (d,  $J = 5.9$  Hz, 2H), 2.26 (d,  $J = 0.7$  Hz, 3H);  $^{13}\text{C-NMR}$  (100 MHz, DMSO- $d_6$ ):  $\delta(\text{ppm}) = 163.9$ , 161.3 (d,  $J = 242.5$  Hz), 151.2, 148.2, 145.4, 134.8 (d,  $J = 3.0$  Hz), 132.6, 129.6 (d,  $J = 8.2$  Hz), 124.6, 115.1 (d,  $J = 21.3$  Hz), 41.8; (ATR):  $\tilde{\nu} = 3249$  (m,  $\nu_{\text{N-H}}$ ), 3078 (w,  $\nu_{\text{C-H}}$ ), 1638 (s,  $\nu_{\text{C=O}}$ ).

#### 2,6-Dichloro-*N*-(4-fluorobenzyl)nicotinamide (**26b**)

The synthesis was conducted from 2,6-dichloronicotinic acid (500 mg, 2.60 mmol) and 4-fluorobenzylamine in accordance with general procedure D. The crude residue was purified by silica gel column chromatography (ethyl acetate/*n*-hexane 1:1) and successive recrystallization (methanol/water), which yielded **26b** as a colorless solid (673 mg, 2.25 mmol, 86%).  $R_f = 0.63$  (ethyl acetate/*n*-hexane 1:1); mp: 168°C;  $^1\text{H-NMR}$  (400 MHz, DMSO- $d_6$ ):  $\delta(\text{ppm}) = 9.16$  (t,  $J = 5.9$  Hz, 1H), 8.03 (d,  $J = 8.0$  Hz, 1H), 7.67 (d,  $J = 8.0$  Hz, 1H), 7.50–7.32 (m, 2H), 7.26–7.11 (m, 2H), 4.46 (d,  $J = 5.9$  Hz, 2H);  $^{13}\text{C-NMR}$  (100 MHz, DMSO- $d_6$ ):  $\delta(\text{ppm}) = 164.2$ , 161.3 (d,  $J = 242.5$  Hz),

149.2, 145.8, 141.2, 134.8 (d,  $J = 3.0$  Hz), 132.1, 129.3 (d,  $J = 8.1$  Hz), 123.6, 115.1 (d,  $J = 21.3$  Hz), 41.9; (ATR):  $\tilde{\nu} = 3253$  (m,  $\nu_{\text{N-H}}$ ), 3052 (w,  $\nu_{\text{C-H}}$ ), 1638 (s,  $\nu_{\text{C=O}}$ ), 1574 (m,  $\delta_{\text{N-H}}$ ).

#### 2-Chloro-*N*-(4-fluorobenzyl)-4-methyl-6-morpholinonicotinamide (**27a**)

Compound **26a** (600 mg, 1.92 mmol) was dissolved in 2-propanol (50 ml). Morpholine (835  $\mu\text{l}$ , 9.58 mmol, 5.0 equiv.) was added, and the reaction mixture was stirred under reflux. After 3 d, it was cooled to room temperature, and all volatiles were removed under reduced pressure. The crude residue was purified by flash chromatography (mobile phase: ethyl acetate/*n*-hexane with 50%–100% ethyl acetate), which yielded **27a** as a pale yellow solid (160 mg, 0.44 mmol, 23%).  $R_f = 0.26$  (ethyl acetate/*n*-hexane 1:1); mp: 186°C;  $^1\text{H-NMR}$  (400 MHz, DMSO- $d_6$ ):  $\delta(\text{ppm}) = 8.88$  (t,  $J = 6.0$  Hz, 1H), 7.45–7.33 (m, 2H), 7.22–7.12 (m, 2H), 6.70 (s, 1H), 4.40 (d,  $J = 6.0$  Hz, 2H), 3.73–3.60 (m, 4H), 3.51–3.38 (m, 4H), 2.14 (s, 3H);  $^{13}\text{C-NMR}$  (100 MHz, DMSO- $d_6$ ):  $\delta(\text{ppm}) = 165.5$ , 161.2 (d,  $J = 242.1$  Hz), 157.9, 148.5, 144.4, 135.4 (d,  $J = 3.0$  Hz), 129.4 (d,  $J = 8.1$  Hz), 122.5, 115.0 (d,  $J = 21.3$  Hz), 106.1, 65.8, 44.9, 41.7, 19.1.

#### 2-Chloro-*N*-(4-fluorobenzyl)-6-morpholinonicotinamide (**27b**)

Compound **26b** (600 mg, 2.01 mmol) was dissolved in methanol (30 ml). Morpholine (437  $\mu\text{l}$ , 5.02 mmol, 2.5 equiv.) was added, and the reaction mixture was stirred under reflux. After 24 h, it was cooled to room temperature, and all volatiles were removed under reduced pressure. The crude residue was purified by flash chromatography (mobile phase: ethyl acetate/*n*-hexane with 50%–100% ethyl acetate), which yielded **27b** as a pale yellow solid (180 mg, 0.51 mmol, 26%).  $R_f = 0.33$  (ethyl acetate/*n*-hexane 1:1); mp: 153°C;  $^1\text{H-NMR}$  (400 MHz, DMSO- $d_6$ ):  $\delta(\text{ppm}) = 8.77$  (t,  $J = 6.1$  Hz, 1H), 7.67 (d,  $J = 8.6$  Hz, 1H), 7.40–7.31 (m, 2H), 7.20–7.10 (m, 2H), 6.81 (d,  $J = 8.6$  Hz, 1H), 4.39 (d,  $J = 6.0$  Hz, 2H), 3.70–3.63 (m, 4H), 3.53–3.44 (m, 4H);  $^{13}\text{C-NMR}$  (100 MHz, DMSO- $d_6$ ):  $\delta(\text{ppm}) = 165.4$ , 161.2 (d,  $J = 242.1$  Hz), 158.4, 145.1, 139.9, 135.4 (d,  $J = 3.0$  Hz), 129.2 (d,  $J = 8.3$  Hz), 120.2, 115.0 (d,  $J = 21.3$  Hz), 104.8, 65.7, 44.7, 41.9; (ATR):  $\tilde{\nu} = 3261$  (m,  $\nu_{\text{N-H}}$ ), 2970 (w,  $\nu_{\text{C-H}}$ ), 1623 (s,  $\nu_{\text{C=O}}$ ), 1556 (m,  $\delta_{\text{N-H}}$ ).

#### *N*-(4-Fluorobenzyl)-4-methyl-6-morpholinonicotinamide (**28a**)

The synthesis was conducted from **27a** (130 mg, 0.36 mmol) following general procedure E. The crude residue was purified by silica gel column chromatography (ethyl acetate) and successive recrystallization (methanol/water) to obtain **28a** as a colorless solid (75 mg, 0.23 mmol, 64%).  $R_f = 0.34$  (ethyl acetate/*n*-hexane 3:1); mp: 192°C;  $^1\text{H-NMR}$  (400 MHz, DMSO- $d_6$ ):  $\delta(\text{ppm}) = 8.71$  (t,  $J = 6.0$  Hz, 1H), 8.23 (s, 1H), 7.41–7.31 (m, 2H), 7.21–7.11 (m, 2H), 6.70 (s, 1H), 4.40 (d,  $J = 6.0$  Hz, 2H), 3.72–3.65 (m, 4H), 3.53–3.46 (m, 4H), 2.34 (s, 3H);  $^{13}\text{C-NMR}$  (100 MHz, DMSO- $d_6$ ):  $\delta(\text{ppm}) = 167.1$ , 161.1 (d,  $J = 242.1$  Hz), 159.4, 147.3, 146.9, 135.9 (d,  $J = 3.2$  Hz), 129.0 (d,  $J = 8.1$  Hz), 121.9, 115.0 (d,  $J = 21.3$  Hz), 107.8, 65.9, 44.8, 41.7, 20.0; (ATR):  $\tilde{\nu} = 3285$  (m,  $\nu_{\text{N-H}}$ ), 2930 (w,  $\nu_{\text{C-H}}$ ), 1621 (s,  $\nu_{\text{C=O}}$ ), 1604 (m,  $\delta_{\text{N-H}}$ ); ESI-HRAM-MS ( $m/z$ ): calcd. for  $[\text{C}_{18}\text{H}_{21}\text{N}_3\text{O}_2\text{F}+\text{H}]^+$  330.1612, found 330.1616; cpd purity (220 nm): 99.6%.

*N*-(4-Fluorobenzyl)-6-morpholinonicotinamide (28b)

The synthesis was conducted from **27b** (110 mg, 0.32 mmol) following general procedure E. The crude residue was purified by silica gel column chromatography (ethyl acetate) and successive recrystallization (methanol/water) to obtain **28b** as a colorless solid (64 mg, 0.20 mmol, 65%).  $R_f = 0.43$  (ethyl acetate/*n*-hexane 3:1); mp: 212°C;  $^1\text{H-NMR}$  (400 MHz, DMSO- $d_6$ ):  $\delta$ (ppm) = 8.83 (t,  $J = 6.0$  Hz, 1H), 8.66 (d,  $J = 2.5$  Hz, 1H), 8.01 (dd,  $J = 9.0, 2.5$  Hz, 1H), 7.39–7.29 (m, 2H), 7.19–7.09 (m, 2H), 6.86 (d,  $J = 9.0$  Hz, 1H), 4.43 (d,  $J = 5.9$  Hz, 2H), 3.72–3.65 (m, 4H), 3.59–3.52 (m, 4H);  $^{13}\text{C-NMR}$  (100 MHz, DMSO- $d_6$ ):  $\delta$ (ppm) = 164.9, 161.1 (d,  $J = 241.0$  Hz), 160.0, 147.9, 136.5, 136.0 (d,  $J = 3.0$  Hz), 129.2 (d,  $J = 8.1$  Hz), 118.8, 114.9 (d,  $J = 21.2$  Hz), 105.6, 65.9, 44.7, 41.7; (ATR):  $\tilde{\nu} = 3298$  (m,  $\nu_{\text{N-H}}$ ), 2966 (w,  $\nu_{\text{C-H}}$ ), 1627 (s,  $\nu_{\text{C=O}}$ ), 1597 (s,  $\delta_{\text{N-H}}$ ); ESI-HRAM-MS ( $m/z$ ): calcd. for  $[\text{C}_{17}\text{H}_{19}\text{N}_3\text{O}_2\text{F}+\text{H}]^+$  316.1456, found 316.1463; cpd purity (220 nm): 97.9%.

*N*-(4-Fluorobenzyl)-2-isopropoxy-4-methylnicotinamide (29)

The synthesis was conducted from **16b** (1.00 g, 3.0 mmol) following general procedure E. The crude residue was purified by silica gel column chromatography (ethyl acetate/*n*-hexane 2:3) and successive recrystallization (methanol/water) to obtain **29** as a colorless solid (591 mg, 1.96 mmol, 66%).  $R_f = 0.57$  (ethyl acetate/*n*-hexane 1:1); mp: 107°C;  $^1\text{H-NMR}$  (400 MHz, DMSO- $d_6$ ):  $\delta$ (ppm) = 8.78 (t,  $J = 6.2$  Hz, 1H), 8.02 (d,  $J = 5.2$  Hz, 1H), 7.48–7.38 (m, 2H), 7.21–7.10 (m, 2H), 6.84 (d,  $J = 5.3$  Hz, 1H), 5.24 (sept,  $J = 6.2$  Hz, 1H), 4.43 (d,  $J = 6.1$  Hz, 2H), 2.18 (s, 3H), 1.26 (d,  $J = 6.2$  Hz, 6H);  $^{13}\text{C-NMR}$  (100 MHz, DMSO- $d_6$ ):  $\delta$ (ppm) = 165.5, 161.1 (d,  $J = 241.8$  Hz), 159.2, 146.2, 146.0, 135.6 (d,  $J = 3.0$  Hz), 128.9 (d,  $J = 8.1$  Hz), 121.5, 118.3, 114.8 (d,  $J = 21.2$  Hz), 67.9, 41.3, 21.9, 18.1; (ATR):  $\tilde{\nu} = 3283$  (m,  $\nu_{\text{N-H}}$ ), 3066, 2992 (w,  $\nu_{\text{C-H}}$ ), 1629 (s,  $\nu_{\text{C=O}}$ ), 1588 (m,  $\delta_{\text{N-H}}$ ); ESI-HRAM-MS ( $m/z$ ): calcd. for  $[\text{C}_{17}\text{H}_{20}\text{N}_2\text{O}_3\text{F}+\text{H}]^+$  303.1503, found 303.1498; cpd purity (220 nm): 99.4%.

*Ethyl 4-ethyl-6-methyl-2-oxo-1,2,3,4-tetrahydropyrimidine-5-carboxylate* (33)

Urea (16.5 g, 275 mmol, 1.1 equiv.) was suspended in ethanol (60 ml). Afterward, ethyl 3-oxobutanoate (31.6 ml, 250 mmol), propanal (19.7 ml, 275 mmol, 1.1 equiv.), and a catalytic amount of acetic acid were added. The mixture was stirred in a closed vessel at 90°C. After 20 h, the reaction mixture was poured into water. The resulting precipitate was filtered off and recrystallized from ethanol. Finally the recrystallized product was washed with a small amount of a mixture of ethanol and water (1:1) to obtain **33** as a colorless solid (17.0 g, 80 mmol 32%).  $R_f = 0.41$  (ethyl acetate); mp: 183°C (lit mp: 179°C–181°C)<sup>[62]</sup>;  $^1\text{H-NMR}$  (400 MHz, DMSO- $d_6$ ):  $\delta$ (ppm) = 8.91 (s, 1H), 7.28 (s, 1H), 4.15–3.99 (m, 3H), 2.17 (s, 3H), 1.42 (qd,  $J = 7.4, 5.3$  Hz, 2H), 1.19 (t,  $J = 7.1$  Hz, 3H), 0.79 (t,  $J = 7.4$  Hz, 3H);  $^{13}\text{C-NMR}$  (100 MHz, DMSO- $d_6$ ):  $\delta$ (ppm) = 165.5, 152.8, 148.4, 98.8, 59.0, 51.3, 29.6, 17.7, 14.2, 8.5; IR (ATR):  $\tilde{\nu} = 3241, 3117$  (m,  $\nu_{\text{N-H}}$ ), 2960 (w,  $\nu_{\text{C-H}}$ ), 1720, 1701 (s,  $\nu_{\text{C=O}}$ ).

*Ethyl 6-ethyl-4-methyl-2-oxo-1,2-dihydropyrimidine-5-carboxylate* (34)

Nitric acid (50%, 25 ml) was cooled to  $-10^\circ\text{C}$ . Subsequently, compound **33** (8.50 g, 40.1 mmol) was added in portions over a period of 5 min

while maintaining the temperature at  $-10^\circ\text{C}$ . After complete addition, the mixture was stirred additional 10 min at  $-10^\circ\text{C}$ . Afterward,  $\text{K}_2\text{CO}_3$  was added to adjust the pH to 7. The resulting aq. solution was extracted with ethyl acetate (10 × 100 ml). The combined organic phases were washed with brine, dried over  $\text{Na}_2\text{SO}_4$ , filtrated, and concentrated under reduced pressure to obtain **34** as an orange solid (7.30 g, 34.7 mmol, 87%).  $R_f = 0.45$  (DCM/methanol 9:1); mp: 99°C;  $^1\text{H-NMR}$  (400 MHz, DMSO- $d_6$ ):  $\delta$ (ppm) = 12.14 (s, 1H), 4.27 (q,  $J = 7.1$  Hz, 2H), 2.64 (q,  $J = 7.5$  Hz, 2H), 2.33 (s, 3H), 1.29 (t,  $J = 7.1$  Hz, 3H), 1.14 (t,  $J = 7.5$  Hz, 3H);  $^{13}\text{C-NMR}$  (100 MHz, DMSO- $d_6$ ):  $\delta$ (ppm) = 165.4, 155.2, 108.5, 61.0, 27.9, 20.8, 13.9, 12.5 (two  $^{13}\text{C}$  signals are apparently missing, possibly due to overlapping since the number of  $^{13}\text{C}$  signals of the predecessor compound **33** and the successor compound **35** is correct); IR (ATR):  $\tilde{\nu} = 2978$  (w,  $\nu_{\text{C-H}}$ ), 1709, 1645 (s,  $\nu_{\text{C=O}}$ ), 1556 (m,  $\delta_{\text{N-H}}$ ).

*Ethyl 2-chloro-6-ethyl-4-methyl-1,2-dihydropyrimidine-5-carboxylate* (35)

Compound **34** (1.10 g, 5.2 mmol) was dissolved in phosphorus oxychloride (3.20 ml, 18.4 mmol, 10.6 equiv.) and stirred for 1 h at  $110^\circ\text{C}$ . Subsequently, all volatiles were removed under reduced pressure. The residue was suspended in ice water (100 ml), and the resulting suspension was extracted with ethyl acetate (3 × 100 ml). The combined organic phases were washed with brine, dried over  $\text{Na}_2\text{SO}_4$ , filtrated, and concentrated under reduced pressure. The crude residue was purified by silica gel column chromatography (ethyl acetate/*n*-hexane 1:3), which yielded **35** as an orange liquid (540 mg, 2.36 mmol, 45%).  $R_f = 0.74$  (ethyl acetate/*n*-hexane 1:3);  $^1\text{H-NMR}$  (400 MHz, DMSO- $d_6$ ):  $\delta$ (ppm) = 4.41 (q,  $J = 7.1$  Hz, 2H), 2.75 (q,  $J = 7.5$  Hz, 2H), 2.48 (s, 3H), 1.33 (t,  $J = 7.1$  Hz, 3H), 1.20 (t,  $J = 7.5$  Hz, 3H);  $^{13}\text{C-NMR}$  (100 MHz, DMSO- $d_6$ ):  $\delta$ (ppm) = 171.7, 167.7, 165.8, 159.5, 124.8, 62.1, 28.3, 22.2, 13.8, 12.4; IR (ATR):  $\tilde{\nu} = 2981$  (w,  $\nu_{\text{C-H}}$ ), 1726 (s,  $\nu_{\text{C=O}}$ ).

*2-Chloro-4-ethyl-6-methylpyrimidine-5-carboxylic acid* (36)

Compound **35** (2.74 g, 12.0 mmol) was dissolved in THF (20 ml). The resulting solution was added to a solution of KOH (1.87 g, 47.9 mmol, 4.0 equiv.) in water (80 ml). The resulting mixture was stirred at room temperature for 12 h. Afterward, it was extracted with ethyl acetate (100 ml). The organic phase was discarded, and the aq. phase was acidified to pH 2–3 with conc. aq. HCl. Subsequently, it was extracted with ethyl acetate again (5 × 100 ml). The combined organic phases were washed with brine, dried over  $\text{Na}_2\text{SO}_4$ , filtrated, and concentrated under reduced pressure. The resulting dark brown solid (1.74 g, 8.7 mmol, 72%) was used for the following reaction without characterization or any further purification.

*2-Chloro-4-ethyl-N*-(4-fluorobenzyl)-6-methylpyrimidine-5-carboxamide (37)

Compound **36** (650 mg, 3.24 mmol), HATU (1.48 g, 3.9 mmol, 1.2 equiv.), DIPEA (1130  $\mu\text{l}$ , 6.48 mmol, 2.0 equiv.) and 4-fluorobenzylamine (555  $\mu\text{l}$ , 4.86 mmol, 1.5 equiv.) were successively dissolved in DMF (10 ml). The mixture was stirred at room temperature. After 8 h, the reaction was quenched by the addition of water (100 ml). The resulting suspension was

extracted with ethyl acetate (100 ml). The organic phase was washed with water (2 × 100 ml) and brine, dried over Na<sub>2</sub>SO<sub>4</sub>, filtrated, and concentrated under reduced pressure. Finally, the crude residue was purified by silica gel column chromatography (ethyl acetate/*n*-hexane 1:1), which yielded **37** as a colorless oil (420 mg, 1.37 mmol, 42%). *R*<sub>f</sub> = 0.51 (ethyl acetate/*n*-hexane 1:1); mp: 172°C; <sup>1</sup>H-NMR (400 MHz, DMSO-*d*<sub>6</sub>): δ(ppm) = 9.14 (t, *J* = 5.9 Hz, 1H), 7.44–7.35 (m, 2H), 7.25–7.14 (m, 2H), 4.46 (d, *J* = 5.9 Hz, 2H), 2.63 (q, *J* = 7.5 Hz, 2H), 2.35 (s, 3H), 1.15 (t, *J* = 7.5 Hz, 3H); <sup>13</sup>C-NMR (100 MHz, DMSO-*d*<sub>6</sub>): δ(ppm) = 170.7, 166.6, 165.0, 161.3 (d, *J* = 242.8 Hz), 158.5, 134.8 (d, *J* = 3.0 Hz), 129.7 (d, *J* = 8.2 Hz), 128.9, 115.2 (d, *J* = 21.3 Hz), 41.9, 27.7, 21.5, 12.5; IR (ATR):  $\tilde{\nu}$  = 3259 (m,  $\nu_{\text{N-H}}$ ), 3080, 2977 (w,  $\nu_{\text{C-H}}$ ), 1637 (s,  $\nu_{\text{C=O}}$ ), 1608 (m,  $\delta_{\text{N-H}}$ ).

#### Ethyl 4-ethyl-6-methyl-2-morpholinopyrimidine-5-carboxylate (**38**)

Compound **35** (4.72 g, 20.7 mmol) was dissolved in ethanol (100 ml). Morpholine (5.35 ml, 62.0 mmol, 3.0 equiv.) was added, and the reaction mixture was stirred at 80°C. After 2 h, volatiles were removed under reduced pressure. The resulting crude residue was purified by silica gel column chromatography (ethyl acetate/*n*-hexane 2:8) to obtain **38** as a yellow oil (5.20 g, 18.6 mmol, 90%). *R*<sub>f</sub> = 0.79 (ethyl acetate/*n*-hexane 1:3); <sup>1</sup>H-NMR (400 MHz, DMSO-*d*<sub>6</sub>): δ (ppm) = 4.29 (q, *J* = 7.1 Hz, 2H), 3.83–3.73 (m, 4H), 3.70–3.61 (m, 4H), 2.65 (q, *J* = 7.5 Hz, 2H), 2.34 (s, 3H), 1.30 (t, *J* = 7.1 Hz, 3H), 1.15 (t, *J* = 7.5 Hz, 3H); <sup>13</sup>C-NMR (100 MHz, DMSO-*d*<sub>6</sub>): δ(ppm) = 170.1, 167.4, 165.8, 159.7, 114.0, 65.9, 60.7, 43.7, 28.8, 23.3, 13.9, 12.6; (ATR):  $\tilde{\nu}$  = 2972 (w,  $\nu_{\text{C-H}}$ ), 1711 (s,  $\nu_{\text{C=O}}$ ).

#### 4-Ethyl-6-methyl-2-morpholinopyrimidine-5-carboxylic acid (**39**)

Compound **38** (5.00 g, 17.9 mmol) was dissolved in ethanol (10 ml). A solution of KOH (4.93 g, 89.5 mmol) in water (20 ml) was added, and the reaction mixture was stirred at 80°C. After 4 h, all volatiles were removed under reduced pressure. The residue was dissolved in water (10 ml), and the resulting solution was acidified to pH 2–3 with conc. aq. HCl. Afterward, it was extracted with ethyl acetate (3 × 100 ml). The combined organic phases were dried over Na<sub>2</sub>SO<sub>4</sub>, filtrated, and concentrated under reduced pressure. The crude residue was purified by silica gel column chromatography (ethyl acetate/acetic acid 9:1) and successive recrystallization (toluene/*n*-hexane) to obtain **39** as a beige-colored solid (3.79 g, 15.1 mmol, 84%). *R*<sub>f</sub> = 0.68 (ethyl acetate/toluene/acetic acid 5:5:1); mp: 130°C; <sup>1</sup>H-NMR (400 MHz, DMSO-*d*<sub>6</sub>): δ (ppm) = 13.02 (s, 1H), 3.86–3.70 (m, 4H), 3.70–3.58 (m, 4H), 2.69 (q, *J* = 7.5 Hz, 2H), 2.36 (s, 3H), 1.15 (t, *J* = 7.5 Hz, 3H); <sup>13</sup>C-NMR (100 MHz, DMSO-*d*<sub>6</sub>): δ(ppm) = 169.8, 169.1, 165.5, 159.7, 115.2, 66.0, 43.7, 28.8, 23.5, 12.6; (ATR):  $\tilde{\nu}$  = 2967 (w,  $\nu_{\text{C-H}}$ ), 3300–2500 (b,  $\nu_{\text{O-H}}$ ), 1675 (s,  $\nu_{\text{C=O}}$ ).

#### 4-Ethyl-N-(4-fluorobenzyl)-6-methyl-2-morpholinopyrimidine-5-carboxamide (**40a**)

The synthesis was conducted from **37** (380 mg, 1.24 mmol) and morpholine in accordance with general procedure C. The crude residue was purified by silica gel column chromatography (ethyl acetate/*n*-hexane 1:1) and successive recrystallization (methanol/water), which yielded **40a** as a colorless solid (324 mg, 0.90 mmol, 73%). *R*<sub>f</sub> = 0.66

(ethyl acetate/*n*-hexane 3:2); mp: 187°C; <sup>1</sup>H-NMR (400 MHz, DMSO-*d*<sub>6</sub>): δ(ppm) = 8.82 (t, *J* = 6.0 Hz, 1H), 7.42–7.32 (m, 2H), 7.23–7.12 (m, 2H), 4.40 (d, *J* = 5.9 Hz, 2H), 3.72–3.69 (m, 4H), 3.65–3.62 (m, 4H), 2.46 (q, *J* = 7.5 Hz, 2H, partially overlapped by DMSO signal), 2.19 (s, 3H), 1.11 (t, *J* = 7.5 Hz, 3H); <sup>13</sup>C-NMR (100 MHz, DMSO-*d*<sub>6</sub>): δ(ppm) = 167.7, 167.4, 163.3, 161.2 (d, *J* = 243.5 Hz), 160.0, 135.5 (d, *J* = 3.2 Hz), 129.5 (d, *J* = 8.1 Hz), 119.7, 115.0 (d, *J* = 21.3 Hz), 66.0, 43.8, 41.9, 27.8, 22.0, 12.5; IR (ATR):  $\tilde{\nu}$  = 3241 (m,  $\nu_{\text{N-H}}$ ), 2975 (w,  $\nu_{\text{C-H}}$ ), 1628 (s,  $\nu_{\text{C=O}}$ ); ESI-HRAM-MS (*m/z*): calcd. for [C<sub>19</sub>H<sub>24</sub>N<sub>4</sub>O<sub>2</sub>F+H]<sup>+</sup> 359.1878, found 359.1878; cpd purity (220 nm): 99.7%.

#### 4-Ethyl-6-methyl-2-morpholino-N-[3-(trifluoromethyl)benzyl]pyrimidine-5-carboxamide (**40b**)

The synthesis was conducted from **39** (250 mg, 1.00 mmol) and (3-(trifluoromethyl)phenyl)methanamine (214 μl, 1.49 mmol, 1.5 equiv.) following general procedure D. The crude residue was purified by silica gel column chromatography (ethyl acetate/*n*-hexane 2:3) and successive recrystallization (methanol/water), which yielded **40b** as a colorless solid (320 mg, 0.78 mmol, 79%). *R*<sub>f</sub> = 0.50 (ethyl acetate/*n*-hexane 1:1); mp: 162°C; <sup>1</sup>H-NMR (400 MHz, DMSO-*d*<sub>6</sub>): δ(ppm) = 8.94 (t, *J* = 6.1 Hz, 1H), 7.72–7.68 (m, 1H), 7.68–7.56 (m, 3H), 4.52 (d, *J* = 6.0 Hz, 2H), 3.77–3.68 (m, 4H), 3.68–3.56 (m, 4H), 2.48 (m, 2H, overlapped by DMSO signal), 2.21 (s, 3H), 1.12 (t, *J* = 7.5 Hz, 3H); <sup>13</sup>C-NMR (100 MHz, DMSO-*d*<sub>6</sub>): δ (ppm) = 167.7, 167.6, 163.3, 160.0, 140.8, 131.6, 129.4, 129.1 (q, *J* = 31.3 Hz), 124.3 (q, *J* = 270.7 Hz), 123.8 (q, *J* = 3.9 Hz), 123.6 (q, *J* = 4.0 Hz), 119.5, 66.0, 43.8, 42.1, 27.8, 21.9, 12.4; (ATR):  $\tilde{\nu}$  = 3251 (m,  $\nu_{\text{N-H}}$ ), 2978 (w,  $\nu_{\text{C-H}}$ ), 1634 (s,  $\nu_{\text{C=O}}$ ), 1571 (m,  $\delta_{\text{N-H}}$ ); ESI-HRAM-MS (*m/z*): calcd. for [C<sub>20</sub>H<sub>24</sub>N<sub>4</sub>O<sub>2</sub>F<sub>3</sub>+H]<sup>+</sup> 409.1846, found 409.1845; cpd purity (220 nm): 99.7%.

#### N-(3,3-Dimethylbutyl)-4-ethyl-6-methyl-2-morpholinopyrimidine-5-carboxamide (**40c**)

The synthesis was conducted from **39** (250 mg, 1.00 mmol) and 3,3-dimethylbutan-1-amine hydrochloride (274 mg, 1.99 mmol, 2.0 equiv.) following general procedure D. Deviating from general procedure D, triethylamine (416 μl, 2.99 mmol, 3.0 equiv.) was added and to the reaction mixture. The crude residue was purified by silica gel column chromatography (ethyl acetate/*n*-hexane 2:3) and successive recrystallization (methanol/water), which yielded **40c** as a colorless solid (269 mg, 0.80 mmol, 81%). *R*<sub>f</sub> = 0.59 (ethyl acetate/*n*-hexane 1:1); mp: 159°C; <sup>1</sup>H-NMR (400 MHz, DMSO-*d*<sub>6</sub>): δ(ppm) = 8.22 (t, *J* = 5.6 Hz, 1H), 3.74–3.67 (m, 4H), 3.67–3.60 (m, 4H), 3.22 (m, 2H), 2.50 (m, 2H, overlapped by DMSO signal), 2.21 (s, 3H), 1.45–1.37 (m, 2H), 1.14 (t, *J* = 7.5 Hz, 3H), 0.92 (s, 9H); <sup>13</sup>C-NMR (100 MHz, DMSO-*d*<sub>6</sub>): δ(ppm) = 167.5, 167.0, 163.2, 159.9, 120.2, 66.0, 43.8, 42.5, 35.5, 29.6, 29.2, 27.8, 22.0, 12.5; (ATR):  $\tilde{\nu}$  = 3226 (w,  $\nu_{\text{N-H}}$ ), 3067, 2952 (m,  $\nu_{\text{C-H}}$ ), 1620 (m,  $\nu_{\text{C=O}}$ ); ESI-HRAM-MS (*m/z*): calcd. for [C<sub>18</sub>H<sub>30</sub>N<sub>4</sub>O<sub>2</sub>+H]<sup>+</sup> 335.2442, found 335.2444; cpd purity (220 nm): 100.0%.

#### 2-Chloro-4-methyl-6-morpholinonicotinonitrile (**42**)

2,6-Dichloro-4-methylnicotinonitrile (1.50 g, 8.0 mmol) was dissolved in methanol (15 ml). The solution was cooled to 0°C, and a solution of morpholine (1.75 ml, 20.1 mmol, 2.5 equiv.) in methanol (5 ml) was

added dropwise under stirring. After complete addition, the cooling was removed, and the reaction mixture was stirred for 16 h at room temperature. Subsequently, all volatiles were removed under reduced pressure, and the residue was dissolved in ethyl acetate (100 ml). The resulting solution was extracted with water (2 × 100 ml), washed with brine, dried over Na<sub>2</sub>SO<sub>4</sub>, filtrated, and concentrated under reduced pressure. The crude residue was purified by flash chromatography (mobile phase: ethyl acetate/*n*-hexane with 30%–70% ethyl acetate), which yielded **42** as a colorless solid (1.33 g, 5.6 mmol, 70%). *R*<sub>f</sub> = 0.45 (ethyl acetate/*n*-hexane 1:1); mp: 156°C (lit mp: 158°C–160°C)<sup>63</sup>; <sup>1</sup>H-NMR (400 MHz, DMSO-*d*<sub>6</sub>): δ(ppm) = 6.88 (d, *J* = 0.8 Hz, 1H), 3.78–3.64 (m, 4H), 3.64–3.49 (m, 4H), 2.36 (d, *J* = 0.8 Hz, 3H); <sup>13</sup>C-NMR (100 MHz, DMSO-*d*<sub>6</sub>): δ(ppm) = 158.3, 153.5, 151.1, 115.9, 105.5, 95.9, 65.6, 44.5, 20.3; (ATR):  $\tilde{\nu}$  = 2982 (w,  $\nu_{C-H}$ ), 2211 (m,  $\nu_{C=N}$ ).

#### 4-Methyl-6-morpholinoisoxazolo[5,4-*b*]pyridin-3-amine (43)

Acetohydroxamic acid (556 mg, 7.40 mmol, 2.2 equiv.) and potassium *tert*-butoxide (755 mg, 6.73 mmol, 2.0 equiv.) were set under an atmosphere of argon and dissolved in dry DMF (10 ml). The resulting mixture was stirred at room temperature for 30 min. Subsequently, a solution of **42** (800 mg, 3.37 mmol) in dry DMF (10 ml) was added. The reaction mixture was stirred at 50°C for 5 h. Afterward, it was concentrated under reduced pressure. The resulting residue was purified by flash chromatography (mobile phase: ethyl acetate/*n*-hexane with 50–90% ethyl acetate), which yielded **43** as a colorless solid (343 mg, 1.45 mmol, 43%). *R*<sub>f</sub> = 0.43 (ethyl acetate/*n*-hexane 3:1); mp: 223°C (decomp.); <sup>1</sup>H-NMR (400 MHz, DMSO-*d*<sub>6</sub>): δ(ppm) = 6.56 (d, *J* = 1.1 Hz, 1H), 5.80 (s, 2H), 3.72–3.65 (m, 4H), 3.59–3.52 (m, 4H), 2.49 (d, *J* = 0.8 Hz, 3H); <sup>13</sup>C-NMR (100 MHz, DMSO-*d*<sub>6</sub>): δ (ppm) = 169.5, 159.7, 158.8, 145.5, 103.4, 97.3, 65.8, 45.0, 18.4; (ATR):  $\tilde{\nu}$  = 3473, 3293 (m,  $\nu_{N-H}$ ), 2961 (w,  $\nu_{C-H}$ ).

#### *N*-(4-Fluorobenzyl)-4-methyl-6-morpholinoisoxazolo[5,4-*b*]pyridin-3-amine (44)

Compound **43** (333 mg, 1.41 mmol) was suspended in dry DCM (30 ml). The suspension was set under an atmosphere of argon. 4-Fluorobenzaldehyde (181 μl, 1.69 mmol, 1.2 equiv.) was added, and the mixture was stirred at room temperature. After 1 h, triethylsilane (675 μl, 4.23 mmol, 3.0 equiv.) and TFA (324 μl, 4.23 mmol, 3.0 equiv.) were added, the temperature was raised to 60°C, and stirring was continued for 24 h. Afterward, 70 ml of DCM was added, and the resulting solution was extracted with a sat. aq. NaHCO<sub>3</sub> solution (100 ml). The organic phase was dried over Na<sub>2</sub>SO<sub>4</sub>, filtrated, and concentrated under reduced pressure. The resulting residue was purified by flash chromatography (mobile phase: ethyl acetate/*n*-hexane with 40%–70% ethyl acetate) and successive recrystallization (methanol/water), which yielded **44** as a colorless solid (386 mg, 1.12 mmol, 80%). *R*<sub>f</sub> = 0.39 (ethyl acetate/*n*-hexane 1:1); mp: 150°C; <sup>1</sup>H-NMR (400 MHz, DMSO-*d*<sub>6</sub>): δ (ppm) = 7.49–7.39 (m, 2H), 7.19–7.09 (m, 2H), 6.65 (t, *J* = 6.1 Hz, 1H), 6.57 (d, *J* = 1.0 Hz, 1H), 4.36 (d, *J* = 6.0 Hz, 2H), 3.71–3.64 (m, 4H), 3.58–3.51 (m, 4H), 2.53 (d, *J* = 0.8 Hz, 3H); <sup>13</sup>C-NMR (100 MHz, DMSO-*d*<sub>6</sub>): δ(ppm) = 169.5, 161.1 (d, *J* = 241.9 Hz), 159.6, 158.3, 145.3, 135.8 (d, *J* = 3.0 Hz), 129.4 (d, *J* = 8.2 Hz), 114.8 (d, *J* = 21.3 Hz), 103.4, 96.9, 65.8,

45.3, 45.0, 18.8; (ATR):  $\tilde{\nu}$  = 3470 (m,  $\nu_{N-H}$ ), 2965 (w,  $\nu_{C-H}$ ); ESI-HRAM-MS (*m/z*): calcd. for [C<sub>18</sub>H<sub>20</sub>N<sub>4</sub>O<sub>2</sub>F+H]<sup>+</sup> 343.1565, found 343.1561; cpd purity (220 nm): 100.0%.

#### 2-Methoxy-4-methyl-6-morpholinocotinonitrile (45)

Compound **42** (768 mg, 3.23 mmol) was dissolved in dry methanol (30 ml). A 25% solution of sodium methoxide in methanol (2.96 ml, 12.92 mmol, 4.0 equiv.) was added, and the reaction mixture was stirred under reflux in an apparatus equipped with a CaCl<sub>2</sub> drying tube. After 24 h, it was cooled to room temperature and concentrated under reduced pressure. The residue was dissolved in ethyl acetate (100 ml), and the resulting solution was extracted with water (2 × 100 ml). The organic phase was washed with brine, dried over Na<sub>2</sub>SO<sub>4</sub>, filtrated, and concentrated under reduced pressure. Finally, the crude residue was purified by silica gel column chromatography (ethyl acetate/*n*-hexane 1:1), which yielded **45** as a colorless solid (678 mg, 2.91 mmol, 90%). *R*<sub>f</sub> = 0.56 (ethyl acetate/*n*-hexane 1:1); mp: 150°C; <sup>1</sup>H-NMR (400 MHz, DMSO-*d*<sub>6</sub>): δ(ppm) = 6.42 (d, *J* = 0.9 Hz, 1H), 3.88 (s, 3H), 3.71–3.64 (m, 4H), 3.64–3.57 (m, 4H), 2.29 (d, *J* = 0.8 Hz, 3H); <sup>13</sup>C-NMR (100 MHz, DMSO-*d*<sub>6</sub>): δ(ppm) = 164.1, 158.2, 153.8, 116.3, 99.5, 81.6, 65.7, 53.5, 44.4, 19.9; (ATR):  $\tilde{\nu}$  = 2972 (w,  $\nu_{C-H}$ ), 2206 (m,  $\nu_{C=N}$ ).

#### *N*'-Hydroxy-2-methoxy-4-methyl-6-morpholinocotinimidamide (46)

Compound **45** (644 mg, 2.76 mmol) was suspended in ethanol (50 ml). A 50% aq. solution of hydroxylamine (1.63 ml, 27.6 mmol, 10.0 equiv.) was added, and the reaction mixture was stirred in a closed vessel at 90°C for 4 d. After 24, 48, and 62 h, additional hydroxylamine solution (each time 1.63 ml, 27.6 mmol, 10.0 equiv.) was added. To terminate the reaction, it was cooled to room temperature, and all volatiles were removed under reduced pressure. The crude residue was purified by flash chromatography (mobile phase: DCM/methanol with 0%–10% methanol), which yielded **46** as a colorless solid (730 mg, 2.74 mmol, 99%). *R*<sub>f</sub> = 0.69 (DCM/methanol 9:1); mp: 211°C; <sup>1</sup>H-NMR (400 MHz, DMSO-*d*<sub>6</sub>): δ(ppm) = 9.04 (s, 1H), 6.20 (s, 1H), 5.45 (s, 2H), 3.75 (s, 3H), 3.72–3.65 (m, 4H), 3.45–3.38 (m, 4H), 2.14 (s, 3H); <sup>13</sup>C-NMR (100 MHz, DMSO-*d*<sub>6</sub>): δ(ppm) = 160.3, 157.1, 150.2, 148.3, 106.3, 99.2, 65.9, 52.5, 45.1, 19.0; (ATR):  $\tilde{\nu}$  = 3470, 3323, 3229 (m,  $\nu_{N-H}/\nu_{O-H}$ ), 2949 (w,  $\nu_{C-H}$ ), 1713 (m,  $\nu_{C=N}$ ).

#### 4-[5-(5-Benzyl-1,2,4-oxadiazol-3-yl)-6-methoxy-4-methylpyridin-2-yl]morpholine (47)

Compound **46** (250 mg, 0.94 mmol) was dissolved in 20 ml of DCM, and triethylamine (196 μl, 1.41 mmol, 1.5 equiv.) was added in one portion. The reaction mixture was cooled to 0°C, and a solution of 2-phenylacetyl chloride (188 μl, 1.41 mmol, 1.5 equiv.) in DCM (5 ml) was added dropwise. After complete addition, stirring at 0°C was continued for 1 h. Subsequently, all volatiles were removed under reduced pressure. The residue was dissolved in THF (10 ml) and treated with a 1 M solution of tetra-*n*-butylammonium fluoride in THF (939 μl, 0.94 mmol, 1.0 equiv.). The reaction mixture was stirred at room temperature for 2 h. Afterward, it was dissolved in ethyl acetate (100 ml) and extracted with water (100 ml). The organic

phase was washed with brine, dried over Na<sub>2</sub>SO<sub>4</sub>, filtrated, and concentrated under reduced pressure. The crude residue was purified by flash chromatography (mobile phase: ethyl acetate/*n*-hexane with 10%–50% ethyl acetate), which yielded **47** as a colorless solid (125 mg, 0.34 mmol, 36%). *R*<sub>f</sub> = 0.64 (ethyl acetate/*n*-hexane 1:1); mp: 115°C; <sup>1</sup>H-NMR (400 MHz, DMSO-*d*<sub>6</sub>): δ(ppm) = 7.40–7.35 (m, 4H), 7.31 (m, 1H), 6.36 (s, 1H), 4.40 (s, 2H), 3.75 (s, 3H), 3.77–3.66 (m, 4H), 3.55–3.48 (m, 4H), 2.09 (s, 3H); <sup>13</sup>C-NMR (100 MHz, DMSO-*d*<sub>6</sub>): δ (ppm) = 177.6, 165.1, 160.5, 158.0, 150.8, 134.3, 129.0, 128.7, 127.3, 99.7, 97.3, 65.8, 52.9, 44.7, 31.9, 19.7; (ATR):  $\tilde{\nu}$  = 2954 (w,  $\nu_{C-H}$ ); ESI-HRAM-MS (*m/z*): calcd. for [C<sub>20</sub>H<sub>23</sub>N<sub>4</sub>O<sub>3</sub>+H]<sup>+</sup> 367.1765, found 367.1763; cpd purity (220 nm): 99.4%.

#### (2-Methoxy-4-methyl-6-morpholinopyridin-3-yl)methanamine (48)

Compound **45** (600 mg, 2.57 mmol) was dissolved in a saturated solution of ammonia in methanol (50 ml). 1.00 g of a Raney nickel suspension in water (50%) was washed with methanol several times and added to the reaction mixture. The suspension was carefully set under a hydrogen atmosphere (balloon pressure) and stirred at 50°C. After 5 h, the catalyst was removed by filtration, and the filtrate was concentrated under reduced pressure. The resulting residue was dissolved in ethyl acetate and filtrated through a pad of silica gel, which was subsequently rinsed with an additional 250 ml of ethyl acetate. The obtained filtrate was discarded. Afterward, the silica gel pad was rinsed with 100 ml of a mixture of methanol and conc. aq. ammonia solution (9:1) to elute the desired product. The filtrate was concentrated under reduced pressure to obtain **48** as a colorless oil (434 mg, 1.83 mmol, 71%), used for the following reaction without any further purification and characterization.

#### 4-Fluoro-N-[(2-methoxy-4-methyl-6-morpholinopyridin-3-yl)methyl]benzamide (49)

Compound **48** (434 mg, 1.83 mmol) was dissolved in DCM (20 ml). Triethylamine (507  $\mu$ l, 3.66 mmol, 2.0 equiv.) was added in one portion. The reaction mixture was cooled to 0°C, and a solution of 4-fluorobenzoyl chloride (325  $\mu$ l, 2.75 mmol, 1.5 equiv.) in DCM (20 ml) was added dropwise over a period of 30 min. Cooling was removed, and the reaction mixture was stirred at room temperature. After 16 h, the reaction mixture was concentrated under reduced pressure. The crude residue was purified by flash chromatography (mobile phase: ethyl acetate/*n*-hexane with 30%–50% ethyl acetate) and successive recrystallization (methanol/water), which yielded **49** as a colorless solid (422 mg, 1.17 mmol, 64%). *R*<sub>f</sub> = 0.63 (ethyl acetate/*n*-hexane 1:1); mp: 180°C; <sup>1</sup>H-NMR (400 MHz, DMSO-*d*<sub>6</sub>): δ(ppm) = 8.31 (t, *J* = 4.7 Hz, 1H), 7.96–7.86 (m, 2H), 7.30–7.19 (m, 2H), 6.21 (s, 1H), 4.35 (d, *J* = 4.7 Hz, 2H), 3.81 (s, 3H), 3.73–3.66 (m, 4H), 3.44–3.37 (m, 4H), 2.25 (s, 3H); <sup>13</sup>C-NMR (100 MHz, DMSO-*d*<sub>6</sub>): δ(ppm) = 165.0, 163.7 (d, *J* = 249.0 Hz), 160.7, 156.6, 150.2, 130.9 (d, *J* = 3.0 Hz), 130.0 (d, *J* = 8.8 Hz), 114.9 (d, *J* = 21.6 Hz), 106.7, 100.1, 65.9, 52.7, 45.2, 34.6, 19.0; (ATR):  $\tilde{\nu}$  = 3309 (m,  $\nu_{N-H}$ ), 2972 (w,  $\nu_{C-H}$ ), 1623 (s,  $\nu_{C=O}$ ), 1599 (s,  $\delta_{N-H}$ ); ESI-HRAM-MS (*m/z*): calcd. for [C<sub>19</sub>H<sub>23</sub>N<sub>3</sub>O<sub>4</sub>F+H]<sup>+</sup> 360.1718, found 360.1713; cpd purity (220 nm): 99.6%.

#### Methyl 6-chloro-2-methoxy-4-methylnicotinate (50)

Compound **15a** (2.25 g, 11.2 mmol) was dissolved in dry DMF (30 ml). K<sub>2</sub>CO<sub>3</sub> (2.31 g, 16.7 mmol, 1.5 equiv.) was added, and the mixture was stirred for 30 min. Afterward, methyl iodide (1.04 ml, 16.7 mmol, 1.5 equiv.) was added dropwise, and the reaction mixture was stirred at room temperature for 8 h. Subsequently, the reaction was quenched by the addition of 150 ml of water. The resulting suspension was extracted with ethyl acetate (150 ml). The organic phase was successively washed with a sat. aq. solution of NaHCO<sub>3</sub> (2 × 100 ml) and brine, dried over Na<sub>2</sub>SO<sub>4</sub>, filtrated, and concentrated under reduced pressure to obtain **50** as a pale yellow solid (2.36 g, 10.9 mmol, 98%). *R*<sub>f</sub> = 0.50 (ethyl acetate/*n*-hexane 1:9); mp: 70°C; <sup>1</sup>H-NMR (400 MHz, DMSO-*d*<sub>6</sub>): δ(ppm) = 7.11 (d, *J* = 0.7 Hz, 1H), 3.85 (s, 3H), 3.82 (s, 3H), 2.24 (d, *J* = 0.6 Hz, 3H); <sup>13</sup>C-NMR (100 MHz, DMSO-*d*<sub>6</sub>): δ(ppm) = 165.7, 159.7, 150.8, 147.9, 118.1, 115.6, 54.4, 52.5, 18.4; (ATR):  $\tilde{\nu}$  = 3034, 2954 (w,  $\nu_{C-H}$ ), 1717 (s,  $\nu_{C=O}$ ).

#### Methyl 2-methoxy-4-methyl-6-morpholinonicotinate (51)

Compound **50** (800 mg, 3.71 mmol) was dissolved in NMP (10 ml). Triethylamine (1030  $\mu$ l, 7.42 mmol, 2.0 equiv.) and morpholine (388  $\mu$ l, 4.45 mmol, 1.2 equiv.) were added successively, and the resulting solution was stirred at 90°C for 2 d. Afterward, the reaction mixture was dissolved in ethyl acetate (100 ml) and extracted with water (3 × 100 ml). The organic phase was washed with brine, dried over Na<sub>2</sub>SO<sub>4</sub>, filtrated, and concentrated under reduced pressure. The crude residue was purified by flash chromatography (mobile phase: ethyl acetate/*n*-hexane with 30%–40% ethyl acetate), which yielded **51** as a colorless solid (386 mg, 1.45 mmol, 39%). *R*<sub>f</sub> = 0.64 (ethyl acetate/*n*-hexane 1:1); mp: 123°C; <sup>1</sup>H-NMR (400 MHz, DMSO-*d*<sub>6</sub>): δ(ppm) = 6.26 (d, *J* = 0.8 Hz, 1H), 3.79 (s, 3H), 3.73 (s, 3H), 3.71–3.64 (m, 4H), 3.56–3.45 (m, 4H), 2.20 (d, *J* = 0.6 Hz, 3H); <sup>13</sup>C-NMR (100 MHz, DMSO-*d*<sub>6</sub>): δ(ppm) = 166.9, 160.1, 157.5, 150.0, 103.9, 99.6, 65.8, 52.9, 51.5, 44.6, 19.9; (ATR):  $\tilde{\nu}$  = 2918 (w,  $\nu_{C-H}$ ), 1747 (s,  $\nu_{C=O}$ ).

#### 2-Methoxy-4-methyl-6-morpholinonicotinohydrazide (52)

Compound **51** (250 mg, 0.94 mmol) was suspended in an 80% aq. solution of hydrazine hydrate (20.0 ml, 303 mmol, 323 equiv.). The suspension was heated to reflux, and methanol was added until complete dissolution of methyl 2-methoxy-4-methyl-6-morpholinonicotinate. Subsequently, stirring under reflux was continued. After 24 h, all volatiles were removed under reduced pressure. The crude residue was purified by flash chromatography (mobile phase: DCM/methanol with 0%–10% methanol), which yielded **52** as a beige-colored solid (168 mg, 0.63 mmol, 67%). *R*<sub>f</sub> = 0.73 (DCM/methanol 9:1); mp: 158°C; <sup>1</sup>H-NMR (400 MHz, DMSO-*d*<sub>6</sub>): δ(ppm) = 9.08 (s, 1H), 6.20 (s, 1H), 4.55 (s, 2H), 3.75 (s, 3H), 3.72–3.65 (m, 4H), 3.48–3.40 (m, 4H), 2.13 (s, 3H); <sup>13</sup>C-NMR (100 MHz, DMSO-*d*<sub>6</sub>): δ(ppm) = 165.4, 159.0, 157.1, 148.9, 108.3, 99.4, 65.9, 52.6, 45.0, 19.1; (ATR):  $\tilde{\nu}$  = 3308 (m,  $\nu_{N-H}$ ), 2977 (w,  $\nu_{C-H}$ ), 1593 (s,  $\nu_{C=O}$ ).

#### 2-(4-Fluorophenyl)-N'-(2-methoxy-4-methyl-6-morpholinonicotinoyl)acetohydrazonamide (53)

Compound **56** (169 mg, 0.83 mmol, 1.4 equiv.) was added in portions to a solution of sodium methoxide (45 mg, 0.83 mmol, 1.4 equiv.) in dry methanol (20 ml) at 0°C. After complete addition, the cooling was



removed, and the reaction mixture was stirred at room temperature. Subsequently, compound **52** (158 mg, 0.59 mmol) was added, and stirring at room temperature was continued for 24 h. Afterward, volatiles were removed under reduced pressure, and the residue was purified by silica gel column chromatography (DCM/methanol 9:1), which yielded **53** as a colorless solid (111 mg, 0.28 mmol, 47%).  $R_f = 0.57$  (DCM/methanol 9:1); mp: 219°C;  $^1\text{H-NMR}$  (400 MHz, DMSO- $d_6$ ):  $\delta(\text{ppm}) = 9.45$  (s, 1H), 7.47–7.34 (m, 2H), 7.28–7.09 (m, 2H), 6.23 (s, 1H), 6.08 (s, 2H), 3.76 (s, 3H), 3.73–3.59 (m, 4H), 3.54–3.41 (m, 4H), 3.37 (s, 2H), 2.15 (s, 3H);  $^{13}\text{C-NMR}$  (100 MHz, DMSO- $d_6$ ):  $\delta(\text{ppm}) = 161.1$ , 161.0 (d,  $J = 240.0$  Hz), 159.1, 157.0, 152.3, 149.0, 134.0, 130.6 (d,  $J = 8.0$  Hz), 114.9 (d,  $J = 21.1$  Hz), 99.5, 65.9, 52.7, 45.1, 39.1, 19.1; (ATR):  $\tilde{\nu} = 3389$ , 3220 (m,  $\nu_{\text{N-H}}$ ), 3047, 2986 (w,  $\nu_{\text{C-H}}$ ), 1653 (m,  $\nu_{\text{C=O}}$ ).

#### 4-[5-[5-(4-Fluorobenzyl)-1H-1,2,4-triazol-3-yl]-6-methoxy-4-methylpyridin-2-yl]morpholine (**54**)

Compound **52** (133 mg, 0.50 mmol),  $\text{K}_2\text{CO}_3$  (35 mg, 0.25 mmol, 0.5 equiv.), and 2-(4-fluorophenyl)acetonitrile (180  $\mu\text{l}$ , 1.50 mmol, 3.0 equiv.) were dissolved in *n*-butanol (2 ml) and stirred in a closed vessel at 150°C in a microwave reactor. After 4 h, the reaction was cooled to room temperature, and all volatiles were removed under reduced pressure. The residue was dissolved in ethyl acetate (100 ml) and extracted with water (100 ml). The organic phase was washed with brine, dried over  $\text{Na}_2\text{SO}_4$ , filtrated, and concentrated under reduced pressure. The crude residue was purified by silica gel column chromatography (ethyl acetate/*n*-hexane 1:1), which yielded **54** as a colorless solid (90 mg, 0.23 mmol, 47%).  $R_f = 0.41$  (ethyl acetate/*n*-hexane 1:1); mp: 164°C;  $^1\text{H-NMR}$  (400 MHz, DMSO- $d_6$ ):  $\delta(\text{ppm}) = 11.35$  (s, 1H), 7.43–7.32 (m, 2H), 7.06–6.95 (m, 2H), 6.16 (s, 1H), 4.13 (s, 2H), 4.01 (s, 3H), 3.87–3.80 (m, 4H), 3.62–3.55 (m, 4H), 2.70 (s, 3H);  $^{13}\text{C-NMR}$  (100 MHz, DMSO- $d_6$ ):  $\delta(\text{ppm}) = 162.3$ , 161.8 (d,  $J = 242.0$  Hz), 160.6, 157.1, 152.7, 152.5, 134.4, 130.6 (d,  $J = 7.9$  Hz), 115.3 (d,  $J = 21.2$  Hz), 101.9, 98.7, 66.8, 53.9, 45.3, 34.2, 23.4; (ATR):  $\tilde{\nu} = 3220$  (m,  $\nu_{\text{N-H}}$ ), 2977 (w,  $\nu_{\text{C-H}}$ ), ESI-HRAM-MS ( $m/z$ ): calcd. for  $[\text{C}_{20}\text{H}_{23}\text{N}_5\text{O}_2\text{F}+\text{H}]^+$  384.1830, found 384.1833; cpd purity (220 nm): 98.6%.

#### Methyl 2-(4-fluorophenyl)acetimidate hydrochloride (**56**)

2-(4-Fluorophenyl)acetonitrile (3.00 ml, 25.0 mmol) was dissolved in dry methanol (20.0 ml, 49 mmol, 2.0 equiv.). The reaction mixture was set under an atmosphere of argon and cooled to 0°C. HCl gas was passed through the solution for 3 h under stirring. Afterward, all volatiles were removed under reduced pressure. The residue was suspended in dry THF, filtered off, and rinsed with additional dry THF to obtain **56** as a colorless solid (2.94 g, 14.5 mmol, 58%). Mp: 157°C;  $^1\text{H-NMR}$  (400 MHz,  $\text{CDCl}_3$ ):  $\delta(\text{ppm}) = 12.91$  (s, 1H), 11.83 (s, 1H), 7.48–7.38 (m, 2H), 7.10–6.99 (m, 2H), 4.28 (s, 3H), 4.06 (s, 2H);  $^{13}\text{C-NMR}$  (100 MHz,  $\text{CDCl}_3$ ):  $\delta(\text{ppm}) = 178.2$ , 162.9 (d,  $J = 247.9$  Hz), 131.6 (d,  $J = 8.2$  Hz), 126.9 (d,  $J = 3.3$  Hz), 116.4 (d,  $J = 21.8$  Hz), 61.3, 38.4; (ATR):  $\tilde{\nu} = 3100$ –2600 (b,  $\nu_{\text{N-H}}$ ), 1652 (m,  $\nu_{\text{C=N}}$ ).

#### 1-Amino-2-(4-fluorophenyl)ethan-1-iminium chloride (**57**)

Compound **56** (2.20 g, 10.8 mmol) was dissolved in dry methanol (25 ml). Ammonia gas was passed through the solution for 30 min. Subsequently,

the reaction vessel was closed, and the mixture was stirred at room temperature. After 24 h, all volatiles were removed under reduced pressure. The resulting mucilaginous substance was treated with ethyl acetate to obtain **57** as a colorless solid, which was filtered off (1.25 g, 6.6 mmol, 61%). Mp: 134°C;  $^1\text{H-NMR}$  (400 MHz, MeOH- $d_4$ ):  $\delta(\text{ppm}) = 7.75$ –7.29 (m, 2H), 7.29–6.99 (m, 2H), 3.82 (s, 2H);  $^{13}\text{C-NMR}$  (100 MHz, MeOH- $d_4$ ):  $\delta(\text{ppm}) = 171.6$ , 164.1 (d,  $J = 245.5$  Hz), 132.2 (d,  $J = 8.2$  Hz), 130.5 (d,  $J = 3.3$  Hz), 117.1 (d,  $J = 22.0$  Hz), 38.6; (ATR):  $\tilde{\nu} = 3300$ –2600 (b,  $\nu_{\text{N-H}}$ ), 1669 (s,  $\nu_{\text{C=N}}$ ).

### 4.1.3 | $\text{Log}D_{7.4}$ estimation

The  $\text{log}D_{7.4}$  estimation was carried out as previously reported by employing a standard HPLC-based method.<sup>[23]</sup> Briefly, the capacity factors of seven reference substances with known  $\text{log}D_{7.4}$  values were determined from their retention times (acetophenone, benzene, ethyl benzoate, benzophenone, phenyl benzoate, diphenyl ether, bibenzyl) with uracil used as a dead-time marker. The logarithm of the capacity factors was then plotted against the corresponding  $\text{log}D_{7.4}$  values to obtain a calibration function, which was used to calculate the  $\text{log}D_{7.4}$  values for each compound of interest. For HPLC analysis, a Phenomenex Luna 5  $\mu\text{m}$  Phenyl-Hexyl 100 Å column (150  $\times$  4.6 mm) was used with a mixture of methanol (75%) and 10 mM Tris/HCl buffer (25%) at pH 7.4 as mobile phase at a flow rate of 1.0 ml/min. The compounds of interest were dissolved in methanol (2 mg/ml), and the retention time was determined as the mean value from two measurements. The reference substances were injected as a mixture, which was prepared by dissolving 2 mg of a reference substance in 1 ml of methanol and subsequently combining 50  $\mu\text{l}$  aliquots of each reference solution. The reference mixture was measured before and after the compounds of interest. Then, the mean retention time from both measurements was used to calculate the calibration function.

## 4.2 | Biology

### 4.2.1 | $K_{V7.2/3}$ channel opening activity

The FLIPR Potassium Assay Kit (Molecular Devices) was used to determine the  $K_{V7.2/3}$  channel opening activity of the synthesized analogs according to the protocol of the assay kit. HEK-293 cells transfected with KCNQ2/3 were obtained from SB Drug Discovery. The cell culture and the data analysis were carried out as previously described elsewhere.<sup>[24,64]</sup> Briefly, the cells were grown in minimum essential medium with non-essential amino acids (Thermo Fisher Scientific), supplemented with 10% heat-inactivated fetal bovine serum, 2 mM L-glutamine, 4  $\mu\text{g/ml}$  blasticidin S-HCl, 1% penicillin/streptomycin and 0.78 mg/ml G418 sulfate. The cells had been seeded at densities of 60,000 cells/well in 100  $\mu\text{l}$  of cell culture media using black-walled 96-well plates with a clear bottom (4titude Vision Plates from Azenta Life Sciences) suitable for fluorimetric measurements. After incubation for 24 h, 100  $\mu\text{l}$  of loading buffer containing

the fluorescent dye and probenecid as an inhibitor for the anion-exchange protein were added. Afterward, the plates were incubated for 1 h at room temperature under the exclusion of light. The test compounds were serially diluted in DMSO and added to the wells to obtain a final DMSO concentration of 1% (V/V). Equally treated wells containing loading buffer and 1% DMSO without test compound were deemed as the vehicle control. After an additional 30 min of incubation, fluorimetric measurements were performed at extinction/emission wavelengths of 485 nm and 535 nm with an Infinite F200 Pro plate reader (Tecan). The baseline fluorescence signal was recorded for 20 s. Subsequently, a stimulus buffer (25 mM K<sup>+</sup>, 15 mM TI<sup>+</sup>) was added to each well, and measuring the fluorescence intensity was continued for 2.5 min. The resulting data were processed by normalizing the measured fluorescence intensity with the average baseline signal ( $F/F_0$ ). A correction was then performed by calculating the difference between the normalized vehicle control signal and the normalized baseline signal and subtracting the result from the  $F/F_0$  value. To obtain a concentration-activity curve, the maximal corr.  $\Delta F/F_0$  values were plotted against the logarithmic compound concentration. Relative EC<sub>50</sub> values were calculated with GraphPad Prism 6 by determining the inflection point of the resulting sigmoidal curves. The corresponding  $E_{\max}$  values as a measure for the intrinsic activity were determined by relating the maximum corr.  $\Delta F/F_0$  value of a specific compound to the maximum corr.  $\Delta F/F_0$  value of flupirtine, which was defined as 100%. All results are means of at least three independent experiments  $\pm$  standard deviation (SD).

#### 4.2.2 | Hepatic cell viability

The culturing of the TAMH and HEP-G2 cells and the MTT cell viability assay were carried out as previously described.<sup>[24,64]</sup> Briefly, TAMH mouse liver cells (School of Pharmacy, University of Washington, Seattle, WA, USA) were grown in serum-free DMEM/F12 medium supplemented with 5% PANEXIN NTA, 10 mM nicotinamide, and 10  $\mu$ g/ml gentamicin. HEP-G2 human liver cancer cells (DSMZ, Braunschweig, Germany) were cultured in RPMI 1640 (PAN Biotech), supplemented with 10% heat-inactivated fetal bovine serum and 1% penicillin/streptomycin. Both cell lines were seeded into 96-well plates with 20,000 cells per well for TAMH and 15,000 cells per well for HEP-G2 and incubated at 37°C in a 5% CO<sub>2</sub> atmosphere. After 24 h, the medium was replaced with fresh culture medium containing the test compounds at defined concentrations. For this purpose, the compounds were dissolved in DMSO and serially diluted in the corresponding culture medium to achieve a final concentration of 1% DMSO (V/V). Equally treated wells containing 1% DMSO without test compound were deemed as the vehicle control. Additional wells without cells were treated analogously to the control wells to determine the background optical density (OD). After 24 h of incubation with the test compounds, the medium was replaced with fresh medium containing 10% (V/V) of a 2.5 mg/ml solution of 3-(4,5-dimethylthiazol-2-yl)-2,5-diphenyltetrazolium bromide (MTT). After an additional 4 h of incubation, the culture medium

in each well was removed, and DMSO (50  $\mu$ l) was added to dissolve the formazan crystals. Afterward, ODs were determined at 570 nm by using a SpectraMax 190 microplate reader. A correction of the OD values of the test compound (T) and control (C) wells by subtracting the blank value followed. Subsequently, the  $T/C_{\text{corr.}}$ -ratios were calculated and plotted against the logarithmic compound concentration to obtain a dose-response curve. After interpolation of the sigmoidal standard curve with GraphPad Prism 6, the LD<sub>50</sub> and LD<sub>25</sub> values were determined as the concentrations that reduced cell viability to 50% and 75%, respectively. If no reduction in cell viability to 75% was observed at the maximum concentration possible without precipitating the compounds, the LD<sub>25</sub> value was reported as higher than the highest concentration tested. All results are the means of at least three independent experiments  $\pm$  SD.

### 4.3 | Molecular modeling

If not stated otherwise, all calculations were performed using the Schrodinger software suite release 2022-1 (Schrödinger, LLC, 2022).

#### 4.3.1 | Structure preparation

The heterotetrameric protein structure of the KCNQ2/3 potassium channel was taken from previous studies<sup>[23]</sup> and is based on the cryo-EM structure of KCNQ2 with bound retigabine (PDB 7CR2),<sup>[36]</sup> while two opposing chains were used as a template for homology modeling within the Multiple Sequence Viewer in Maestro. Finally, the obtained model was prepared by the Protein Preparation Wizard<sup>[65]</sup> to optimize the protonation states and the hydrogen bond network, followed by a restraint minimization with OPLS4 force field parameters.<sup>[66]</sup>

#### 4.3.2 | Molecular docking

All ligands were prepared using the Ligand Preparation application in Maestro and then docked into the heterotetrameric KCNQ2/3 model using an induced fit approach<sup>[67]</sup> in Glide (version 94137)<sup>[68]</sup> with standard sampling protocol of protein sidechains and an implicit membrane representation. The resulting 20 docking poses per compound were visually analyzed and selected. The compounds **14** and **18a** were re-docked into the same KCNQ2/3 retigabine binding site after molecular dynamics simulations using the Glide XP scoring function<sup>[69]</sup> for direct comparison.

#### 4.3.3 | Molecular dynamics simulations

The previously generated protein structure was prepared for molecular dynamics simulation using Desmond System Builder. The POPC bilayer membrane<sup>[70]</sup> position was placed on the

transmembrane helices, and the system was solvated in an orthorhombic box with a 1 nm buffer around the protein with explicit TIP3P<sup>[71]</sup> water molecules and 0.15 M NaCl salt concentration. OPLS4 force field parameters<sup>[66]</sup> were applied in all simulations. Since the binding pockets are highly conserved, four different ligands (retigabine, **18a**, **18c**, **49**) were used in a single molecular dynamics run after molecular docking. The molecular system was minimized for 500 ps and equilibrated using the standard protocol (distributed with Desmond v6.9<sup>[72]</sup>) for membrane systems at 300 K and NpT ensemble.<sup>[73]</sup> The production run was performed for 50 ns with a timestep of 2 fs. The temperature and pressure were maintained by a Langevin thermostat and a Langevin barostat, respectively. The snapshots were saved to the trajectory every 20 ps and analyzed using the Simulation Interaction Diagram in Maestro.

## ACKNOWLEDGMENTS

Konrad W. Wurm and Frieda-Marie Bartz are funded by grants DFG LI 765/7-2 and DFG BE 1287/6-2 awarded to Andreas Link and Patrick J. Bednarski by the Deutsche Forschungsgemeinschaft (DFG—German Research Foundation). We thank Ms. Anne Schüttler and Ms. Maria Hühr for excellent technical assistance. Open Access funding enabled and organized by Projekt DEAL.

## CONFLICT OF INTEREST

The authors declare no conflict of interest.

## ORCID

Andreas Link  <http://orcid.org/0000-0003-1262-6636>

## REFERENCES

- [1] V. Barrese, J. B. Stott, I. A. Greenwood, *Annu. Rev. Pharmacol. Toxicol.* **2018**, *58*, 625. <https://doi.org/10.1146/annurev-pharmtox-010617-052912>
- [2] D. A. Brown, G. M. Passmore, *Br. J. Pharmacol.* **2009**, *156*, 1185. <https://doi.org/10.1111/j.1476-5381.2009.00111.x>
- [3] M. M. Shah, M. Migliore, I. Valencia, E. C. Cooper, D. A. Brown, *Proc. Natl. Acad. Sci. USA.* **2008**, *105*, 7869. <https://doi.org/10.1073/pnas.0802805105>
- [4] H. C. Peters, H. Hu, O. Pongs, J. F. Storm, D. Isbrandt, *Nat. Neurosci.* **2005**, *8*, 51. <https://doi.org/10.1038/nn1375>
- [5] F. A. Vigil, C. M. Carver, M. S. Shapiro, *Front. Physiol.* **2020**, *11*, 688. <https://doi.org/10.3389/fphys.2020.00688>
- [6] M. Borgini, P. Mondal, R. Liu, P. Wipf, *RSC Med. Chem.* **2021**, *12*, 483. <https://doi.org/10.1039/D0MD00328J>
- [7] a) F. A. Vigil, E. Bozdemir, V. Bugay, S. H. Chun, M. Hobbs, I. Sanchez, S. D. Hastings, R. J. Veraza, D. M. Holstein, S. M. Sprague, C. M. Carver, J. E. Cavazos, R. Brenner, J. D. Lechleiter, M. S. Shapiro, *J. Cereb. Blood Flow Metab.* **2019**, *40*, 1256–1273. <https://doi.org/10.1177/0271678X19857818>; b) J. Ren, J. Guo, S. Zhu, Q. Wang, R. Gao, C. Zhao, C. Feng, C. Qin, Z. He, C. Qin, Z. Wang, L. Zang, *Biol. Pharm. Bull.* **2021**, *44*, 169. <https://doi.org/10.1248/bpb.b20-00504>
- [8] S. Costi, M.-H. Han, J. W. Murrugh, *CNS Drugs* **2022**, *36*, 207. <https://doi.org/10.1007/s40263-021-00885-y>
- [9] M. A. Überall, G. H. H. Mueller-Schwefe, B. Terhaag, *Curr. Med. Res. Opin.* **2012**, *28*, 1617. <https://doi.org/10.1185/03007995.2012.726216>
- [10] J. A. French, B. W. Abou-Khalil, R. F. Leroy, E. M. T. Yacubian, P. Shin, S. Hall, H. Mansbach, V. Nohria, *Neurology* **2011**, *76*, 1555. <https://doi.org/10.1212/WNL.0b013e3182194bd3>
- [11] A. Nissenkorn, P. Kornilov, A. Peretz, L. Blumkin, G. Heimer, B. Ben-Zeev, B. Attali, *Epileptic Disord.* **2021**, *23*, 695. <https://doi.org/10.1684/epd.2021.1315>
- [12] D. Rudin, J. Spoendlin, A. L. Cismaru, E. Liakoni, N. Bonadies, U. Amstutz, C. R. Meier, S. Krähenbühl, M. Haschke, *Eur. J. Intern. Med.* **2019**, *68*, 36. <https://doi.org/10.1016/j.ejim.2019.07.029>
- [13] C. Bock, A. Link, *Future Med. Chem.* **2019**, *11*, 337. <https://doi.org/10.4155/fmc-2018-0350>
- [14] K. W. Wurm, F.-M. Bartz, L. Schulig, A. Bodtke, P. J. Bednarski, A. Link, *ChemMedChem* **2022**, *17*, e202200262. <https://doi.org/10.1002/cmdc.202200262>
- [15] M. C. Michel, P. Radziszewski, C. Falconer, D. Marschall-Kehrel, K. Blot, *Br. J. Clin. Pharmacol.* **2012**, *73*, 821. <https://doi.org/10.1111/j.1365-2125.2011.04138.x>
- [16] S. Clark, A. Antell, K. Kaufman, *Ther. Adv. Drug Saf.* **2015**, *6*, 15. <https://doi.org/10.1177/2042098614560736>
- [17] M. R. Groseclose, S. Castellino, *Chem. Res. Toxicol.* **2019**, *32*, 294. <https://doi.org/10.1021/acs.chemrestox.8b00313>
- [18] K. Methling, P. Reszka, M. Lalk, O. Vrana, E. Scheuch, W. Siegmund, B. Terhaag, P. J. Bednarski, *Drug Metab. Dispos.* **2009**, *37*, 479. <https://doi.org/10.1124/dmd.108.024364>
- [19] C. C. Hernandez, R. A. Tarfa, J. Miguel I. Limcaoco, R. Liu, P. Mondal, C. Hill, R. Keith Duncan, T. Zzounopoulos, C. R. J. Stephenson, M. J. O'Meara, P. Wipf, *Bioorg. Med. Chem. Lett.* **2022**, *71*, 128841. <https://doi.org/10.1016/j.bmcl.2022.128841>
- [20] P. Bloms-Funke, M. Bankstahl, J. Bankstahl, C. Kneip, W. Schröder, W. Löscher, *Neuropharmacology* **2022**, *203*, 108884. <https://doi.org/10.1016/j.neuropharm.2021.108884>
- [21] M. D. Aleo, J. Aubrecht, P. D. Bonin, D. A. Burt, J. Colangelo, L. Luo, S. Schomaker, R. Swiss, S. Kirby, G. C. Rigdon, P. Dua, *Pharmacol. Res. Perspect.* **2019**, *7*, e00467. <https://doi.org/10.1002/prp2.467>
- [22] (a) Y.-M. Zhang, H.-Y. Xu, H.-N. Hu, F.-Y. Tian, F. Chen, H.-N. Liu, L. Zhan, X.-P. Pi, J. Liu, Z.-B. Gao, F.-J. Nan, *J. Med. Chem.* **2021**, *64*, 5816. <https://doi.org/10.1021/acs.jmedchem.0c02252>; (b) S. Musella, L. Carotenuto, N. Iraci, G. Baroli, T. Ciaglia, P. Nappi, M. G. Basilicata, E. Salvati, V. Barrese, V. Vestuto, G. Pignataro, G. Pepe, E. Sommella, V. Di Sarno, M. Manfra, P. Campiglia, I. Gomez-Monterrey, A. Bertamino, M. Tagliatalata, C. Ostacolo, F. Miceli, *J. Med. Chem.* **2022**, *65*, 11340. <https://doi.org/10.1021/acs.jmedchem.2c00911>
- [23] K. W. Wurm, F.-M. Bartz, L. Schulig, A. Bodtke, P. J. Bednarski, A. Link, *ACS Omega* **2022**, *7*, 7989. <https://doi.org/10.1021/acsomega.1c07103>
- [24] A. S. Surur, C. Bock, K. Beirow, K. Wurm, L. Schulig, M. K. Kindermann, W. Siegmund, P. J. Bednarski, A. Link, *Org. Biomol. Chem.* **2019**, *17*, 4512. <https://doi.org/10.1039/C9OB00511K>
- [25] S. Kühnert, G. Bahrenberg, A. Kless, W. Schroder, S. Lucas (Grünenthal GmbH), *US /0258947 A1*, 2012.
- [26] A. P. Kourounakis, D. Xanthopoulos, A. Tzara, *Med. Res. Rev.* **2020**, *40*, 709. <https://doi.org/10.1002/med.21634>
- [27] A. A. Kadi, S. M. Amer, H. W. Darwish, M. W. Attwa, *RSC Adv.* **2017**, *7*, 36279. <https://doi.org/10.1039/c7ra06341e>
- [28] S. L. Degorce, M. S. Bodnarchuk, J. S. Scott, *ACS Med. Chem. Lett.* **2019**, *10*, 1198. <https://doi.org/10.1021/acsmchemlett.9b00248>
- [29] H. Zhao, H. Fu, R. Qiao, *J. Org. Chem.* **2010**, *75*, 3311. <https://doi.org/10.1021/jo100345t>
- [30] J. L. Yap, K. Hom, S. Fletcher, *Tetrahedron Lett.* **2011**, *52*, 4172. <https://doi.org/10.1016/j.tetlet.2011.06.007>
- [31] P. K. Gadekar, A. Roychowdhury, P. S. Kharkar, V. M. Khedkar, M. Arkile, H. Manek, D. Sarkar, R. Sharma, V. Vijayakumar,

- S. Sarveswari, *Eur. J. Med. Chem.* **2016**, *122*, 475. <https://doi.org/10.1016/j.ejmech.2016.07.001>
- [32] (a) W. Jaspers, A. Oliveira, R. Prieto-Díaz, M. Majellaro, J. Åqvist, E. Sotelo, H. Gutiérrez-de-Terán, *Molecules* **2017**, *22*, 1945. <https://doi.org/10.3390/molecules22111945>; (b) J. Cai, X. Fradera, M. van Zeeland, M. Dempster, K. S. Cameron, D. J. Bennett, J. Robinson, L. Popplestone, M. Baugh, P. Westwood, J. Bruin, W. Hamilton, E. Kinghorn, C. Long, J. C. M. Uitdehaag, *Bioorg. Med. Chem. Lett.* **2010**, *20*, 4507. <https://doi.org/10.1016/j.bmcl.2010.06.043>; (c) H. W. Lee, B. Y. Kim, J. B. Ahn, S. K. Kang, J. H. Lee, J. S. Shin, S. K. Ahn, S. J. Lee, S. S. Yoon, *Eur. J. Med. Chem.* **2005**, *40*, 862. <https://doi.org/10.1016/j.ejmech.2005.03.019>
- [33] C. Zhao, Y. H. Choi, D. B. Khadka, Y. Jin, K.-Y. Lee, W.-J. Cho, *Bioorg. Med. Chem.* **2016**, *24*, 789. <https://doi.org/10.1016/j.bmc.2015.12.047>
- [34] E. A. Arnott, L. C. Chan, B. G. Cox, B. Meyrick, A. Phillips, *J. Org. Chem.* **1653**, 2011, 76. <https://doi.org/10.1021/jo102262k>
- [35] H.-P. Gong, Z.-J. Quan, X.-C. Wang, *Chem. Pap.* **2022**, *76*, 2529. <https://doi.org/10.1007/s11696-021-02044-5>
- [36] X. Li, Q. Zhang, P. Guo, J. Fu, L. Mei, D. Lv, J. Wang, D. Lai, S. Ye, H. Yang, J. Guo, *Cell Res.* **2021**, *31*, 52. <https://doi.org/10.1038/s41422-020-00410-8>
- [37] M. T. Rahman, A. M. Decker, L. Lauder milk, R. Maitra, W. Ma, S. Ben Hamida, E. Darcq, B. L. Kieffer, C. Jin, *J. Med. Chem.* **2021**, *64*, 12397. <https://doi.org/10.1021/acs.jmedchem.1c01075>
- [38] H. C. Shen, F.-X. Ding, Q. Deng, S. Xu, X. Tong, X. Zhang, Y. Chen, G. Zhou, L.-Y. Pai, M. Alonso-Galicia, S. Roy, B. Zhang, J. R. Tata, J. P. Berger, S. L. Colletti, *Bioorg. Med. Chem. Lett.* **2009**, *19*, 5716. <https://doi.org/10.1016/j.bmcl.2009.08.006>
- [39] M. I. Antczak, Y. Zhang, C. Wang, J. Doran, J. Naidoo, S. Voruganti, N. S. Williams, S. D. Markowitz, J. M. Ready, *J. Med. Chem.* **2017**, *60*, 3979. <https://doi.org/10.1021/acs.jmedchem.7b00271>
- [40] M. G. Palermo, *Tetrahedron Lett.* **1996**, *37*, 2885. [https://doi.org/10.1016/0040-4039\(96\)00425-X](https://doi.org/10.1016/0040-4039(96)00425-X)
- [41] K. Biernacki, M. Daško, O. Ciupak, K. Kubiński, J. Rachon, S. Demkowicz, *Pharmaceuticals* **2020**, *13*, 111. <https://doi.org/10.3390/ph13060111>
- [42] A. R. Gangloff, J. Litvak, E. J. Shelton, D. Sperandio, V. R. Wang, K. D. Rice, *Tetrahedron Lett.* **2001**, *42*, 1441. [https://doi.org/10.1016/S0040-4039\(00\)02288-7](https://doi.org/10.1016/S0040-4039(00)02288-7)
- [43] N. Y. Khromova, M. M. Fedorov, S. I. Malekin, A. V. Kutkin, *Russ. J. Org. Chem.* **2016**, *52*, 1490. <https://doi.org/10.1134/S1070428016100195>
- [44] S. Ueda, H. Nagasawa, *J. Am. Chem. Soc.* **2009**, *131*, 15080. <https://doi.org/10.1021/ja905056z>
- [45] K.-S. Yeung, M. E. Farkas, J. F. Kadow, N. A. Meanwell, *Tetrahedron Lett.* **2005**, *46*, 3429. <https://doi.org/10.1016/j.tetlet.2005.02.167>
- [46] A. D. Bochevarov, E. Harder, T. F. Hughes, J. R. Greenwood, D. A. Braden, D. M. Philipp, D. Rinaldo, M. D. Halls, J. Zhang, R. A. Friesner, *Int. J. Quantum Chem.* **2013**, *113*, 2110. <https://doi.org/10.1002/qua.24481>
- [47] M. Xie, G. Zhu, Y. Hu, H. Gu, *J. Phys. Chem. C* **2011**, *115*, 20596. <https://doi.org/10.1021/jp206544a>
- [48] J. D. Mottishaw, H. Sun, *J. Phys. Chem. A* **2013**, *117*, 7970. <https://doi.org/10.1021/jp403679x>
- [49] J. Payandeh, M. Volgraf, *Nat. Rev. Drug Discov.* **2021**, *20*, 710. <https://doi.org/10.1038/s41573-021-00240-2>
- [50] A. Schenzer, *J. Neurosci.* **2005**, *25*, 5051. <https://doi.org/10.1523/JNEUROSCI.0128-05.2005>
- [51] Assessment report for flupirtine containing medicinal products, 2013, Accessed July 21, 2022. [https://www.ema.europa.eu/en/documents/referral/flupirtine-containing-medicines-article-107i-procedure-prac-assessment-report\\_en.pdf](https://www.ema.europa.eu/en/documents/referral/flupirtine-containing-medicines-article-107i-procedure-prac-assessment-report_en.pdf)
- [52] N. Vineela Karthik Naguri, K. Ravi Babu Komaram, S. Tamilisetty Vidya Sagar, *Asian J. Pharm. Clin. Res.* **2019**, *12*, 84. <https://doi.org/10.22159/ajpcr.2019.v12i4.31699>
- [53] W. Siegmund, C. Modess, E. Scheuch, K. Methling, M. Keiser, A. Nassif, D. Roskopf, P. J. Bednarski, J. Borlak, B. Terhaag, *Br. J. Clin. Pharmacol.* **2015**, *79*, 501. <https://doi.org/10.1111/bcp.12522>
- [54] J. G. Kenna, J. Utrecht, *Drug Metab. Dispos.* **2018**, *46*, 1658. <https://doi.org/10.1124/dmd.118.082719>
- [55] (a) P. Nicoletti, A. N. Werk, A. Sawle, Y. Shen, T. J. Urban, S. A. Coulthard, E. S. Bjornsson, I. Cascorbi, A. Floratos, T. Stammschulte, U. Gundert-Remy, M. R. Nelson, G. P. Aithal, A. K. Daly, *Pharmacogenet. Genomics* **2016**, *26*, 218. <https://doi.org/10.1097/FPC.0000000000000209>; (b) F. Puls, C. Agne, F. Klein, M. Koch, K. Rifai, M. P. Manns, J. Borlak, H. H. Kreipe, *Virchows Arch.* **2011**, *458*, 709. <https://doi.org/10.1007/s00428-011-1087-9>
- [56] A. Segovia-Zafra, D. E. Di Zeo-Sánchez, C. López-Gómez, Z. Pérez-Valdés, E. García-Fuentes, R. J. Andrade, M. I. Lucena, M. Villanueva-Paz, *Acta Pharm. Sin. B* **2021**, *11*, 3685. <https://doi.org/10.1016/j.apsb.2021.11.013>
- [57] G. A. Kullak-Ublick, R. J. Andrade, M. Merz, P. End, A. Benesic, A. L. Gerbes, G. P. Aithal, *Gut* **2017**, *66*, 1154. <https://doi.org/10.1136/gutjnl-2016-313369>
- [58] T. Mosmann, *J. Immunol. Methods* **1983**, *65*, 55. [https://doi.org/10.1016/0022-1759\(83\)90303-4](https://doi.org/10.1016/0022-1759(83)90303-4)
- [59] (a) T. Ramirez, A. Strigun, A. Verlohner, H.-A. Huener, E. Peter, M. Herold, N. Bordag, W. Mellert, T. Walk, M. Spitzer, X. Jiang, S. Sperber, T. Hofmann, T. Hartung, H. Kamp, B. van Ravenzwaay, *Arch. Toxicol.* **2018**, *92*, 893. <https://doi.org/10.1007/s00204-017-2079-6>; (b) M. Davis, B. D. Stamper, *BioMed Res. Int.* **2016**, *2016*, 4780872. <https://doi.org/10.1155/2016/4780872>
- [60] K. McEuen, J. Borlak, W. Tong, M. Chen, *Int. J. Mol. Sci.* **2017**, *18*, 1335. <https://doi.org/10.3390/ijms18071335>
- [61] N. T. T. Tham, S.-R. Hwang, J.-H. Bang, H. Yi, Y.-I. Park, S.-J. Kang, H.-G. Kang, Y.-S. Kim, H.-O. Ku, *J. Vet. Sci.* **2019**, *20*, 34. <https://doi.org/10.4142/jvs.2019.20.1.34>
- [62] A. Mobinikhaledi, N. Forughifar, J. A. Alipour Safari, E. Amini, *J. Heterocycl. Chem.* **2007**, *44*, 697. <https://doi.org/10.1002/jhet.5570440329>
- [63] U. Galli, E. Ciruolo, A. Massarotti, J. Margaria, G. Sorba, E. Hirsch, G. Tron, *Molecules* **2015**, *20*, 17275. <https://doi.org/10.3390/molecules200917275>
- [64] C. Bock, A. S. Surur, K. Beirou, M. K. Kindermann, L. Schulig, A. Bodtke, P. J. Bednarski, A. Link, *ChemMedChem* **2019**, *14*, 952. <https://doi.org/10.1002/cmdc.201900112>
- [65] G. Madhavi Sastry, M. Adzhigirey, T. Day, R. Annabhimoju, W. Sherman, *J. Comput.-Aided Mol. Des.* **2013**, *27*, 221. <https://doi.org/10.1007/s10822-013-9644-8>
- [66] C. Lu, C. Wu, D. Ghoreishi, W. Chen, L. Wang, W. Damm, G. A. Ross, M. K. Dahlgren, E. Russell, C. D. von Bargen, R. Abel, R. A. Friesner, E. D. Harder, *J. Chem. Theory Comput.* **2021**, *17*, 4291. <https://doi.org/10.1021/acs.jctc.1c00302>
- [67] W. Sherman, T. Day, M. P. Jacobson, R. A. Friesner, R. Farid, *J. Med. Chem.* **2006**, *49*, 534. <https://doi.org/10.1021/jm050540c>
- [68] (a) R. A. Friesner, J. L. Banks, R. B. Murphy, T. A. Halgren, J. J. Klicic, D. T. Mainz, M. P. Repasky, E. H. Knoll, M. Shelley, J. K. Perry, D. E. Shaw, P. Francis, P. S. Shenkin, *J. Med. Chem.* **2004**, *47*, 1739. <https://doi.org/10.1021/jm0306430>; (b) T. A. Halgren, R. B. Murphy, R. A. Friesner, H. S. Beard, L. L. Frye, W. T. Pollard, J. L. Banks, *J. Med. Chem.* **2004**, *47*, 1750. <https://doi.org/10.1021/jm030644s>
- [69] R. A. Friesner, R. B. Murphy, M. P. Repasky, L. L. Frye, J. R. Greenwood, T. A. Halgren, P. C. Sanschagrin, D. T. Mainz, *J. Med. Chem.* **2006**, *49*, 6177. <https://doi.org/10.1021/jm051256o>

- [70] M. Kurki, A. Poso, P. Bartos, M. S. Miettinen, *J. Chem. Inf. Model.* **2022**,. <https://doi.org/10.1021/acs.jcim.2c00395>
- [71] P. Mark, L. Nilsson, *J. Phys. Chem. A* **2001**, *105*, 9954. <https://doi.org/10.1021/jp003020w>
- [72] K. J. Bowers, E. Chow, H. Xu, R. O. Dror, M. P. Eastwood, B. A. Gregersen, J. L. Klepeis, I. Kolossvary, M. A. Moraes, F. D. Sacerdoti, J. K. Salmon, Y. Shan, D. E. Shaw, in *SC '06: Proceedings of the 2006 ACM/IEEE conference on Supercomputing* (Ed: B. Horner-Miller), ACM Press, New York, USA, **2006**, 84–es. <https://doi.org/10.1145/1188455>
- [73] M. Ikeguchi, *J. Comput. Chem.* **2004**, *25*, 529. <https://doi.org/10.1002/jcc.10402>

## SUPPORTING INFORMATION

Additional supporting information can be found online in the Supporting Information section at the end of this article.

**How to cite this article:** K. W. Wurm, F.-M. Bartz, L. Schulig, A. Bodtke, P. J. Bednarski, A. Link, *Arch. Pharm.* **2023**;356:e2200473. <https://doi.org/10.1002/ardp.202200473>